

ALTERATIONS IN DIASTASE ACTIVITY AND SOME PHYSICAL PROPERTIES OF THERMALLY TREATED HONEY FROM SELECTED AREAS IN SOUTHERN NIGERIA.

Adedayo, O. O.; Ochigbo, S. S.*

Department of Chemistry
Federal University of Technology, Minna. Nigeria.

*Corresponding Author: stephenochigbo@futminna.edu.ng, stephen_ochigbo@yahoo.com;
Tel:+234 (0) 813 228 6172

ABSTRACT

Based on experimental design patterned after conditions applicable to processing technologies in Nigerian honey industry, samples of honey from selected areas in three zones of Southern Nigeria were heated in a thermostatic water bath under varied temperatures (50 °C, 60 °C, 80 °C, 100 °C) and time (60, 180, 300 and 420 min). From the result, it was observed that thermal treatment under certain conditions of combination of temperature and time leads to loss of diastase activity and physical properties such as colour and viscosity of the samples. Diastase activity (measured as Diastase Number DN) was within specified limits at 50 °C and 60 °C at the maximum heating time of 420 min. There was considerable loss of diastase activity at 80 °C for 300 min and 420 min while no diastase activity was recorded in all samples at these times at 100°C. It was concluded that the most appropriate temperature and time combination for entrepreneurs considering thermal treatment of these honey type in the area of study is 60 °C for a period up to 420 min, irrespective of the initial values of DN within the regulated standards.

Keywords: Honey, Diastase activity, Diastase Number, Thermal treatment.

INTRODUCTION

Honey gathering and usage is almost as old as man. In all climes and cultures honey is widely valued as good natural product. In religious settings, the Holy Bible tells of King Solomon encouraging the use of honey, the Promised Land was frequently regarded as the land flowing with 'milk and honey'. In Holy Hadith, prophet Mohammed recommended honey to one of his followers as remedy for diarrhoea and the Quran has an entire Surah called al-Nahl which translates as 'the Honey Bee' [1, 2].

Honey which is a sweet, viscous, golden or amber coloured liquid produced by honeybees is basically of two types based on where the bees obtained the start-up material; blossom honey and honeydew honey. Blossom honey is the honey obtained from nectar of plants. The honeybees gather the nectar and processed it in honeycomb. It is also called nectar honey. Honeydew is the sticky syrupy secretion of aphids and *hemiptera* sucked from phloem sap of plants. Instead of taking nectars from plants, Honeybees gather these secretions, combine them with substances of their own and

transform them to honey [3]. One of the main hurdles encountered by entrepreneurs in the honey industry is quality deterioration as a result of fermentation. If honey is left unheated during processing, fermentation sets in within few days of storage due to high moisture content and yeast count. Hence, both local and industrial honey processing require a considerable amount of heat treatment in order to reduce moisture content to a level that delays fermentation [4]. Industrially, honey decrystallization, pasteurization and liquefaction are frequently achieved by convection method in which honey containers is placed in a thermostat heated air or water. However, time and temperature required is speculative since honey quality is largely dependent on the geographical origin and the plant species on which the bees obtained nectars [3]. Findings in a separate clime may be used as reference for another but such would not suffice in dealing with quality issues relating to thermal conditions necessary in completely different area. The desirability of thermal treatment to eliminate the challenges of viscosity, fermentation and crystallization come with its own problems. Honey contains thermolabile substances, key to its appeal and vast usefulness. Improper application of heat has the potential to damage honey quality by altering the physico-chemical quality parameters through the formation of Hydroxymethylfurfural (HMF), inactivation of enzymatic activities and changes in sensory and physical characteristics [5, 6]. As a viscous liquid, honey rheological properties are significant in terms of sensory quality and applications related to handling, processing, hydraulic transport, bottling, storage, quality control and crystallization process [7, 8]. Honey flow properties depend mainly on its

composition (crystal structure), temperature and moisture content. D'Arcy [9] indicated honey with high moisture content have low viscosity. From literature, it has been widely agreed that honey in its liquid states acts like a Newtonian fluid whose viscosity depends mainly on temperature and water content [10, 11]. There are reports, however, indicating non-Newtonian behaviour for some honey [12, 13]. Subjecting honey to thermal treatment changes the colour from its usual golden or light amber to a darker hue as a result of Maillard or non-enzymatic browning reactions [14]. Honey natural colour depends largely on the floral source and mineral contents. Colour is the primary physical property seen by consumers. Indeed, honey pricing rests to a considerable degree on its colour [15]. Though honey is widely consumed in Nigeria, No work has been reported in literature on the effects of thermal treatment on the diastase activity and colour of the honey samples available in Nigeria.

This study is therefore aimed at addressing this gap by investigating the effects of thermal treatment on the diastase activity and colour of fresh honey from Southern parts of Nigeria.

MATERIALS AND METHODS

Materials

Fresh, untreated honey samples used in this study were collected from local bee hunters in three locations of the geo-political zones of Southern Nigeria. The samples were homogenized in the laboratory by constant stirring for 5 min, preventing air from being stirred into the samples. Particles, debris and lifeless bees were removed by passing the honey through 0.5 mm sieve.

Quality assurance of the fresh honey samples was subsequently conducted in the laboratory by the measurements of Hydroxymethylfurfural (HMF) content, diastase activity, pH and acidity (free, lactone and total acidity), Moisture content, viscosity, colour value, density, electrical conductivity and sugars

(apparent reducing sugars and apparent sucrose). Afterwards, the samples were kept at room temperature in HDPE containers and stored in dark polythene bags for a week before the commencement of thermal treatments. The samples were coded as stated in Table I

Table I. Coding of Fresh Honey Samples

Code	Honey Sample
EB	Ehor via Benin City, Edo State, South-South, Nigeria
IA	Ihiala via Onitsha, Anambra State, South-East, Nigeria
SW	Olokuta via Ore, Ondo State, South-West, Nigeria

Experimental Design

The design of the thermal treatment on the fresh honey samples is shown in Table II. The temperatures and time were chosen to represent the feasible ranges of conditions obtainable in Nigerian honey processing industry. Each of the sample (150 g) was weighed into a 250 mL beaker, well-sealed and treated thermally by heating in temperature-controlled water bath

(Techmel & Techmel, USA Model TT42D) at specified conditions enumerated in the experimental design. The treatments of samples were performed in duplicates. After each thermal treatment, the samples were cooled rapidly under a running tap and kept in clean and well-closed PET bottles for subsequent characterizations.

Table II: Experimental Design of the Thermal Treatment Conditions of the Honey Samples

Sample	Heating		Immersion time		
	Temperature	60 min	180 min	300 min	420 min
Ehor, EB	50°C	EB ₁	EB ₂	EB ₃	EB ₄
	60°C	EB ₅	EB ₆	EB ₇	EB ₈
	80 °C	EB ₉	EB ₁₀	EB ₁₁	EB ₁₂
	100 °C	EB ₁₃	EB ₁₄	EB ₁₅	EB ₁₆
Ihiala, IA	50°C	IA ₁	IA ₂	IA ₃	IA ₄

..

	60°C	IA ₅	IA ₆	IA ₇	IA ₈
	80 °C	IA ₉	IA ₁₀	IA ₁₁	IA ₁₂
	100 °C	IA ₁₃	IA ₁₄	IA ₁₅	IA ₁₆
Ore, SW	50°C	SW ₁	SW ₂	SW ₃	SW ₄
	60°C	SW ₅	SW ₆	SW ₇	SW ₈
	80 °C	SW ₉	SW ₁₀	SW ₁₁	SW ₁₂
	100 °C	SW ₁₃	SW ₁₄	SW ₁₅	SW ₁₆

Determination of Physico-chemical Properties

Dynamic Viscosity

The dynamic viscosity or viscosity coefficient η is the tangential force per unit surface, known as shearing stress τ and expressed in Pascal, necessary to move, parallel to the sliding plane, a layer of liquid of 1 square meter at a rate (v) of 1 meter per second relative to a parallel layer at a distance (x) of 1 meter. The ratio dv/dx is a speed gradient for the rate of shear D expressed in reciprocal seconds (s^{-1}), hence $\eta = \tau / D$. The time required for the level of the honey to drop from a pre-determined mark (above) to another (below) is measured with a stop-watch. The validity of the result is ensured with two consecutive readings not different by more than 1 % [16].

$$\text{Dynamic viscosity } \eta = K\rho t$$

t = flow time, in seconds.

ρ = density of the honey expressed in mg/mm^3

K = Constant of the viscometer, expressed in mm^2/s

The result was expressed as Pa.s (Pascal seconds).

Density

The density was determined by dividing the weight in air of the honey that fill a pycnometer at 20° by weight in air of water needed to fill the pycnometer after making allowance for the thrust of the air [16].

The density was calculated from the expression:

$$\rho_{20} = \frac{998.2(M_1 + A)}{M_2 + A}$$

Where

M_1 = Apparent weight of honey (g)

M_2 = Apparent weight of water (g)

A = the correction factor for the thrust of the air, $0.0012 M_2$

998.2 = the density of water at 20° in Kg/m^3

The result is expressed in $g\ cm^{-3}$.

Diastase Activity

The Goethe unit which is the unit of Diastase activity is defined as the amount in mL of 1 % starch hydrolyzed by an enzyme in 1 g of honey per hour at 40 °C. The Diastase activity is expressed as Diastase number [17]. In principle, a standard starch solution, capable of developing, with iodine, a blue colour in a defined range of intensity, is acted upon by the enzyme in the sample under standard conditions. The diminution in the blue colour is measured at intervals. The diastase activity was determined using the traditional Schade method [18].

The diastase activity was calculated thus;

$$DN = \frac{300}{tx}$$

Where;

DN = Diastase Number (DN)

tx = reaction time in minutes.

Colour Value

The colour value is based on the intensity of colour in honey formed under prescribed conditions and read at 420 nm using spectrophotometer. The honey samples (25 g) were dissolved in 30 mL of water in a beaker and transferred quantitatively to a 50 mL volumetric flask. After making to mark with distilled water, the solution was mixed, filtered through a filter paper with diameter of pores 0.45 µm and degassed. The absorbance of the resulting filtrate was measured at 420 nm using a 10 cm cuvette.

The colour value was calculated thus;

$$\text{Colour value, } C_v = \frac{(A \times 1000)}{B \times C}$$

Where,

A = Absorbance at 420 nm

B = path length in centimetres

C= Concentration of the solution in g/ml

Statistical Analysis

The results of the study were analyzed by Analysis of Variance (ANOVA). The data for the diastase number (DN), viscosity and colour values in treated honey samples were analyzed with one-way ANOVA with a probability limit of p<0.05. Throughout the analysis, differences at p<0.05 were considered significant. Multiple regressions was applied with density and DN values as dependent variable and the sample temperature and heating time in thermostatic water bath as independent variables. Microsoft Excel 2007 and SPSS 16.0 for Windows were used. Experiments were done in triplicates and average results reported.

RESULTS AND DISCUSSION

Table III: Physico-Chemical Properties of Untreated Honey Samples

Parameters	Standard Values ^a	Experimental values		
		SW	EB	IA
pH	_____	5.12±0.02	5.34±0.05	4.91±0.04
Diastase No. (°Goethe)	≥ 8	16.22±0.44	15.65±0.13	23.14±0.68
Density (g/cm ³)	_____	1.368±0.00	1.407±0.00	1.433±0.00
Dynamic Viscosity (Pa.s)	_____	212.32±7.62	435.45±3.83	351.92±2.89
Colour Value	_____	201.10±2.50	379.00±2.12	278.07±2.25

*Standard values as reported by Codex Alimentarius Commission [19]

Results are expressed as mean values ± standard deviations, where n = 3

Diastase Activity in Thermally Treated Honey Samples

Fig. 1 shows the impact of thermal treatment on diastase activity in SW honey at different time and heating temperature. After the first 60 min at 50 °C, the initial value of diastase number, 16.22 °Goethe was reduced to 14.69, 13.97 at 60 °C, 10.89 at 80 °C and 6.96 at 100 °C. For the next

treatment at 180 min the diastase number recorded at 50 °C, 60 °C, 80 °C and 100 °C were 10.95, 9.75, 5.93 and 1.03 respectively. The diastase number in 300 min and 420 min at 50 °C was 7.83 and 4.63 respectively. At 60 °C for the same 300 min and 420 min the diastase number was 6.15 and 3.30 respectively.

The diastase activity was not detectable at

300 and 420 min under the 80 °C and 100 °C thermal intensity. This result is in concordance to those obtained by Cozmuta *et al.* [20]. The slight area of divergence is that complete inactivation of enzymes occurred at 120 min under 100 °C but in this particular honey such total denaturation was obtained at 100 °C after 300 min. The longer the immersion time the more rapid the inactivation process.

The coefficient of determination, R^2 value of 0.998 for SW diastase loss at 60 min shows that only 0.2 % of the regression variances do not depend on the variable. At 180 min the percentage of variance was 99.9 % while the regression coefficient for 300 and 420 min shows that the direction of relationship between DN and its independent variables was negative.

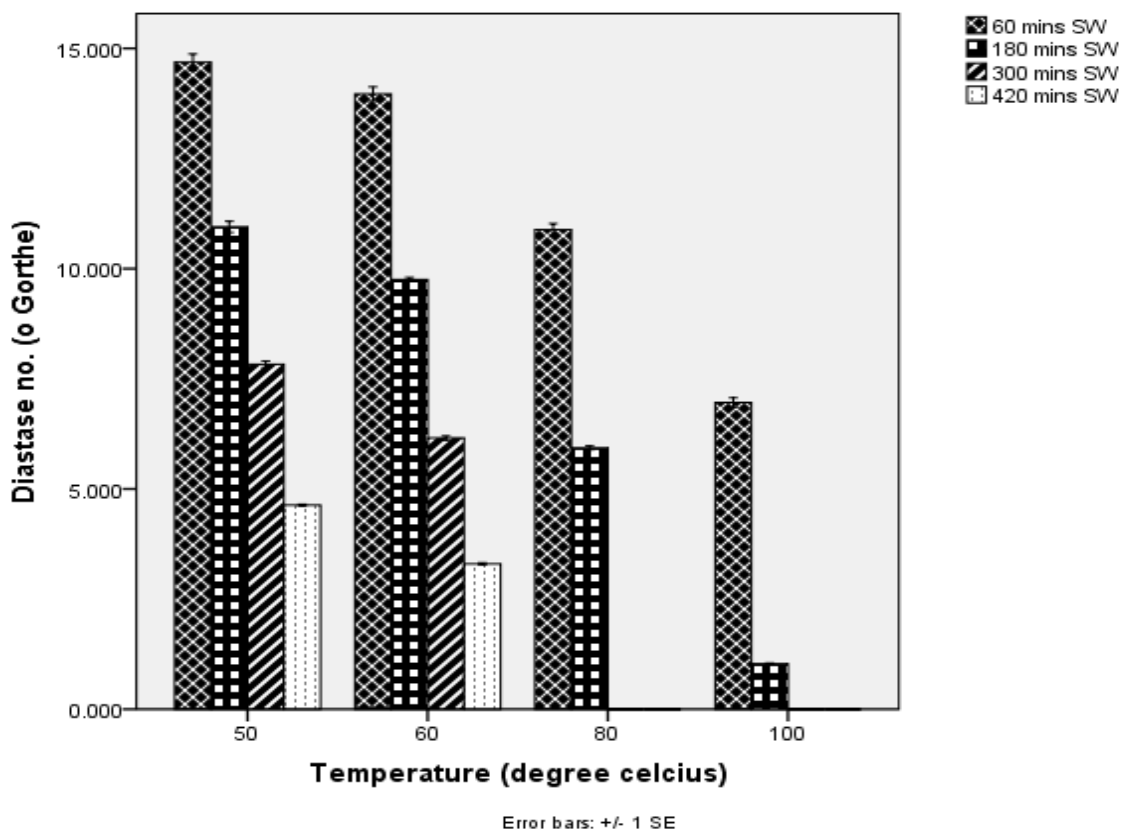


Fig. 1: Impact of Thermal Treatment on Diastase Activity in SW Honey

Fig. 2 shows the effects of thermal treatment on EB honey under the applied conditions. The initial diastase number was reduced at 50 °C for 60 min by 14.7 %, 30.22 % at 180 min, 48.37 % at 300 min and 66.96 % at 420 min. This result is in concordance to what was obtained by other researchers who also observed a continual and consistent reduction in DN at higher temperature [20, 21]. The diastase

activity falls below the minimum specification of 8 °Goethe at 60 °C in 300 min. However, the Codex alimentarius [19] gave another limit of 3 °Goethe for honey with low natural enzyme content. If the preceding position is taken into consideration, the honey diastase quality was finally compromised at 80 °C for 300 min with a DN value of 2.89 °Goethe. As

..

seen in Fig. 3 no diastase activity was detectable in 180 to 420 min at 100 °C.

The percentage of variance between the variables was 97.4 % for 60 min, 99.5 % for 180 min, 91.0 % for 300 min and 90.3 % for

420 min. The regression coefficient was positive for 60 and 180 min but negative for 300 and 420 min. At all the heating temperature and immersion time, DN values varied significantly ($p < 0.05$) except at 80 °C and 100 °C for 420 min.

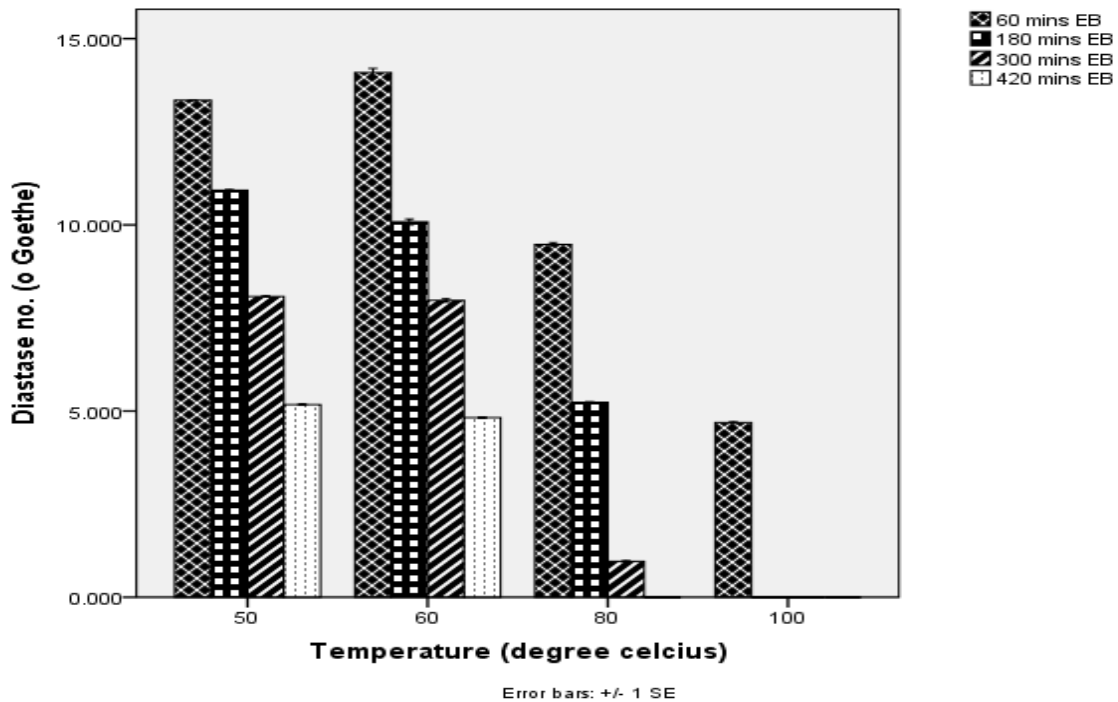


Fig 2: Impact of Thermal Treatment on Diastase Activity in EB Honey at Different Temperature and Time

The extent of diastase activity reduction in IA honey under thermal treatment is graphically presented in Fig. 3. The initial diastase number of 23.14 was reduced to 19.42 at 50 °C during the first 60 min. In 180 min, the initial value was reduced to 15.54, 12.17 in 300 min and 9.53 in 420 min. At 60 °C the diastase number was 19.37 in 60 min, 14.85 in 180 min, 10.92 in 300 min and 8.11 in 420 min. The reduction at 80 °C was 43.34 % for 60 min, 68.54 % in 180 min, 91.27 % in 300 min and 100 % in

420 min. At 100 °C the diastase activity was reduced by 65.25 % in 60 min, 91.44 % in 180 min and 100 % in 300 to 420 min. The R^2 value 0.978 at 60 min shows that only 2 % of the regression variances do not depend on the variable. The percentage of variance in 180 min for all heating temperature was 98.0 %, 95.2 % in 300 min and 93.4 % in 420 min. The regression coefficient was only positive in 60 min and negative in the remaining immersion time.

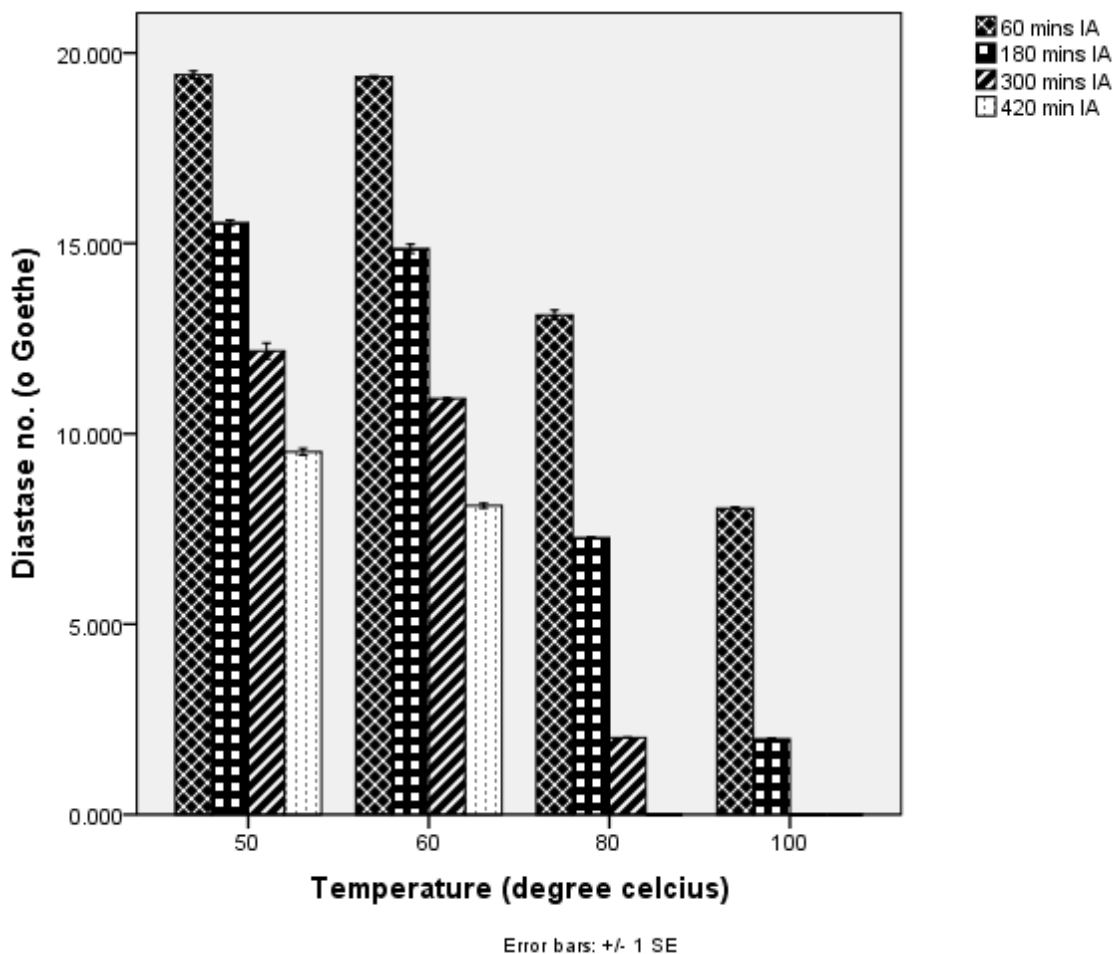


Fig 3. Impact of Thermal Treatment on Diastase Activity in IA Honey at Different Temperature and Time

At 100 °C, the ratio of diastase loss was higher for EB in 60 and 180 min. This explains why the diastase activity loss was 100 % for EB in 180 min, a condition obtainable in SW and IA in 300 to 420 min. This result is in partial agreement with the one reported by Tosi *et al.* [21] that diastase activity was not observable at 100 °C in 0 – 20 min. In this study, the distaste activity was still observable in 60 min at 100 °C to an appreciable 4.69 °Goethe for EB, 6.96 °Goethe for SW and 8.04 °Goethe for IA. In short time, at every heating temperature the diastase activity was still detectable in all tested honey. No diastase activity was recorded in all samples at 100 °C in 300 to 420 min.

From the statistical analysis, the diastase numbers varied insignificantly ($p>0.05$) for SW at 80 °C and 100 °C in 300 and 420 min. In EB the diastase number varied significantly ($p<0.05$) at all heating temperature and time except in 420 min at 80 °C and 100 °C. However, for IA at 50 °C and 60 °C in 60 min and 80 °C and 100 °C in 420 min the diastase number varied insignificantly ($p>0.05$). It could be deduced that length of immersion time and temperature increase contributed to enzyme inactivation but the loss of diastase was more dependent on heating period. Cozmuta *et al.* [20] and Tosi *et al.* [21] advanced a hypothesis for diastase activity loss by thermal effects based on structural changes in the molecules of the

enzymes. When under intense heat enzyme molecules acquire enough kinetic energy to surmount the mutual repulsive forces within the electron clouds of their constituent atoms. This phenomenon makes them align, leading to transition state of the molecules and irreversible denaturation of the enzymes.

Colour Analysis in Thermally Treated Honey

The results of colour analysis in SW, EB and IA honeys after thermal treatment in various conditions are represented in Fig. 4, 5 and 6 respectively. Naturally, honey colour varies widely and depends on the floral source and region [22]. The colour of the honey samples were changed in varying degree during the thermal conditioning. A darker hue was observed as a result of non-enzymatic browning or Maillard reaction [23]. These changes result in higher absorbance reading and have deepening effects on the colour values.

In SW the initial value increased by 0.15 % in 60 min at 50 °C and 30.12 % in 420 min

at the same temperature. At 100 °C in the same 60 min the increase in value was 21.77 %. In this honey, effect of time is more pronounced than temperature. The colour values only became heightened at higher temperature in extended period alone. At the maximum condition applied (420 min at 100 °C) the honey colour changes appeared to vary widely. The increase was 101.29 % for SW, 50.31 % for EB and 78.85 % for IA. In EB the changes in colour tend to proceed gradually such that not many changes were visually observed. This was also shown by the graphical representation.

From the statistical analysis using ANOVA, the colour values in IA varied significantly ($p < 0.05$) at all heating temperature and immersion time. Similar trend was observed in EB except the values in 180 min at 50 °C and 60 °C which did not change significantly ($p > 0.05$). For SW at 50 °C and 60 °C in 60 min, 180 min and 300 min the colour values did not change significantly as observed in the remaining applied conditions.

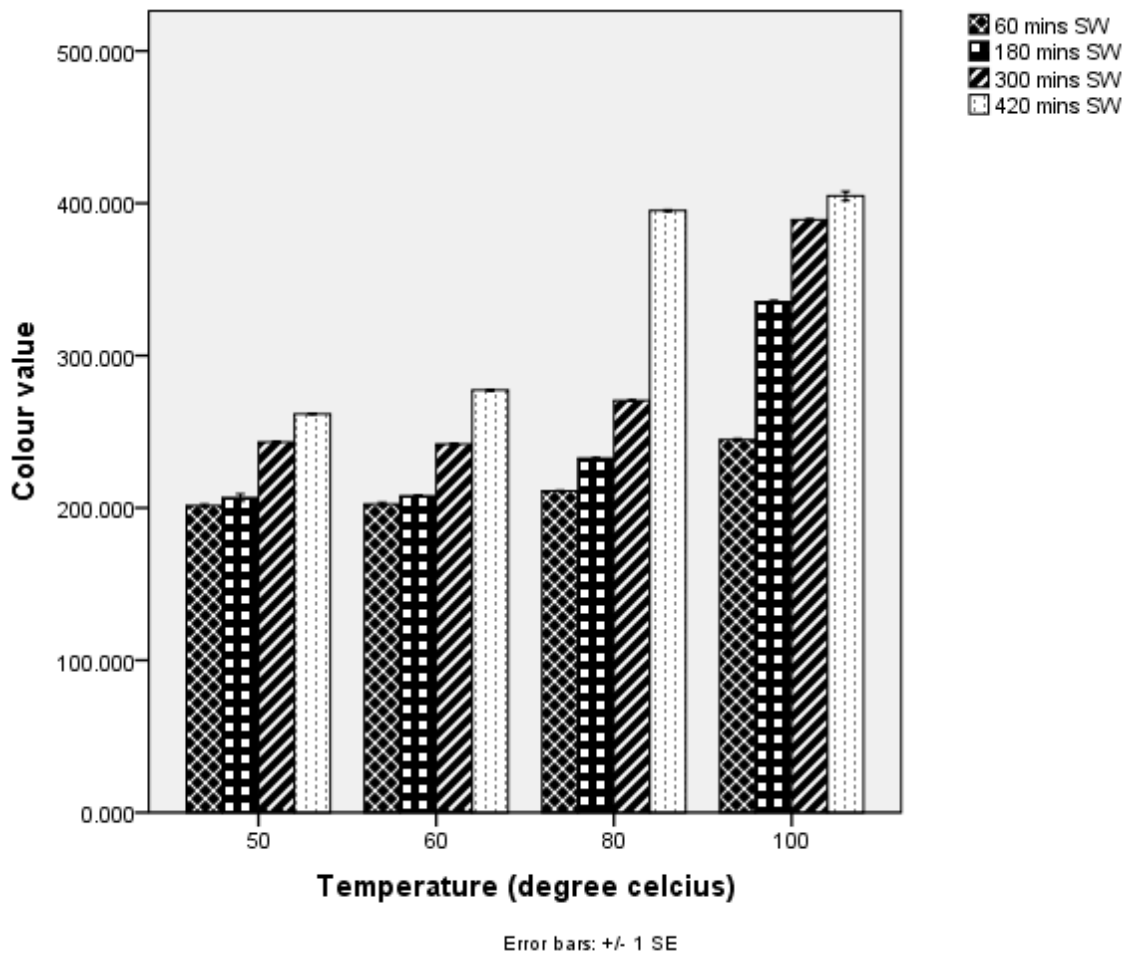


Fig. 4: Colour Changes in Thermally Treated SW Honey Sample

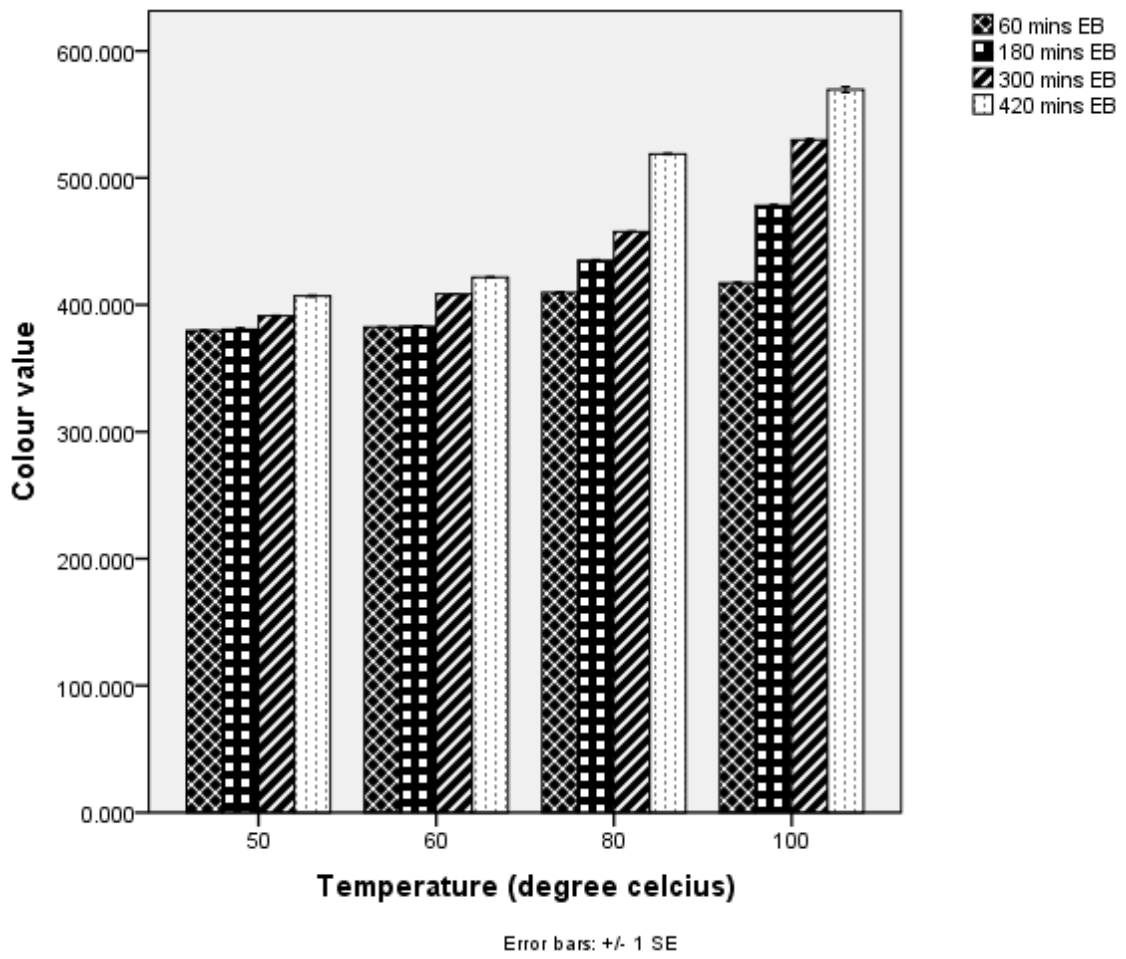


Fig 5: Colour Changes in Thermally Treated EB Honey Sample

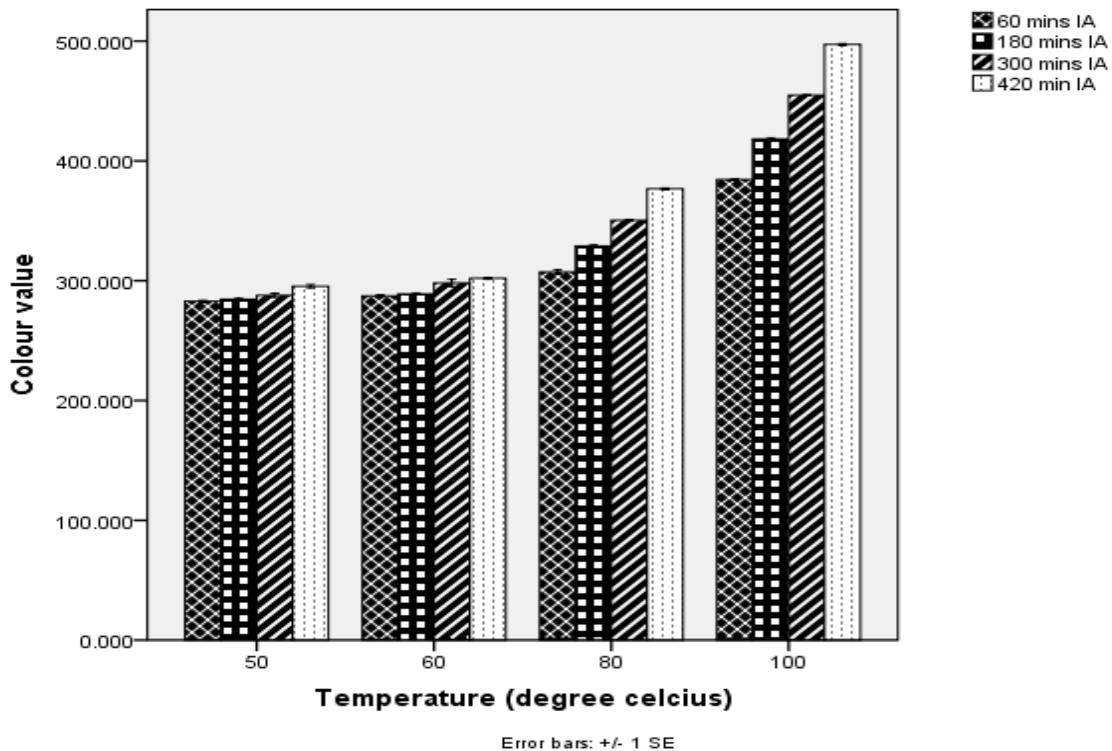


Fig. 6: Colour Changes in Thermally Treated IA Honey Sample

Thermal treatment has effects on the viscosity values of SW, EB and IA honeys. At 50 °C the changes in viscosity in 60 minutes varied widely for the tested honey. From their initial values the changes recorded were 4.79 % for SW, 2.85 % for EB and 0.09 % for IA. For IA at 50 °C in all immersion time there was resistance to change in viscosity such that only 1.26 % was recorded in 420 min in contrast to 12.13 % in EB and 9.59 % in SW.

At higher temperature and extended period, the change in viscosity became more pronounced. In 420 min at 80 °C, the viscosity was reduced by 96.95 % in SW, 85.14 % in EB and 89.12 % in IA in contrast to 49.56 %, 38.07 % and 47.34 % at the same 80 °C in 60 min for SW, EB and IA

respectively. In 420 min at 100 °C the same trend was observed with viscosity value reducing by 99.63 % for SW, 98.72 % for EB and 99.66 % for IA. From the statistical analysis, the viscosity values for the entire samples in every heating temperature and immersion time varied significantly ($p < 0.05$).

As presented in Fig. 7, 8 and 9 the regression chart for density profile of SW, EB and IA honey respectively revealed a minimal impact of heat. The regression coefficient for density was positive in all the investigated honey samples at every applied thermal condition except in 60 minutes for IA honey which exhibited a negative relationship. At no condition was the percentage of variance below 95 %.

..

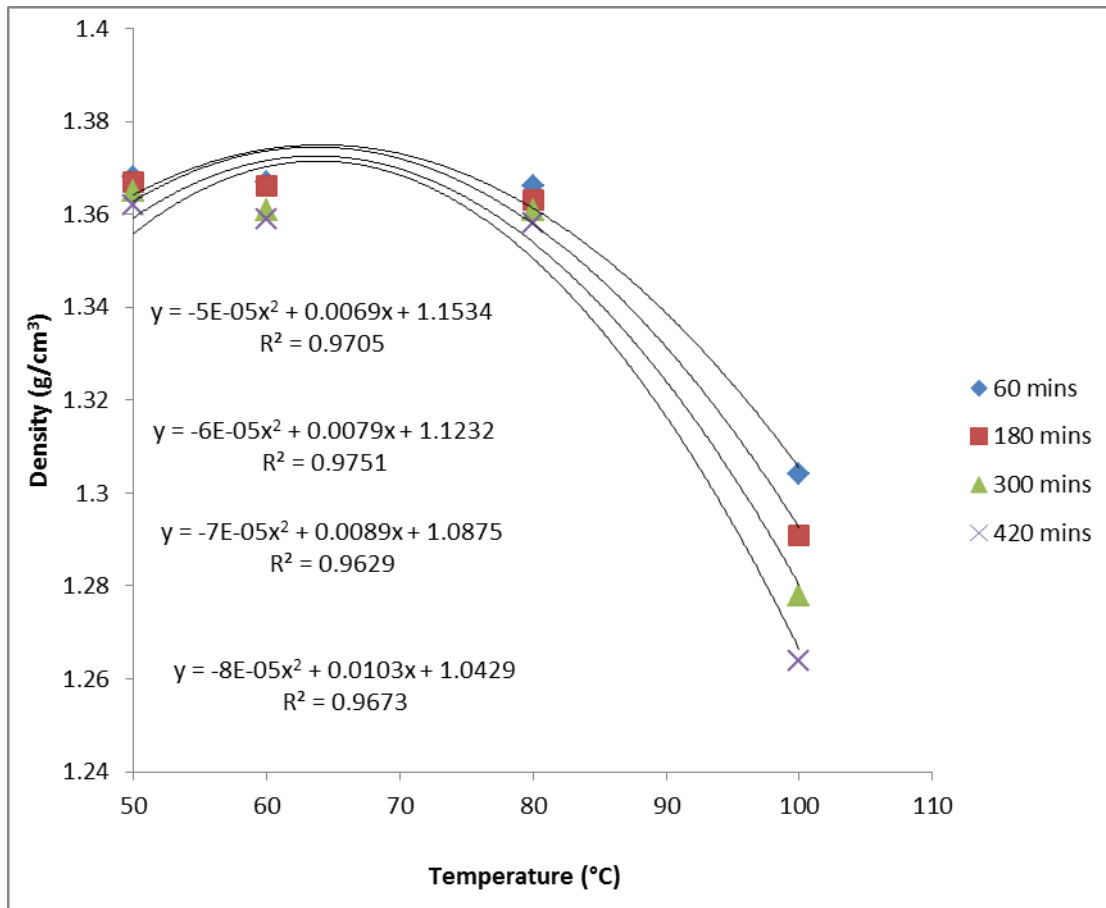


Fig. 7: Regression Chart for Density Profile of Thermally Treated SW Honey

..

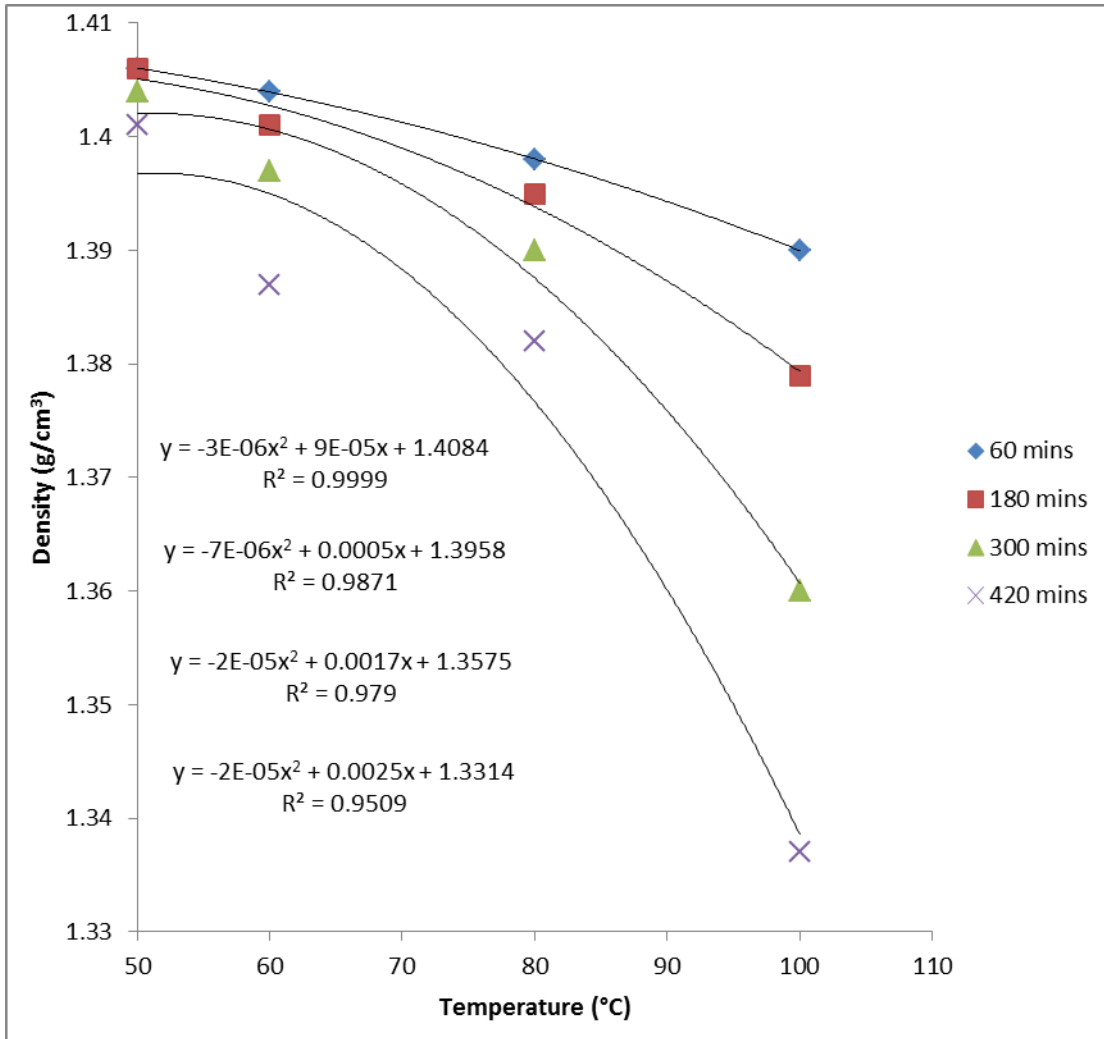


Fig. 8: Regression Chart for Density Profile of Thermally Treated EB Honey

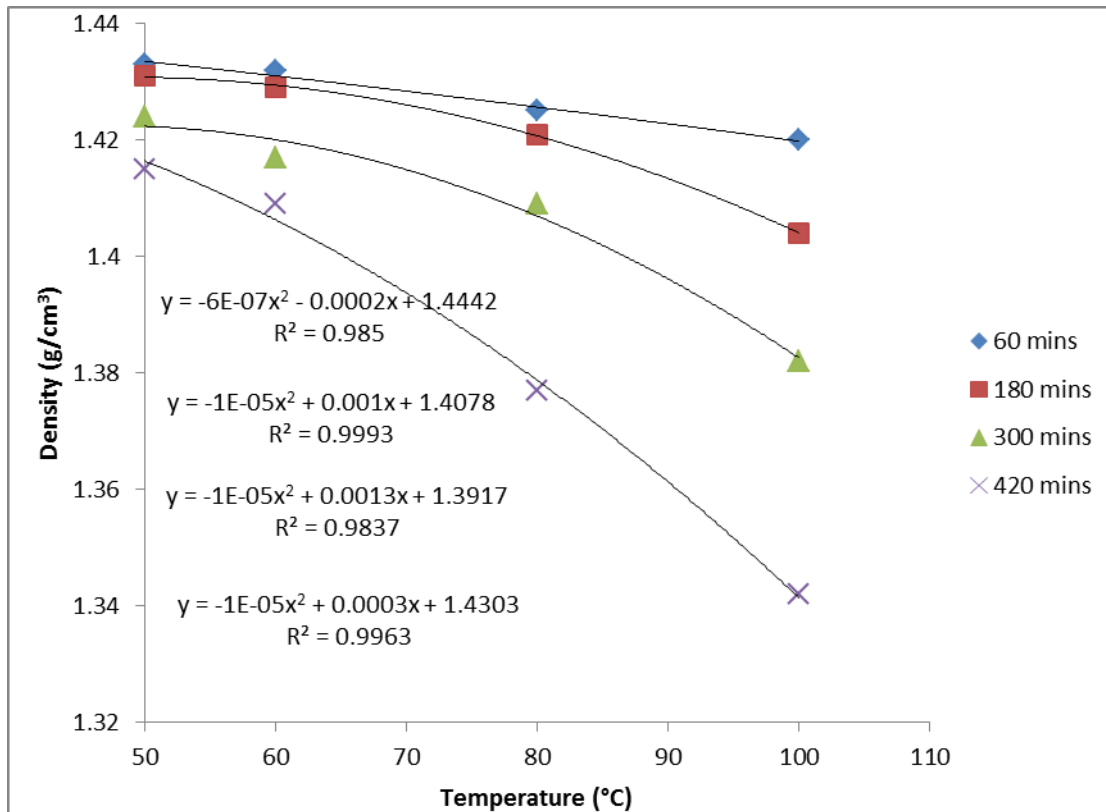


Fig. 9: Regression Chart for Density Profile of Thermally Treated IA Honey

CONCLUSION

The three fresh honey samples have appropriate Diastase Number (DN) at room temperature. It was observed that thermal treatment has significant effects on the diastase activity and physical properties such as colour and viscosity of the samples. Diastase activity (measured as Diastase Number DN) was within specified limits at 50 °C and 60 °C at the maximum heating time of 420 min. There was considerable loss of diastase activity at 80 °C for 300 min and 420 min while no diastase activity was recorded in all samples at the these times at 100 °C. It was concluded that the most appropriate temperature and time combination for entrepreneurs considering thermal

treatment of these honey type in the area of study is 60 °C for a period up to 420 min, irrespective of the initial values of DN within the regulated standards.

Further researches could be conducted on enzymes inactivation during thermal treatment of honey with emphasis on Invertase and glucose-oxidase (GOD). Invertase and GOD are more sensitive to heat than diastase and could be useful in evaluating biochemical deterioration of mildly treated honey. GOD is responsible for the production of gluconolactone and hydrogen peroxide and by extension honey antimicrobial properties. The results of such findings could form the basis for regulation of GOD in honey since none has been formulated up till now.

REFERENCES

1. Bogdanov, S., Jurendic, T. Sieber, R., & Gallmann, P. (2008). Honey for nutrition and health: A review. *American Journal of the College of Nutrition*, 27, 677-689.
2. Wikipedia. (2012). Honey. Retrieved November 15, 2012, from <http://www.en.wikipedia.org/wiki/Honey>
3. Chis, A. & Purcarea, C. (2011). Quality of chestnut honey modified by thermal treatment. *Studia Universitat "Vasile Goldis", Seria Stintele vietii*, 21(3), 573-579.
4. Hebbar, H. U., Nandini, K. E., Lakshmi, M. C., & Subramanian, R. (2003). Microwave and infrared heat processing of honey and its quality. *Food Sci. Technol. Res.*, 9 (1), 49-53.
5. Sahinler, N & Gul, A. (2005). Effect of heating and storage on honey hydroxymethylfurfural and diastase activity. *Journal of Food Technology*, 3 (2), 152-157.
6. Turhan, I., Tetik, N., Karhan, M., Gurel, F. & Tavukeuoglu, H.R. (2008). Quality of honeys influenced by thermal treatment. *Journal of Food Science and Technology* 41, 1396-1399.
7. Bakier, S. (2007). Influence of temperature and water content on the rheological properties of Polish honeys. *Polish Journal of Food and Nutrition Sciences*, 57, (2A) 17-23.
8. James, O. O., Mesubi, M. A., Usman, L. A., Yeye, S. O., Ajanaku, K. O., Ogunniran, K.O., Ajani, O. O. & Siyanbola, T. O. (2009). Physical characterization of some honey samples from North-Central Nigeria. *International Journal of Physical Sciences*, 4(9), 464-470.
9. D'Arcy, E.R. (2007). High-power ultrasound to control honey crystallization. (RIRDC Publication No. 07/145), Brisbane, Australia: Australian Government, Rural Industries Research and Development Corporation.
10. Sopade, P. A., Halley, P. J., Bhandari, B., D'Arcy, B., Doebler, C. & Caffin, N. (2002). Application of the Williams-Landel-Ferry model to the viscosity-temperature relationship of Australian honeys. *Journal of Food Engineering*, 56, 67-75.
11. Zaitoun, S., Al-Majeed, G. A., Al-Malah, K. I. M., & Abu-Jdayil, B. (2001). Rheological properties of selected light colored Jordanian honey. *International Journal of Food Properties*, (4), 1
12. Mossel, B., Bhandari, B., D'Arcy, B., & Caffin, N. (2000). Use of an Arrhenius model to predict rheological behaviour in some Australian honeys. *Lebenswiss Technol.*, 33(8), 545-552.
13. Sopade, P. A., Halley, P. J., D'Arcy, B., Bhandari, B., & Caffin, N. (2004). Friction factors and rheological behaviour of Australian honey in a straight pipe. *Int. J. Food Proper*, 7, 393-405.
14. Bogdanov, S. (2008). Storage, crystallisation and liquefaction of honey. Bee Product Science. Available online <http://www.bee-hexagon.net>
15. Bogdanov, S., Ruoff, K., & Persano Oddo, L. (2004). Physico-chemical methods for the characterization of unifloral honeys: a review. *Apidologie*, 35, S4-S17.
16. British Pharmacopoeia (BP) (2009). *Determination of weight per milliliter, density, relative density*

- and apparent density. Viscosity. Appendix VG and VH.
17. Küçük M., Kolaylı S., Karaoğlu Ş., Ulusoy E., Baltacı C., & Candan F. (2007). Biological activities and chemical composition of three honeys of different types from Anatolia. *Food Chemistry*, 100, 526–534.
 18. AOAC. (1997). Official methods of analysis of the Association of Analytical Chemists 15th Edition, AOAC, Washington, DC.
 19. Codex Alimentarius Commission. (2001). Revised codex standard for honey, Codex STAN 12 – 1981, Rev. 1 (1987), Rev. 2 (2001); FAO/WHO.
 20. Cozmuta, A. M., Cozmuta, L. M., Varga, C., Marian, M., & Peter, A. honey. *Romanian Journal of Food Science*, 1(1), 45-52.
 21. Tosi, E., Martinet, R., Ortega, M., Lucero, H., & Re, E. (2008). Honey diastase activity modified by heating. *Food Chemistry*, 106, 883-887.
 22. White, J. W., & Doner, L. W., (1980). Honey Composition and Properties. In *Beekeeping in the United States Agricultural Handbook* Number 335 Revised October 1980, pp 82–91.
 23. Bogdanov, S. (2009). Honey composition. In *Book of honey*. Bee Product Science. Available online <http://www.bee-hexagon.net>

(2011). Effect of thermal processing on quality of polyfloral

JOMAR 11(2) 2017, 18 - 25
ISSN: 1597-3204

CHEMICAL AND MINERALOGICAL CHARACTERIZATION OF ITAKPE IRON ORE MINE WASTES (TAILINGS)

Alabi, O.O., Gbadamosi, Y., Olatunji T. A. and Ola-Omole O.O

Metallurgical and Materials Engineering Department,
School of Engineering and Engineering Technology, Federal University of Technology, Akure.
Corresponding author: oladunni69alabi@yahoo.com

ABSTRACT

Samples of Itakpe Iron Ore waste dump (tailings) were collected using random sampling method from different locations at the tailings dump sites of National Iron Ore Mining Company (NIOMCO) in Itakpe, Kogi State, Nigeria and properly homogenized to give the head sample. The head sample was chemically analyzed using Energy Dispersive X-Ray Fluorescence Spectrometry (ED-XRFS). Mineralogical analysis was carried out using X-ray Diffraction and Scanning Electron Microscopy (SEM) coupled with Energy Dispersive X-ray Spectroscopy (SEM-EDX). The result showed that it contains 27.71 % Fe₂O₃, 70.1 % SiO₂, and other trace compounds. The qualitative and quantitative XRD analysis of the crude revealed different mineral peaks of which 20.05% Fe₂O₃ and 68.41 % SiO₂ are the major constituents of the ore matrix. SEM micrographs obtained revealed the interlocking nature of the minerals constituting the ore matrix. EDX analysis of regions within the ore matrix revealed the presence of C, O, Al, Si, Fe, Cu, Mg, P and K; such that silicon and iron are the major elemental constituents of the ore matrix while other elements exists in trace form. The crude sample of Itakpe Iron Ore dumped tailings has been found to be coarsely packed and interlocked a haematite rich mineral with magnetite and silica with silica as major impurity. However, easy liberation was facilitated by comminution due to the coarsely packed nature of ore matrix.

Keywords: Dump Tailings, Itakpe, Iron-ore, Characterization

INTRODUCTION

Itakpe iron ore deposit is a magnetite-haematite mineral consisting of 14 ore layers of economic value ranging in grade predominantly from 14.8 – 41 % Fe with an overall average grade of 36 % Fe [1]. It is located at Latitude 07°36¹¹20¹¹ and

Longitude 6°18¹³⁵11¹¹ E in Okehi Local Government Area of Kogi state, Nigeria [1]. The National Iron Ore Mining Company, Itakpe is charged with the mining and processing of this mineral; exploitation method adopted was open-pit mining, and so far, two production batches are being

..

advanced [1]. Furthermore, the ore is currently being processed using magnetic and gravity methods. However, flotation plant is being constructed for future beneficiation of the iron ore [1]. The Itakpe iron ore deposit has a reserve of about 200 million tonnes with an average iron ore content of 36 %. [2] This has to be beneficiated at a rate of 8 million tonnes per year to produce 64 % Fe concentrate as sinter material for the Ajaokuta blast furnace and 68% Fe concentrate as pellet feed for the direct reduction plant at Aladja, all in Nigeria. At this production rate (8 million tonnes per year), large quantities of unwanted siliceous residues called tailings were generated as waste product of the beneficiated iron ore [2, 3]. Research has shown that these tailings contain viable grade of iron which could be processed. [2, 3]. Also, the need for land maximization due to the enormous amount of land occupied by these tailings beckons for drastic methods which can proffer solution to the consequent land underutilization. On this premise, the study was carried out in order to ascertain its qualitative and quantitative characteristics. This will invariably provide an avenue for further research to be carried out towards determination of the best exploitation method to be adopted to separate the iron from the waste.

MATERIALS AND METHOD

Collection of Samples

Samples were collected from different

locations at the tailing dump sites in National Iron Ore Mining Company (NIOMCO) Itakpe, Kogi State, Nigeria, homogenized and 50 kg was weighed out of which 5 kg of the crude was sampled out by cone and quartering sampling method, homogenized and prepared towards analysis.

2.2 Crude Sample Preparation

Crude sample (200 g) was randomly collected, crushed and pulverized to pass through -300+250 μm mesh size and homogenized for characterization.

Chemical Characterization by Energy Dispersive X – Ray Fluorescence Spectrometry (ED – XRFS)

The sample (20.00 g) which pass through a 250 μm mesh sieve, was dried for 1 h in an oven at 105 $^{\circ}\text{C}$ and cooled. Thereafter, the sample was intimately mixed with a binder in the ratio of 5.0 g sample to 1.0 g cellulose flakes binder and pelletized at a pressure of 10-15 tons/inch² in a pelletizing machine. At this stage, the pelletized sample was stored in a desiccator for analysis. The Energy Dispersive X – Ray Fluorescence Spectrometry (ED – XRFS) machine used to determine the various composition of element was allowed to attain the required temperature. The result of analysis was recorded in percentage (%) for minor and major concentrations of elements.

Qualitative and Quantitative Analysis by X-Ray Diffractometer (XRD)

XRD analysis was carried out on the prepared sample using a back loading preparation method. It was analyzed with a PANalytical Empyrean diffractometer with PIXcel detector and fixed slits with Fe filtered Co-K α radiation. The phases were identified using X'Pert Highscore plus software. The relative phase amounts (weight %) were evaluated using the Rietveld method.

Mineralogical Characterization by Scanning Electron Microscopy with Energy Dispersive Spectrometer (SEM-EDX)

Morphological and qualitative analyses of the bulk ore were performed using SEM-EDX. The SEM provided information on the

physical properties of minerals, while EDX provided information on their chemistry. Scanning Electron Microscopy studies for mineral analysis of representative samples were conducted in two stages using SEM model JEOL 840. All the samples were carbon coated in order to make the minerals surface conductive. Samples for analysis were cut, polished, mounts in embedded epoxy resin, and finally polished to obtain a mirror-like surface. The polished surfaces were finally carbon coated before analysis. Qualitative analyses of minerals were carried out on some mounts of the ore using (SEM/EDX) - model JEOL 840, to produce Backscattered Images (BSI).

RESULTS AND DISCUSSION

Results

Table I: Chemical Composition of Crude Sample of Itakpe Iron Ore Tailings

Sample / Assay (%)	SiO ₂	K ₂ O	CaO	V ₂ O ₅	MnO	Fe ₂ O ₃	CuO	ZnO
Crude	70.1	0.967	0.559	0.008	0.068	27.71	0.03	0.00

..

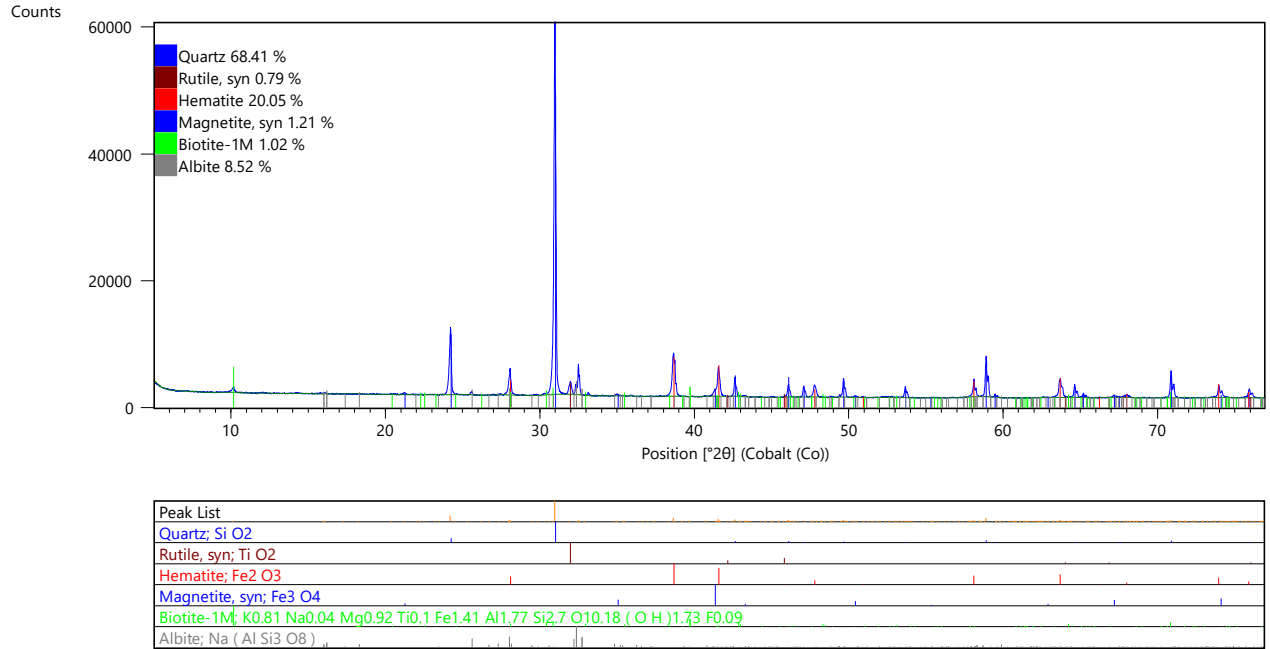
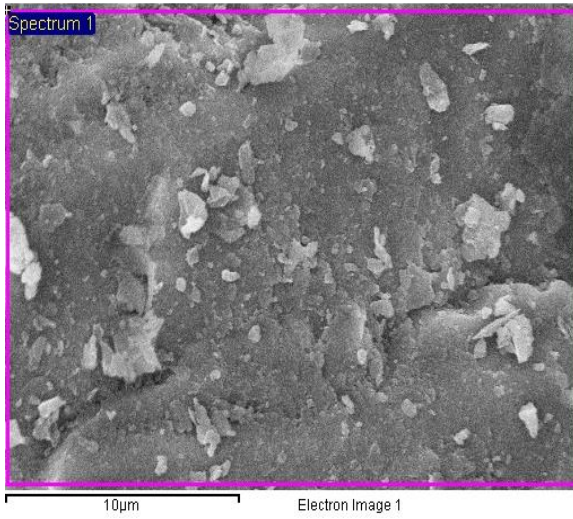
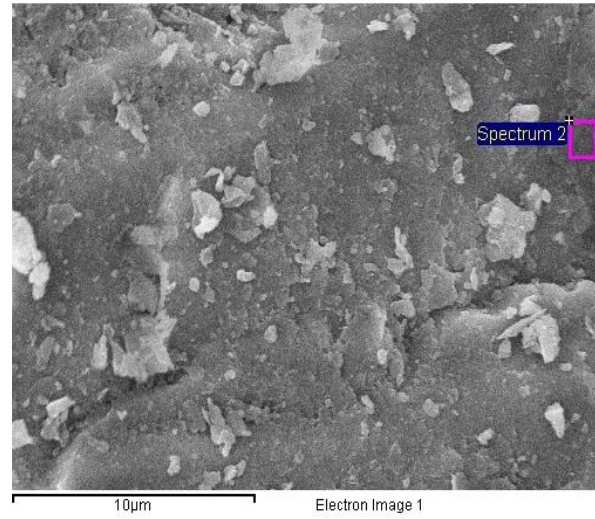


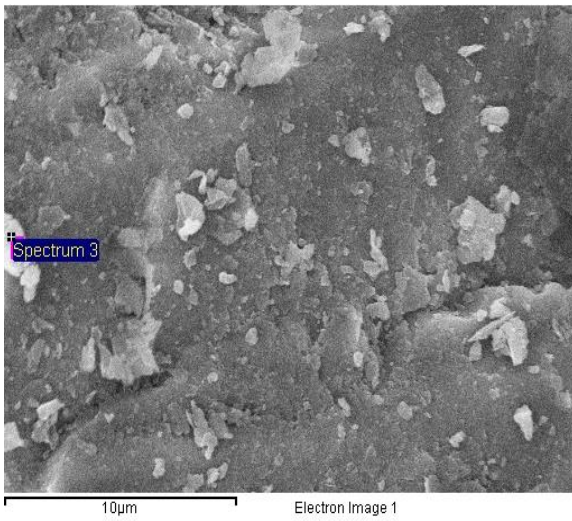
Fig. 1: XRD Pattern of Itakpe Iron Ore Dumped Tailings



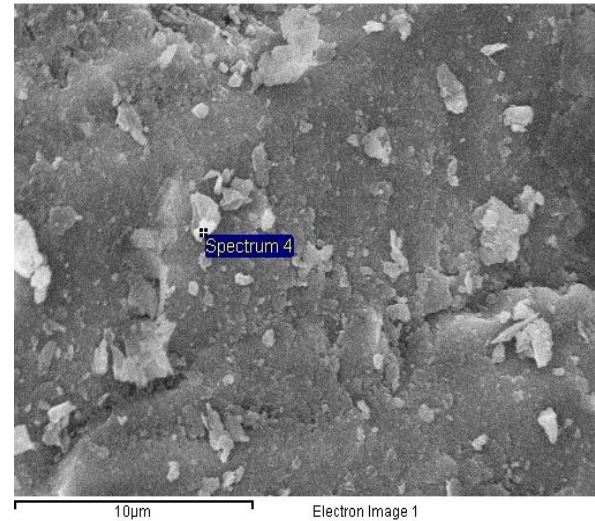
(a)



(b)

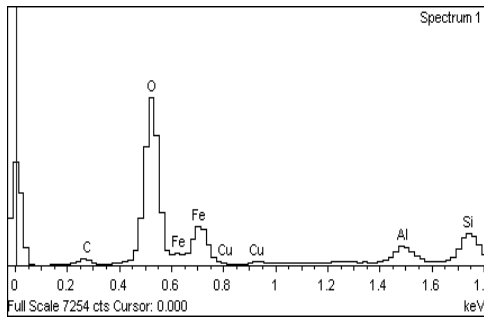


(c)



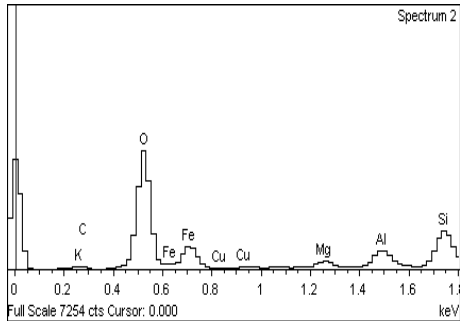
(d)

Plate 1: Scanning Electron Microscopy (SEM) Micrograph of Itakpe Iron Ore Dumped Tailings at 10 µm, showing (a) Holistic analysis, (b,c,d) Point analyses



Element	C	O	Al	Si	Fe	Cu	Total
Weight%	6.97	43.53	2.04	3.45	43.62	0.39	100
Atomic %	13.53	63.48	1.77	2.86	18.22	0.14	

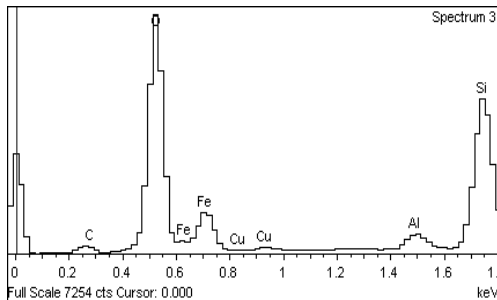
(a)



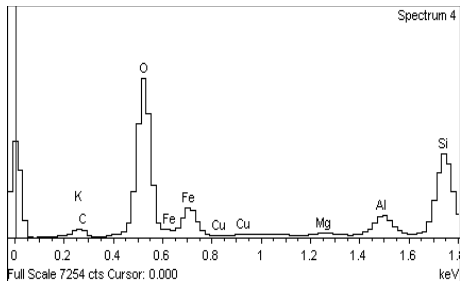
Element	C	O	Mg	Al	Si	P	K	Fe	Cu	Total
Weight%	4.1	37.36	1.4	2.68	5.0	0.8	0.33	47.8	0.2	100
	9	3			4	5		2	9	
Atomic %	8.9	59.60	1.5	2.54	4.5	0.7	0.22	21.8	0.1	
	0	0	0		8	0		5	2	

(b)

Element	C	O	Al	Si	P	Fe	Cu	Total
Weight%	7.25	56.06	1.29	11.98	1.18	21.89	0.35	100
Atomic %	12.03	69.83	0.95	8.50	0.76	7.81	0.11	



(c)



Element	C	O	Mg	Al	Si	K	Fe	Cu	Total
Weight%	7.79	49.16	0.36	2.22	9.22	0.42	30.39	0.44	100
Atomic %	13.78	65.26	0.31	1.75	6.97	0.23	11.56	0.15	

(d)

Fig. 2: Energy Dispersive X-ray Spectroscopy (EDX) peaks for the various elements present in the head sample SEM Micrograph for (a) Holistic analysis, (b,c,d) Point analyses

DISCUSSION

Chemical Characterization

Table 1 shows the chemical composition of crude Itakpe Iron Ore dumped tailings using Energy Dispersive X-ray Fluorescent Spectrometer (ED-XRFS). This reveals that the crude contains 27.71 % Fe_2O_3 , 70.1% SiO_2 and other constituent compounds in trace form, thus confirms the presence of iron in the iron ore dumped tailings. For an ore to be named an iron bearing mineral and also viable for processing, it must certify the standard requirement of 1 – 5 % iron. This report agrees with Yaro and Thomas [6].

Mineralogical Characterization by XRD

Figure 1 presents the XRD pattern and mineralogical assemblage of Itakpe iron ore dumped tailings. The diffractogram reveals the peaks of different minerals present within the ore matrix and their relative phase amount (weight %). The minerals present and their relative phase amounts are as follows: Quartz (68.41 % SiO_2), Rutile (0.79 % TiO_2), Haematite (20.05 % Fe_2O_3), Magnetite (1.21 % Fe_3O_4), Biotite-1M (1.02 %) and Albite (8.52 % ($\text{Na (AlSi}_3\text{O}_8)$)). From the diffractogram, haemitite and silica are found to be predominant in the ore matrix to other minerals. The characterization studies

therefore affirms that, quartz is the major gangue which needs to be separated from the iron bearing mineral in Itakpe iron ore dumped tailings. This beneficiation could be achieved by froth flotation [6].

Plate 1 presents the Scanning Electron Microscopy (SEM) image of the head sample at 10 μm of the homogenized Itakpe Iron Ore Dumped Tailings while Fig. 2 shows the detailed EDX analysis of crude sample. The SEM image revealed the interlocking nature of the minerals within the crystal aggregates in the ore matrix. The micrograph revealed that the minerals are separated by coarse grain boundaries that can facilitate their liberation during comminution, because the more coarse mineral particles are, the easier their liberation [5]. The elemental composition of these interlocked minerals was affirmed by EDX analysis carried out holistically and at specific regions in the ore matrix as shown in Fig. 2 (a, b, c, d). Holistic analysis of elemental composition of the ore sample revealed the presence of C, O, Al, Si, Fe, Cu, Mg, P and K; such that silicon and iron are the prominent constituents of the ore matrix while other elements exist in trace form. The carbon element identified is probably due to the carbon coating treatment of the sample prior to analysis in order to make the mineral surface conductive [7]. The result obtained further complements the analyses done on the sample using XRD and XRF, and also indicates that the ore contained the mineral of interest (iron oxide) and other associated

..

minerals that can hinder the utilization of the ore unless the impurities are drastically reduced or removed.

CONCLUSION

In conclusion, chemical characterization of Itakpe Iron Ore Dumped tailings assayed 27.71 % Fe_2O_3 , 70.1 % SiO_2 and other constituent compounds in trace form, thus confirming the presence of iron in the iron dumped tailings. SEM image reveals the interlocking nature of these minerals within the crystal aggregates of the ore matrix and the EDX analysis at different regions revealed the presence of C, Ti, Al, Mn, Cu, and O within the mineral matrix; such that iron, titanium, and silicon are the major

elemental constituents of the matrix. Finally, the characteristic coarsely packed nature of the minerals present in the ore matrix will foster easier liberation of the iron ore from the gangue by comminution.

On the premise of these findings, keen interest should be directed towards exploitation of Itakpe Iron Ore dumped tailings through any selected beneficiation techniques so as to judiciously re-separate the valuable mineral from the tailings and also re-extract iron from the concentrate product.

REFERENCES

1. NIOMC Project Report (1980) Vol. 2, pp. 1 – 10.
2. Adepoju, S. O. and Olaleye, B. M., (2001) Gravity concentration of silica sand from Itakpe iron. Retrieved 12/13/2017, 12:16 pm.
3. Alabi, O.O. (2016), Beneficiation of Ajabanoko Iron Ore Deposit, Kogi State, Nigeria using Magnetic Methods. International Journal of Civil, Mechanical and Science, Vol 2, Issue 2, 91-93
4. Chunk K. Obasi (1998), Mineralogical Characteristics and Genetic Significance of Hematite in Ore Tailings by Tabling Operation. Nigerian Journal of Engineering Management. Vol. 2, No. 2, 51-55.
5. Wills, B.A. (2006) Mineral Processing Techniques: An Introduction to the Practical Aspect of Ore Treatment and Mineral Recovery. 7th Edition, Elsevier Science & Technology Books, Amsterdam, pp. 225.
6. Yaro, S.A. and Thomas, D.G. (2009) Chemical Mineralogical Characteristics of Kotonkarfe Iron Ore. Journal of Engineering and Technology (JET), Bawero University, Kano, 4 (1), pp. 65-71.
7. Ogundeji F.O., Alabi O.O. and Ajakaiye A. (2018) Determination of Chemical, Mineralogical Composition and Liberation Size of Mandaka

..

Manganese Ore, Niger State, Nigeria.
Journal of Advance Research in

Manufacturing, Material Science and
Metallurgical Engineering; 5 (3): 1 – 5.

**EVALUATION OF *DETARIUM MICROCARPUM* AND *BRACHYSTEGIA EURYCOMA* AS VISCOSIFIER
IN POTASSIUM CHLORIDE – POLYMER DRILLING MUD**

Oboh I. O., Okon A. N.,* and Nseh B. U.

Department of Chemical & Petroleum Engineering,
University of Uyo, Uyo-AKS, Nigeria.

Corresponding author;; email: anietieokon@uniuyo.edu.ng. Phone: 07017067407

ABSTRACT

Drilling through trouble zones, like; high pressure zone, shaly formation, thief zone, among others requires special formulated drilling muds. One of such drilling muds is KCl-Polymer mud to inhibit shaly formation; as water-based mud interactions with the formation leads to pipe sticking. Formulating this KCl-Polymer mud requires enhanced polymers as viscosifiers to achieve some of its basic drilling fluid functions. Regrettably, these polymers are imported and the total dependence on these polymers is worrisome as it results in a high overall well drilling cost in Nigeria. Therefore, this study evaluates the use of *Detarium microcarpum* and *Brachystegia eurycoma* seeds as viscosifiers in the KCl-Polymer mud and results compared with Polyanionic cellulose (PAC R) content for the same mud. The results obtained depict that the *Detarium microcarpum* (*Ofor*) at 2 g content compared favourably with 1g content of PAC R as viscosifier in the KCl-Polymer mud. Also, *Brachystegia eurycoma* (*Achi*) at 5 g content compared with 1 g content of PAC R in the mud. Additionally, at 150 °F, the 5 g content *Brachystegia eurycoma* (*Achi*) had negligible gel strength unlike its *Detarium microcarpum* (*Ofor*) counterpart which had flat gel characteristic even at high temperature. Furthermore, the results depict that the KCl-Polymer mud's yield point (YP) was drastically reduced at low *Detarium microcarpum* and *Brachystegia eurycoma* contents in the mud. Therefore, the viscosifying potential of the *Detarium microcarpum* (*Ofor*) in KCl-Polymer mud for drilling through trouble formations can be exploited; as it seems promising. This development will reduce: over dependence and importation of foreign polymers, total drilling cost and boost the Nigerian economy.

Keywords: *Detarium microcarpum*; *Brachystegia eurycoma*; Viscosifiers; KCl-Polymer; Drilling mud.

INTRODUCTION

Drilling fluids are used in the oil and gas industry for the drilling of boreholes and construction of oil wells [1]. They are heterogeneous mixtures of clay, water and other additives that aid the drilling operations. Thus, they are sometimes seen as the circulating blood of the drilling operation. Depending on the continuous phase, drilling fluid is classified either as water-based mud (WBM) or oil-based mud (OBM). Although a new class has been introduced known as synthetic-based drilling mud (SBM) because of the environmental challenge of the oil-based muds (OBMs) [2]. It is now a well-established fact that the success of a drilling operation relies to a large extent on the physical/rheological properties of the drilling fluid used for lubricating drill bits [3]. Therefore, the importance of drilling fluid otherwise known as 'drilling mud' cannot be over emphasized as the knowledge of drilling fluid is a requisite in the rotary drilling operation in the petroleum industry [4]. Tailoring drilling fluid is an important key to the success of a drilling operation. Failure to do so can result in costly problems, impediment on the equipment longevity and performance, and can ultimately jeopardize overall well objective [5]. The composition of drilling fluid depends on the requirements of the particular drilling operations [6]. During drilling, the deposit of solids in the form of a cake contributes to the borehole stability and limits the invasion of the permeable

zone by the liquid phase and reduces the formation damage [7]. Thus, this characteristic of the drilling mud to perform deposition of solids to form cake is controlled by its viscosity which is enhanced by viscosifier (additive) such as polymers, starch, etc. As such, different types of polymers and chemicals are used by the petroleum industry to design some drilling muds to meet some functional requirements such as appropriate mud rheology, density, fluid loss control property, etc. [8].

The use of conventional water-based muds (WBMs) in drilling sensitive (shale) formations results in the adsorption of water associated with the drilling mud onto the surface of shale [9]. Depending on the shale type, this occurrence may lead to various reactions like swelling, cutting dispersion and increase in pore pressure [10], during drilling operations. The increase in formation pore pressure in turn creates wellbore instability of varying degree as the drilling operation progresses. Therefore, to overcome this formation sensitive challenge with conventional WBMs, Potassium Chloride (KCl)-Polymer based muds are used to inhibit or limit chemical interaction of shale formations. William [11] maintained that the KCl/Polymer mud is suitable for drilling potential productive sands. In addition, Sadiq [12] opined that KCl/Polymer mud advantages include: higher shear thinning, high true yield strength, improved borehole stability, good bit hydraulic and reduced circulating pressure losses. So far,

..

companies involved in design and production of drilling fluid in Nigeria for the oil and gas sector have over the years imported the materials to produce mud or in some cases imported already designed and produced drilling mud [13]. This has been a major challenge to the indigenous companies involved in the oil and gas as they have to import these materials at high costs. In this regard, the indigenous companies find it difficult to compete favourably with their foreign counterparts. Thus, with the emergence of local content in the oil and gas industry by the Federal government under the auspices of Nigerian National Petroleum Corporation (NNPC) there is need to find local drilling mud materials that can substitute the foreign ones. Such local raw materials of interest in recent studies are *Detarium microcarpum* and *Brachystegia eurycoma* seeds popularly known as *Ofor* and *Achi* respectively. Interestingly, some studies in the literature by Uhegbu *et al.* [14], Mariod *et al.* [15], Aviara *et al.* [16], among others have provided the



Plate 1a: *Detarium microcarpum* (Ofor)

physicochemical properties of these seeds. Therefore, this study evaluates the use of local seeds: *Detarium microcarpum* and *Brachystegia eurycoma* as viscosifier in KCl-Polymer based drilling mud.

MATERIALS AND METHODS

Seeds Preparation

The *Detarium microcarpum* and *Brachystegia eurycoma* seeds (as depicted in Plates 1a and 1b respectively) were obtained from local market in Uyo, Akwa Ibom State, Nigeria. The seeds were sorted to remove unviable ones and then washed to remove debris, roasted for 10 - 15 min and soaked immediately in distilled water for 1 h. The cotyledons were extracted from the seeds and soaked overnight in distilled water. Thereafter, the water was decanted and the cotyledons were sun-dried for four (4) days. Finally, the cotyledons were ground and sieved to 125 μm to obtain fine powder. The powders were stored in air-tight containers to avoid contamination.



Plate 1b: *Brachystegia eurycoma* (Achi)

Mud Formulation

According to William [11], the basic components of KCl-Polymer mud are: fresh water or sea water, KCl, inhibiting polymer, viscosity building polymer, stabilized starch, caustic soda and lubricants. Table 1 presents the basic compositions of the base KCl-Polymer mud used for this study. After weighing the various additives as indicated in Table I, 350 mL of fresh water was filled in the mud cup and place under the Hamilton Beach Standard mixer. The various components (additives) were added to the fresh water to formulate the KCl-Polymer mud based on the indicated mixing order presented in Table I. Also, the base *Ofor* and *Achi* muds (i.e. without addition of PAC R) were formulated based on the components indicated in Table II. These formulated KCl-Polymer muds were allowed to age for 24 h

before testing for their various mud properties. The determined mud properties were pH and rheological properties: apparent viscosity, plastic viscosity, yield point and gel strength based on the API Specification 13B [17] recommended practice for field testing water-based drilling fluids. The obtained mud properties are presented in Table III. On the other hand, three mud samples with different local seeds content of 2 g, 3 g and 5 g were prepared to evaluate their potential in KCl-Polymer mud rheological properties. In addition, the KCl-Polymer mud samples were hot rolled at 150 °F for 16 h to assess their performance at high temperature. Thus, the base KCl-Polymer mud and the formulated *Ofor* and *Achi* muds with 3 g and 5 g contents were used for the hot roll evaluation.

Table I: Base Mud Compositions

Mud components	Content	Mixing order	Mixing during (min)
Fresh water, (mL)	350	1	--
Barite, (g)	10	2	5
Soda ash, (g)	0.25	3	2
Caustic soda, (g)	0.25	4	2
Potassium Chloride, (g)	25	5	5
PAC R, (g)	1.0	6	5
PAC L, (g)	1.0	7	2
Biocide, (mL)	0.5	8	2

Table II: Base Compositions for *Ofor* and *Achi* Mud

Mud components	Ofor Mud	Achi Mud	Mixing Time (min)
Fresh water, (mL)	350	350	--
Barite, (g)	10	10	5
Soda ash, (g)	0.25	0.25	2
Caustic soda, (g)	0.25	0.25	2
Potassium Chloride, (g)	25	25	5
Ofor, (g)	1.0	--	5
Achi, (g)	--	1.0	5
PAC L, (g)	1.0	1.0	2
Biocide, (mL)	0.5	0.5	2

Mud Properties Determination

The mud pH and rheological properties were determined as described from previous studies [18,19,20].

RESULTS AND DISCUSSION

A comparison of *Detarium microcarpum* and *Brachystegia eurycoma* seeds as viscosifiers in KCl-Polymer mud otherwise referred to as *Ofor* and *Achi* muds respectively in this study with PAC R was presented in Table III. The obtained mud rheological properties: apparent viscosity, plastic viscosity and yield point from the local seeds (i.e., *Ofor* and *Achi*) muds were less than the base KCl-Polymer mud with PAC R at the same 1 g content. This observation was attributed to the fact that PAC R is a modified polymer enhanced for the purpose of mud viscosifying as additive. Interestingly, the both local seeds muds have the same 10 sec and 10 mins gel strength with the base KCl-Polymer mud. Additionally, the obtained gel

strength values of the base KCl-Polymer and the local seed muds indicated that they all have flat gel strengths; as the obtained 10 seconds and 10 min gel strengths were the same values. This implied that the *Ofor* and *Achi* muds' gel strengths would remain constant during non-circulating time, which is a good requirement for drilling operations. It meant that these muds will not become thick during tripping out of hole; as thick mud will require high pump power to initiate mud circulation when drilling operation commences again. On the other hand, Fig. 1 depicted the rheogram (i.e., shear stress - shear rate profile) of the KCl-Polymer muds, namely: base, *Ofor* and *Achi* muds. Fig. 1 indicated that the base mud which contained PAC R had higher rheological values than the *Ofor* and *Achi* muds. This resulted in the high shear stress - shear rate profile of the base mud than the locally formulated muds.

Table III: Mud Properties for the Base KCl-Polymer Muds

..

Mud Properties	Base Mud	<i>Ofor</i> Mud	<i>Achi</i> Mud
pH Value	11.0	11.0	11.0
Apparent Viscosity, (cP)	16.5	10.5	9.0
Plastic Viscosity, (cP)	14.0	9.0	7.0
Yield Point, (Pa)	4.31	1.44	1.92
Gel Strength, (Pa):	0.48/0.48	0.48/0.48	0.48/0.48

Table IV presents the results for the various mud properties obtained at different seed contents of *Ofor* and *Achi* in the KCl-Polymer mud. The comparisons of the results with the base mud showed that increase in the local seed contents in the KCl-Polymer mud improved their mud rheology. This development meant that the local seeds would require more contents in the mud to perform like the PAC R studied. As observed in the Table 4, the *Ofor* mud properties at 2 g content were comparable with the base mud's properties. Whilst *Achi* mud at 2 g content; even at 3 g, were less comparable with the base mud. These observations were further depicted in the rheogram; as presented in Fig. 2 and 3. As observed in Figs. 2 and 3, at 2 g content, the *Ofor* mud's shear

stress - shear rate profile was close to the base mud's profile than the *Achi* mud's profile. For the 3 g content, the *Ofor* mud's profile was higher than the base mud. This indicated that the increased *Ofor* content improved its viscosifying potential in the KCl-Polymer mud. As stated earlier, the *Achi* mud's profile at 3 g content was less than the base mud's profile. Nevertheless, at 5 g content, the *Ofor* and *Achi* muds' rheological properties were higher than the based mud. The *Ofor* mud's properties were far higher, but *Achi* mud's properties were slightly higher than the base mud in Table IV and Fig. 5. This indicates that more content of *Achi* was required in the KCl-Polymer mud to enhance its viscosifying potential in order to be compared with that of PAC R.

Table IV: Mud Properties of the increased *Ofor* and *Achi* content

Mud Properties	Base Mud	<i>Ofor</i> Mud			<i>Achi</i> Mud		
Content	--	2 g	3 g	5 g	2 g	3 g	5 g
Apparent Viscosity, (cP)	16.5	16.5	38.5	47.0	12.5	14	24.5
Plastic Viscosity, (cP)	14.0	13.0	26.0	30.0	11.0	10.0	19.0

..

Yield Point, (Pa)	4.31	3.35	11.97	16.28	1.44	3.83	5.27
Gel Strength, (Pa):	0.48/0.48	0.48/0.48	0.48/0.96	0.96/1.44	0.48/0.48	0.48/0.96	0.48/0.48

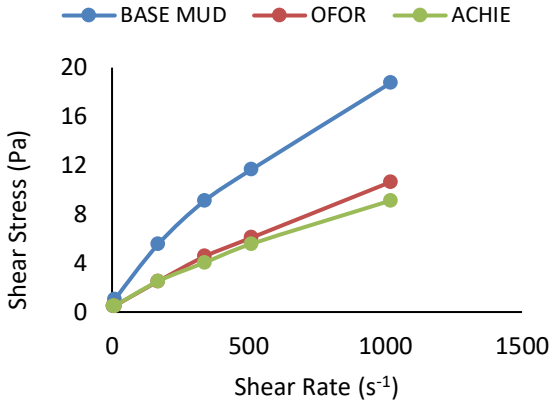


Fig. 2: Comparison of Base Muds

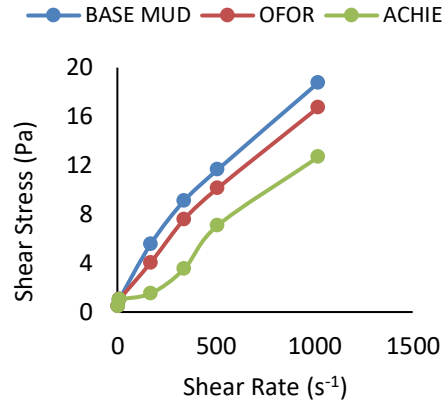


Fig. 3: 2 g *Ofor* and *Achi* Muds vs. Base Mud

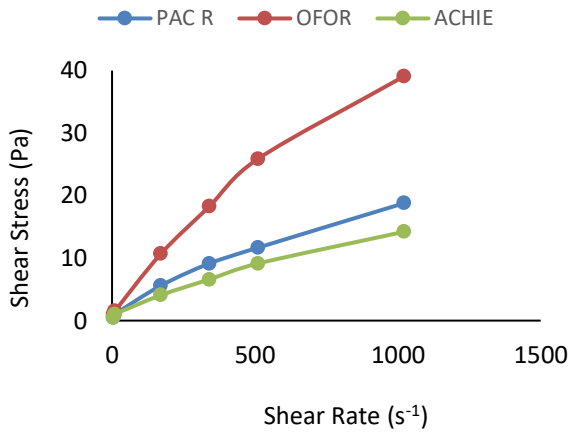


Fig. 4: 3 g *Ofor* and *Achi* Muds vs. Base Mud

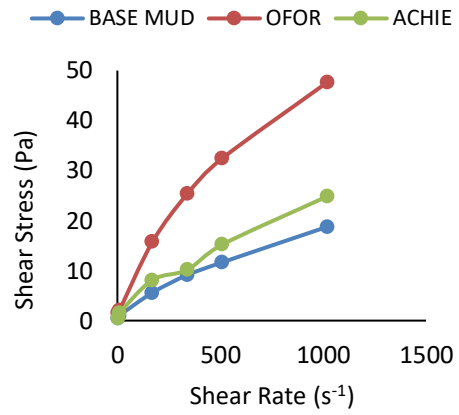


Fig. 5: 5 g *Ofor* and *Achi* Muds vs. Base Mud

..

On the other hand, Table 5 and Figs. 6 and 7 present the results after the base mud and 3 g and 5 g content of the local seed muds were hot rolled at 150 °F for 16 h. Comparison of the muds' properties: apparent viscosity, plastic viscosity and yield point, indicate that *Ofor* muds have higher properties than the base and *Achi* muds. These high mud properties in turn resulted to the high shear stress - shear rate profile (Figs. 6 and 7) obtained for *Ofor* mud when compared to the base and *Achi* muds. Additionally, at 5 g content, the *Achi* mud has the same mud properties and shear stress - shear rate profile with the base mud; as observed in Table 5 and Fig. 7 respectively. Furthermore, the obtained 10 seconds and 10 min gel strengths for the based and *Ofor* mud at 3 g and 5 g content

were the same (Table 5). However, the *Achi* muds have negligible 10 sec and 10 min gel strengths after the hot rolling test. This indicated that high temperature would seriously affect the solid holding potential of the *Achi* mud during non-circulation period. In addition, comparisons of the muds' properties before and after hot rolling as presented in Table 6 showed the percentage decrease in the various KCl-Polymer muds' properties. The results (Table 6) indicated that the muds' yield point was the most affected mud property at high temperature. However, when the content of the local seeds were increased in the KCl-Polymer mud, the percentage decrease of the mud yield point was reduced; as it was in the case for the 5 g content *Ofor* and *Achi* muds.

Table V: The KCl-Polymer Muds' Properties after Hot Rolling at 150 °F

Mud Properties	Base Mud	<i>Ofor</i> Mud		<i>Achi</i> Mud	
		3 g	5 g	3 g	5 g
Content	--	3 g	5 g	3 g	5 g
Apparent Viscosity, (cP)	10.0	16.5	24.0	4.0	10.0
Plastic Viscosity, (cP)	8.0	14.0	17.0	3.0	8.0
Yield Point, (Pa)	1.92	2.39	6.70	0.96	1.92
Gel Strength, (Pa)	0.48/0.48	0.48/0.48	0.48/0.48	--	--

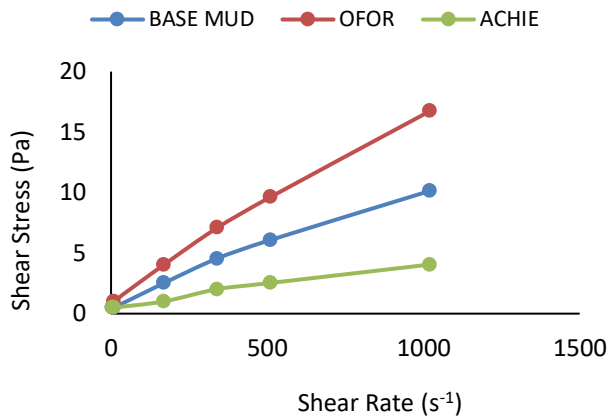


Fig. 6: 3 g *Ofor* and *Achi* Muds vs. Base Mud after hot rolling

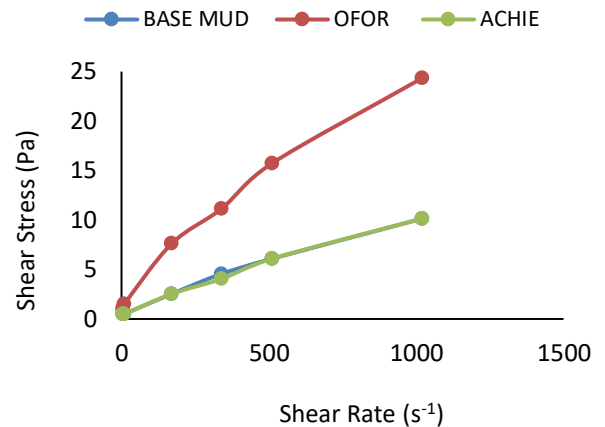


Fig. 7: 5 g *Ofor* and *Achi* Muds vs. Base Mud after hot rolling

Table VI: Percentage Decrease in the KCl-Polymer Muds' Properties after Hot Rolling

Mud Properties	Base Mud	<i>Ofor</i> Mud		<i>Achi</i> Mud	
Content	--	3 g	5 g	3 g	5 g
Apparent Viscosity, (%)	39.39	57.14	48.94	71.43	59.18
Plastic Viscosity, (%)	42.86	46.15	43.33	70.00	57.90
Yield Point, (%)	55.56	80.00	58.82	75.00	63.64

CONCLUSION

The viscosifying potentials of any drilling mud additives are basically to improve the mud's rheological properties and in some cases modify the mud filtration loss characteristic. In the Petroleum industry, these viscosifiers are enhanced polymers that have been for decades for both water-based and oil-based muds. Regrettably, most of them are imported which involves foreign exchange and other contingencies, that will in turn impact on the overall drilling cost. Therefore, there is need to substitute the foreign additives with the locally available material(s). Thus, the study

confirms that KCl-Polymer based mud, 2 g of *Ofor* content compare favourably with 1 g of PAC R (Polyanionic Cellulose), whilst *Achi* required 5 g to compare with that same PAC R content in the mud. Also, the local seeds (i.e., *Ofor* and *Achi*) in KCl-Polymer mud have a flat gel strength characteristic but at high temperature *Achi* solid holding potential (gel strength) becomes negligible. Furthermore, with low local seeds content, the KCl-Polymer mud yield point reduced drastically at high temperature while the performance of *Ofor* content in the KCl-Polymer mud as viscosifier was higher than *Achi*.

..

Further studies should be undertaken to determine the optimum content of these local seeds that would compare favourably to PAC R in drilling mud.

REFERENCES

- [1]. Udoh, F. D., Itah, J. J. and Okon, A. N. (2012). Formulation of Synthetic-Based Drilling Fluid Using Palm Oil Derived Ester. *Asian Journal of Microbiology, Biotechnology and Environmental Science*, Vol. 14, No. 2, pp. 175-180.
- [2]. Agwu, O. E., Okon, A. N. and Udoh, F. D. (2015). A Comparative Study of Diesel Oil and Soybean Oil as Oil-Based Drilling Mud. *Journal of Petroleum Engineering*, Vol. 2015, Article ID 828451, 10 pages.
- [3]. Okon, A. N. (2010). Formulation of Water-Based Drilling Fluid Using Local Clay. Unpublished B. Eng. Project submitted to the Department of Chemical and Petroleum Engineering, University of Uyo, Akwa Ibom State, Nigeria.
- [4]. Udoh, F. D. and Okon, A. N. (2012). Formulation of Water-Based Drilling Fluid Using Local Materials. *Asian Journal of Microbiology, Biotechnology and Environmental Science*, Vol. 14, No. 2, pp. 167-174.
- [5]. Rabia, H. (2000). *Well Engineering and Construction*. London: Graham and Trotman Ltd.
- [6]. Taiwo, A., Joel, O. F. and Kazeem, A. A. (2011). Investigation of Local Polymer (Cassava Starches) as a Substitute for Imported Sample in Viscosity and Fluid Loss Control of Water-Based Drilling Mud. *ARJN Journal of Engineering and Applied Sciences*, Vol. 6, No. 12, pp. 43-48.
- [7]. Peng, S. J. (1990). Filtration Properties of Water Based Drilling Fluid. Unpublished PhD Thesis submitted to Heriot-Watt University, Edinburgh, United Kingdom. p. 28.
- [8]. Amanuallh, M. D., Marsden, J. R. and Shaw, H. F. (1997). An Experimental Study of the Swelling Behavior of Mud Rocks in the Presence of Drilling Mud System. *Canadian Journal of Petroleum Technology*, Vol. 36, No. 3, pp. 45-50.
- [9]. Joel, O. F., Durueke, U. J. and Nwokoye, C. U. (2012). Effect of KCl on Rheological Properties of Shale Contaminated Water-Based Mud. *Global Journal of Researches in Engineering*, Vol. 12, No. 1, pp. 11-17.
- [10]. Chenevert, M. E. and Pernot, V. (1998). Control of Shale Swelling

Pressures using Inhibitive Water Based Muds. Paper presented at the Society of Petroleum Engineers Annual Technical Conference and Exhibition, New Orleans, 27-30 September.

[11]. William, C. L. (2009). *Working Guide to Drilling Equipment and Operations*. Gulf Professional Publishing, Oxford, United Kingdom.

[12]. Sadiq, H. M. (2017). Investigating the Corrosivity of KCl/Polymer Drilling Mud on Downhole Material. *IOSR Journal of Applied Geology and Geophysics*, Vol. 5, No. 3, pp. 44-49.

[13]. Olatunde, A. O., Usman, M. A., Olafadehan, O. A., Adeosun, T. A. and Ufot, O. E. (2012). Improvement of Rheological Properties of Drilling Fluid Using Locally Based Materials. *Journal of Petroleum and Coal*, Vol. 54, No. 1, pp. 65-75.

[14]. Uhegbu, F. O., Onwuchekwu, C. C., Iwela, E. E. J. and Kanu, J. (2009). Effect of Processing Methods on Nutritive and Antinutritive Properties of Seeds of *Brachystegia eurycoma* and *Detarium microcarpum* from Nigeria. *Pakistan Journal of Nutrition*, Vol. 8, No. 4, pp. 316-320.

[15]. Mariod, A. A., Mirghani, M. E. S., Abdul, A. B. and Abdelwahab, S. I. (2009). *Detarium microcarpum* Guill and Perr Fruit Proximate Chemical Analysis and Sensory Characteristics of Concentrated Juice and Jam. *African Journal of Biotechnology*, Vol. 8, No. 17, pp. 4217-4221.

[16]. Aviara, N. A., Onaji, M. E. and Lawal, A. A. (2015). Moisture-dependent Physical Properties of *Detarium microcarpum* Seeds. *Journal of Biosystems Engineering*, Vol. 40, No. 3, pp. 213-223.

[17]. Mahto, V. and Sharma, V. P. (2004). Rheological Study of a Water-Based Oil Well Drilling Fluid. *Journal of Petroleum Science and Engineering*. Vol.45, pp.19-26.

[18]. Okon, A. N., Udoh, F. D. and Bassey, P. G. (2014). Evaluation of Rice Husk as Fluid Loss Control Additive in Water-Based Drilling Mud. Paper presented at the Society of Petroleum Engineers Annual International Conference and Exhibition held in Lagos, Nigeria, 5-7 August.

[19]. Omole, O., Adeleye, J. O., Falode, O., Malomo, S. and Oyedeji, O. A. (2013). Investigation into the Rheological

..

and Filtration Properties of Drilling Mud Formulated with Clays from Northern Nigeria. *Journal of Petroleum and Gas Engineering*, Vol. 4, No. 1, pp. 1-13.

%20Bentonite%20LSGTC%20pres%2013a%20sec%20. Accessed: 12th August, 2017.

- [20]. API 13B Section 9 Bentonite.
www.lonestarbarite.com/specs/API

FORMULATION

*Alabi F. M.¹, Lajide L.¹, Ayodele O.² and Idoko O.³

1. Department of Chemistry, Federal University of Technology, P. M. B. 704 Akure, Ondo State, Nigeria
2. Department of Industrial Chemistry, Ekiti State University, P. M. B. 5363, Ado-Ekiti, Nigeria
3. Chemistry Advance Centre, Sheda Science and Technology Complex, P. M. B. 186 Garki, Abuja, Nigeria

*Corresponding author: alabifortune72@gmail.com

ABSTRACT

There is a growing need for local sourcing of alternative raw materials from agricultural sources to replace synthetic ones obtained from the petrochemical industry because of environmental concerns coupled with the high cost of importation of these raw materials. In this study, the physicochemical properties of extracted Cashew Nut Shell Liquid (CNSL) as a defoamer was studied in comparison with polydimethylsiloxane (PDMS), a synthetic defoamer and Linseed oil, a non-synthetic one. The cashew nut shells were extracted by soxhlet apparatus using hexane as the extracting solvent, and analyzed using standard methods. The results show relatively comparative properties in the extracted CNSL and PDMS and Linseed oil. The refractive index was 1.53 compared to 1.4 and 1.47 of PDMS and Linseed oil; viscosity of 38.5 mPa.s which falls within the acceptable range of PDMS for industrial application; specific gravity of 0.99 g/cm³ to 1.04 g/cm³ and 0.93 g/cm³ of PDMS and Linseed oil, respectively. The saponification and Iodine values for linseed oil were 188 mgKOH/g and 170 Wijs while 105.85 MgKOH/g and 121 Wijs were reported for the extracted CNSL. The GC-MS analysis identified six (6) different compounds in the mass spectrum consisting of mono-unsaturated, di-unsaturated, saturated cardanol and saturated cardol. These compounds could be responsible for its comparative properties with PDMS and Linseed oil as alternative defoamer.

Keywords: Cashew nut shell liquid, defoamer, polydimethylsiloxane, paint formulation

INTRODUCTION

The concern with the paint industry in Nigeria is the local sourcing of raw materials

for production as over 70 % of the raw materials need of the industry is imported [1]. This is as a result of the non-completion

of the second phase of the petrochemical plants which is expected to supply most of the chemical raw materials. Therefore the search for alternative raw materials from available local sources and the development of less polluting raw material are some measures necessary to address the challenge of raw materials for the paint industry in the Country.

The cashew tree is indigenous to Brazil but is now widely cultivated as an economic crop in terms of food source, income, industrial raw materials and foreign exchange, across the tropics especially in Africa and Asia [2]. Major cashew producing countries in these regions are India, Srilanka, Thailand, Malaysia, Indonesia, Tanzania, Kenya, Madagascar, Senegal, Malawi, Angola and Nigeria [3]. In Nigeria cashew production is mainly concentrated in 27 States with increased production from 30,000 MT in 1990 to 836,500 MT in 2012 [4]. Cashew nut shell liquid (CNSL) is a by-product of the cashew processing industry. The cashew nut liquid is extracted from the cashew nut's shell and represents approximately 25 % of the cashews weight and 30-35 % of the nut shells weight [2]. It is a cheap and renewable raw material with many industrial applications in polymer-based industries, synthesis of chemicals and intermediates including bactericides, insecticides and surface active agents [5]. CNSL industrial versatility is as a result of the phenolic constituents such as anacardic acid, cardanol and cardol that easily react forming various

derivatives including polymers and resins [6]. In industry, CNSL polymers and resins are widely employed as friction materials, surface coating, adhesives, laminates, rubber compounding, flame retardants, and anticorrosive paints [7]. They are also recently studied as rubber plasticizers [8] and antioxidant [9], in polyurethanes synthesis [10], in the cure of epoxy resin [11], and in well-known phenol formaldehyde resin [12].

Its common use in the coating industry is in the form of alkyd and epoxy resins in oil based paint formulation as binder and a curing agent to give a wide range of properties.

In the production and application of paint system, foam formation is an undesired side effect that arises. The resultant effect is an increase in production time, difficulty in filling paint vessels with the correct quantity of paint and surface defects such as craters and weak points in dried film [13]. For this reason, defoaming agents such as mineral and silicone oils, are added to prevent these problems. The most commonly used defoaming agent in the paint industry is Polydimethyl Siloxane, a mineral-organic polymer of the siloxane family. This study therefore reports the evaluation of cashew nut shell liquid (CNSL) as a potential natural defoamer in the formulation of paints.

MATERIALS AND METHOD

Materials

..

Cashew (*Anacardium occidentale* Linn) nuts (procured from local cashew traders along the Abuja-Keffi Road, Nigeria), laboratory mortar and pestle, Soxhlet extractor, Abbe Refractometer, NDJ 5S type of viscometer, Finnigan GC 8000 series interfaced with a Voyager Electron Impact-Mass Selective Detector on RTX-5MS column, pH meter (Hanna Instruments Model 211 Microprocessor), reflux condenser, water bath. All reagents used for this analysis are of analytical grade.

Methods

Extraction of Cashew Nut Shell Liquid (CNSL)

The cashew nut was sundried for 14 days, washed and bi-sectioned with manual cashew cracker to separate the nut shell from the kernel. The cashew nut shells were ground using a laboratory mortar and pestle. The extraction was conducted using Soxhlet apparatus and n-hexane as the extracting solvent. The extraction was done for 8 h and the extracted CNSL was stored in a laboratory sample bottle prior to analysis.

Determination of Refractive index

Measurement of the refractive index of the sample was done by means of Abbe Refractometer at 30.6 °C using the method of AOAC (2000).

Determination of Viscosity

The viscosity measurement was carried out at 30 °C by means of NDJ 5S type of viscometer. Rotor 1 was used at the speed of

60 rpm for the determination of viscosity of the CNSL samples.

Determination of pH

Measurement of pH was done using pH meter (Hanna Instruments Model 211 Microprocessor). The pH meter was calibrated using buffer 7 and readings were obtained by inserting the probe of the pH meter into CNSL.

Gas Chromatography - Mass Spectrometer

Gas Chromatography - Mass Spectrometer (GC - MS) analysis was carried out using a Finnigan GC 8000 series, interfaced with a Voyager Electron Impact-Mass Selective Detector, on RTX-5MS column. Sample (1 mg) was dissolved in 10 mL of dichloromethane and 1 µL of this solution was injected into the GC - MS. The temperature was programmed from 50 to 250 °C at 10 °C/ min and maintained at 250 °C for 30 min.

Determination of Specific Gravity

The specific gravity was determined according to AOAC (2000) using pycnometer bottle.

Determination of Acid Value, Saponification value, Iodine value and Free Fatty Acid

The Acid, Saponification, Iodine and Free Fatty Acid values were obtained the method of IPAN (2003).

RESULTS AND DISCUSSION

The results of the physicochemical properties of the extracted CNSL are presented in Table I. The appearance of the final extract was dark brown and can be termed industrial grade similar to reports in literature [3, 14, 7, 15]. The percentage yield of the sample was 64.07 %, the sample was viscous in nature and the refractive index

was 1.53 which indicated that the oil is a little bit thicker when compared with most non-drying oils [16, 17]. The value of the refractive index also compared favourably with polydimethylsiloxane (1.4), a commonly used inorganic defoamer [18] and linseed oil (1.47) which is being used as an organic defoaming agent in paint formulation [19].

Table I: Physicochemical properties of extracted CNSL

Parameter	CNSL
% Yield	64.07
Appearance	Dark brown liquid
Nature	Viscous
Refractive index	1.53
Viscosity at 27 °C (mPa.s)	38.5
Specific gravity (g/cm ³)	0.99
pH	4.29
Saponification value (MgKOH/g)	105.85
Iodine value (Wijs)	121.93
Acid value (MgKOH/g)	124.85
Free fatty Acid (MgKOH/g)	60.92

The viscosity of polydimethylsiloxane (PDMS) ranged from 15-50,000 Centistoke depending on its end use, and the viscosity of the extracted CNSL (38.5 mPa.s) falls within the range of PDMS industrial applications [20]. The specific gravity (0.99 g/cm³) compared favourably with linseed oil (0.93 g/cm³), an organic defoamer; and polydimethylsiloxane (1.04 g/cm³), an inorganic defoamer used in paint formulation [21]. The saponification and iodine values for linseed oil were reported to

be 188 mgKOH/g and 170 Wijs while 105.85 MgKOH/g and 121 Wijs were reported for the extracted CNSL [19, 3, 15]. The pH (4.29) reported in this work confirms the presence of anacardic acid in CNSL which gives the liquid its anti-microbial properties [22].

Figure 1 shows the main lines (1-15) as observed from the GC-MS analysis of the CNSL. Six different compounds (Hit 1-6) were detected in the mass spectrum of each of the lines as presented in Figs 2-16

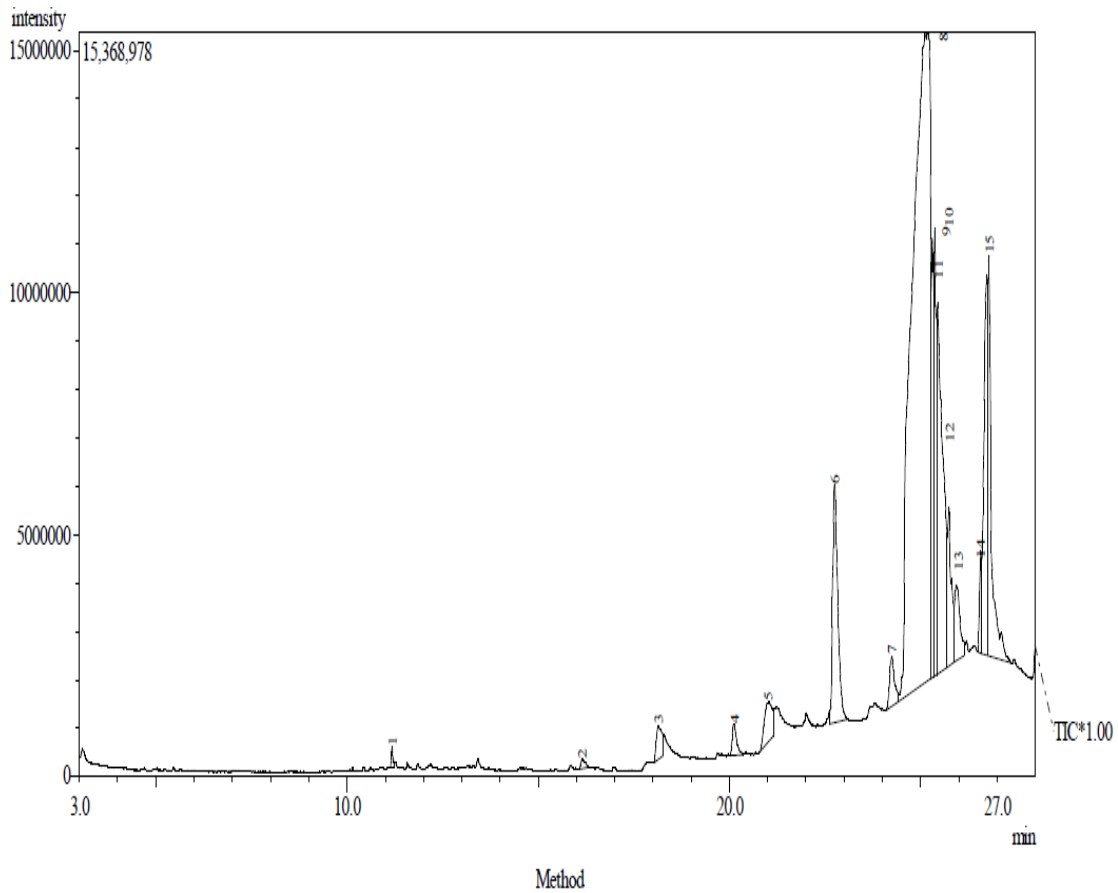


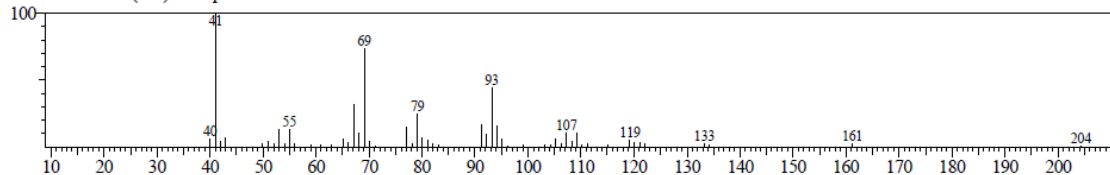
Fig. 1: GC-MS Chromatogram of Cashew Nut Shell Liquid

From the mass spectra, the main constituents identified were cardanols (monounsaturated cardanol peak of 302; di-unsaturated cardanol peak of 300 at lines 8, 9 and 10; and saturated cardanol peak of

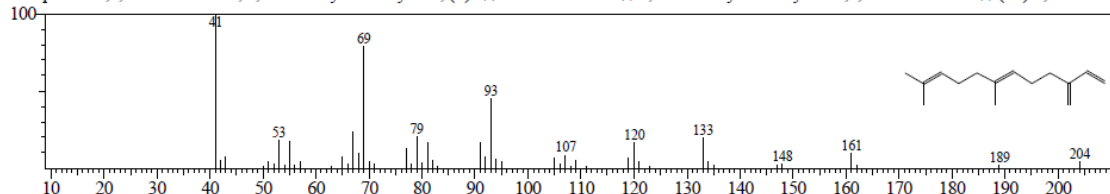
304 at line 6 in Hits 1, 2, and 5). Other relative abundant constituents identified were cardols: saturated cardol at 316 in Line 12.

<< Target >>

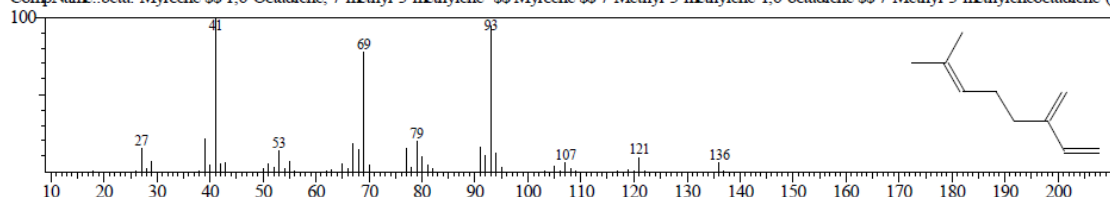
Line#:1 R.Time:11.183(Scan#:983) MassPeaks:55
RawMode:Single 11.183(983) BasePeak:41.00(64963)
BG Mode:11.150(979) Group 1 - Event 1



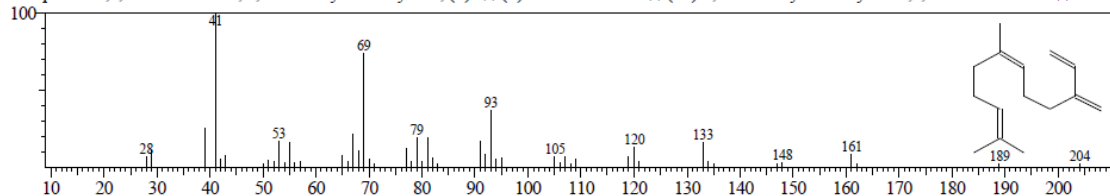
Hit#:1 Entry:43398 Library:NIST05.LIB
SE:90 Formula:C15H24 CAS:18794-84-8 MolWeight:204 RetIndex:1440
CompName:1,6,10-Dodecatriene, 7,11-dimethyl-3-methylene-, (E)- \$\$ beta.-Famesene \$\$ 7,11-Dimethyl-3-methylene-1,6,10-dodecatriene # \$\$



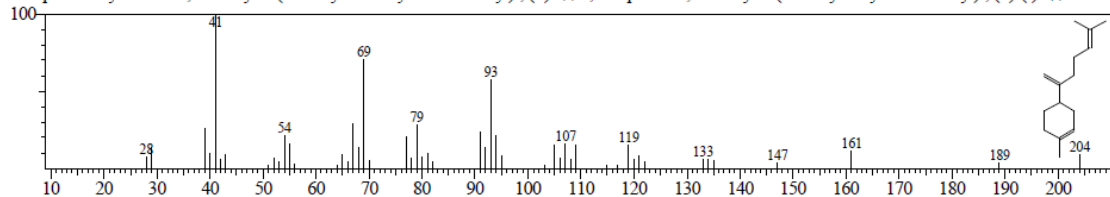
Hit#:2 Entry:6263 Library:NIST05s.LIB
SE:90 Formula:C10H16 CAS:123-35-3 MolWeight:136 RetIndex:958
CompName:.beta.-Myrcene \$\$ 1,6-Octadiene, 7-methyl-3-methylene- \$\$ Myrcene \$\$ 7-Methyl-3-methylene-1,6-octadiene \$\$ 7-Methyl-3-methyleneoctadiene-(1



Hit#:3 Entry:16675 Library:NIST05s.LIB
SE:90 Formula:C15H24 CAS:28973-97-9 MolWeight:204 RetIndex:1440
CompName:1,6,10-Dodecatriene, 7,11-dimethyl-3-methylene-, (Z)- \$\$ (Z)-.beta.-Famesene \$\$ (6Z)-7,11-Dimethyl-3-methylene-1,6,10-dodecatriene # \$\$



Hit#:4 Entry:16676 Library:NIST05s.LIB
SE:89 Formula:C15H24 CAS:495-61-4 MolWeight:204 RetIndex:1500
CompName:Cyclohexene, 1-methyl-4-(5-methyl-1-methylene-4-hexenyl)-, (S)- \$\$ 1,5-Heptadiene, 6-methyl-2-(4-methyl-3-cyclohexen-1-yl)-, (S)-(-)- \$\$ beta.-I



Hit#:5 Entry:43397 Library:NIST05.LIB
SE:89 Formula:C15H24 CAS:77129-48-7 MolWeight:204 RetIndex:1440
CompName:1,6,10-Dodecatriene, 7,11-dimethyl-3-methylene- \$\$ (6E)-7,11-Dimethyl-3-methylene-1,6,10-dodecatriene # \$\$

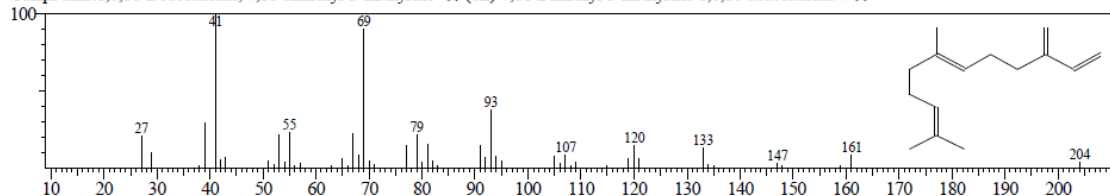
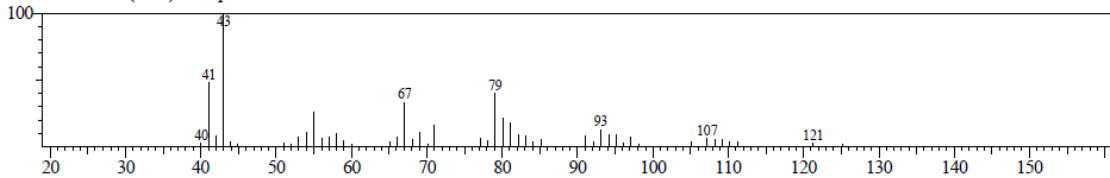


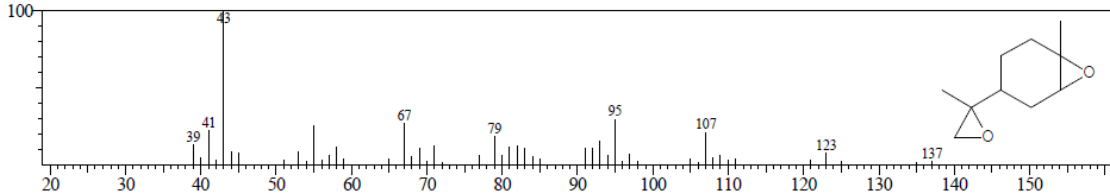
Fig. 2: Line 1 Mass Spectra of Cashew Nut Shell Liquid

<< Target >>

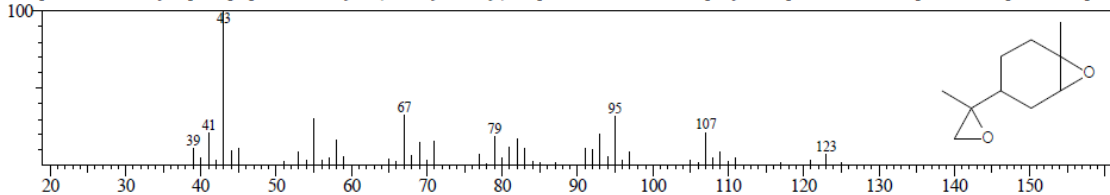
Line# 2 R Time: 16.142 (Scan# 1578) Mass Peaks: 49
Raw Mode: Single 16.142 (1578) Base Peak: 43.00 (44545)
BG Mode: 15.700 (1525) Group 1 - Event 1



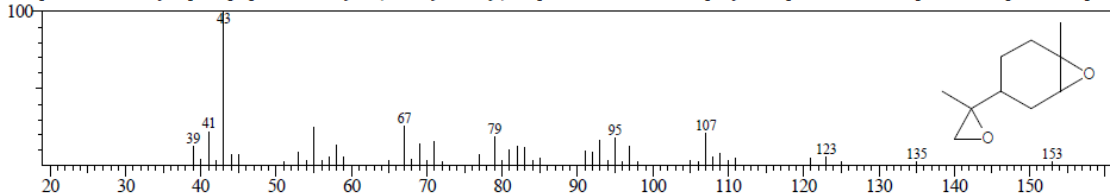
Hit# 1 Entry: 11626 Library: NIST05s.LIB
SE89 Formula: C₁₀H₁₆O₂ CAS: 96-08-2 MolWeight: 168 RetIndex: 1128
CompName: 7-Oxabicyclo[4.1.0]heptane, 1-methyl-4-(2-methoxyiranyl)- \$p\$-Menthane, 1,2:8,9-diepoxy- \$α\$-Limonene diepoxide \$Dipentene diepox



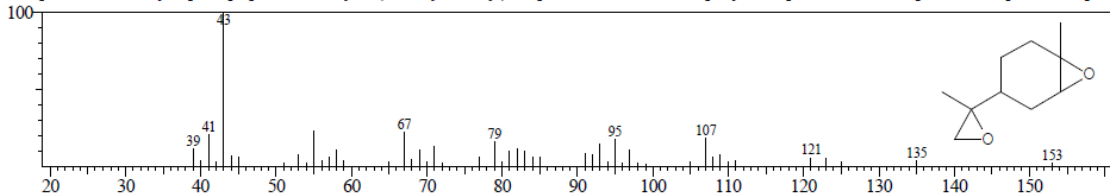
Hit# 2 Entry: 11624 Library: NIST05s.LIB
SE88 Formula: C₁₀H₁₆O₂ CAS: 96-08-2 MolWeight: 168 RetIndex: 1128
CompName: 7-Oxabicyclo[4.1.0]heptane, 1-methyl-4-(2-methoxyiranyl)- \$p\$-Menthane, 1,2:8,9-diepoxy- \$α\$-Limonene diepoxide \$Dipentene diepox



Hit# 3 Entry: 11623 Library: NIST05s.LIB
SE88 Formula: C₁₀H₁₆O₂ CAS: 96-08-2 MolWeight: 168 RetIndex: 1128
CompName: 7-Oxabicyclo[4.1.0]heptane, 1-methyl-4-(2-methoxyiranyl)- \$p\$-Menthane, 1,2:8,9-diepoxy- \$α\$-Limonene diepoxide \$Dipentene diepox



Hit# 4 Entry: 11622 Library: NIST05s.LIB
SE88 Formula: C₁₀H₁₆O₂ CAS: 96-08-2 MolWeight: 168 RetIndex: 1128
CompName: 7-Oxabicyclo[4.1.0]heptane, 1-methyl-4-(2-methoxyiranyl)- \$p\$-Menthane, 1,2:8,9-diepoxy- \$α\$-Limonene diepoxide \$Dipentene diepox



Hit# 5 Entry: 23472 Library: NIST05.LIB
SE87 Formula: C₁₀H₁₆O₂ CAS: 96-08-2 MolWeight: 168 RetIndex: 1128
CompName: 7-Oxabicyclo[4.1.0]heptane, 1-methyl-4-(2-methoxyiranyl)- \$p\$-Menthane, 1,2:8,9-diepoxy- \$α\$-Limonene diepoxide \$Dipentene diepox

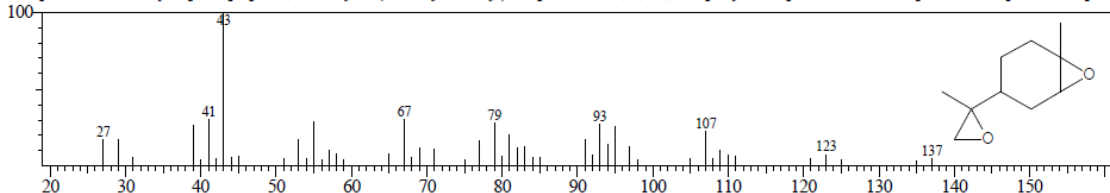
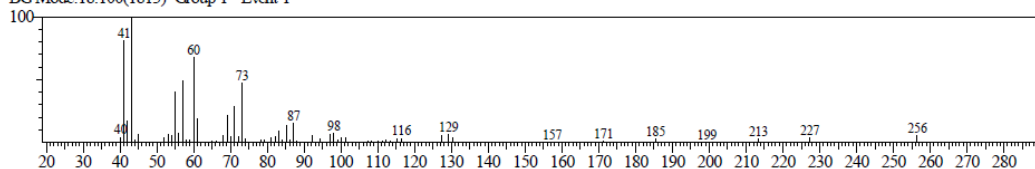


Fig. 3: Line 2 Mass Spectra of Cashew Nut Shell Liquid

<< Target >>

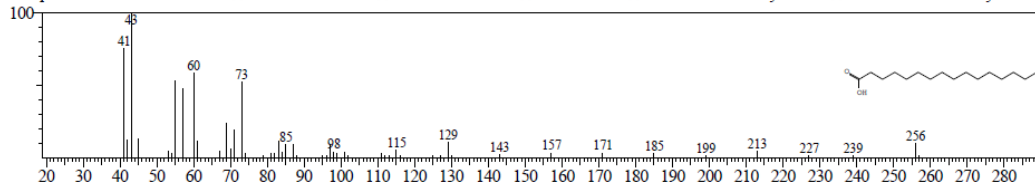
Line# 3 R Time: 18.142(Scan#: 1818) MassPeaks: 65
RawMode: Single 18.142(1818) BasePeak: 43.00(28266)
BG Mode: 18.100(1813) Group 1 - Event 1



Hit# 1 Entry: 21329 Library: NIST05s.LIB

SI: 89 Formula: C16H32O2 CAS: 57-10-3 MolWeight: 256 RetIndex: 1968

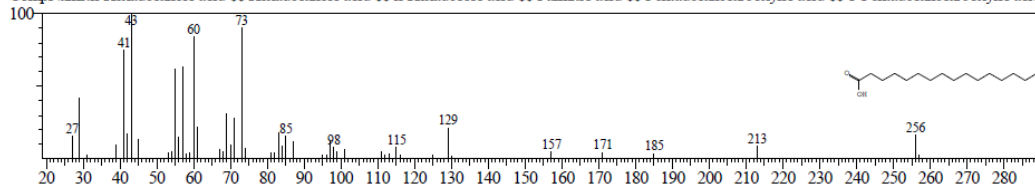
CompName: n-Hexadecanoic acid \$\$ Hexadecanoic acid \$\$ n-Hexadecoic acid \$\$ Palmitic acid \$\$ Pentadecanecarboxylic acid \$\$ 1-Pentadecanecarboxylic acid



Hit# 2 Entry: 74999 Library: NIST05s.LIB

SI: 88 Formula: C16H32O2 CAS: 57-10-3 MolWeight: 256 RetIndex: 1968

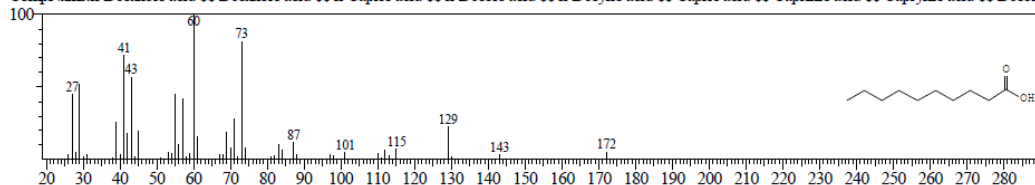
CompName: n-Hexadecanoic acid \$\$ Hexadecanoic acid \$\$ n-Hexadecoic acid \$\$ Palmitic acid \$\$ Pentadecanecarboxylic acid \$\$ 1-Pentadecanecarboxylic acid



Hit# 3 Entry: 12248 Library: NIST05s.LIB

SI: 85 Formula: C10H20O2 CAS: 334-48-5 MolWeight: 172 RetIndex: 1372

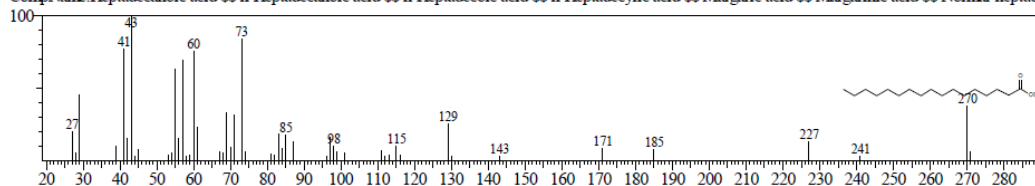
CompName: n-Decanoic acid \$\$ Decanoic acid \$\$ n-Capric acid \$\$ n-Decoic acid \$\$ n-Decylic acid \$\$ Capric acid \$\$ Caprinic acid \$\$ Caprylic acid \$\$ Decoic acid



Hit# 4 Entry: 22212 Library: NIST05s.LIB

SI: 85 Formula: C17H34O2 CAS: 506-12-7 MolWeight: 270 RetIndex: 2067

CompName: Heptadecanoic acid \$\$ n-Heptadecanoic acid \$\$ n-Heptadecoic acid \$\$ n-Heptadecylic acid \$\$ Margaric acid \$\$ Margarinic acid \$\$ Normal-heptadecanoic acid



Hit# 5 Entry: 22977 Library: NIST05s.LIB

SI: 85 Formula: C18H36O2 CAS: 57-11-4 MolWeight: 284 RetIndex: 2167

CompName: Octadecanoic acid \$\$ Stearic acid \$\$ n-Octadecanoic acid \$\$ Humko Industriene R \$\$ Hydrofol Acid 150 \$\$ Hystrene S-97 \$\$ Hystrene T-70 \$\$ Hystrene T-70

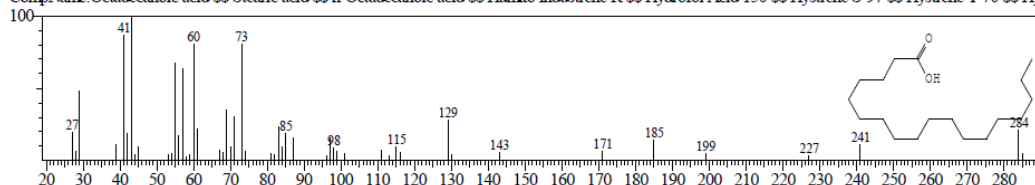
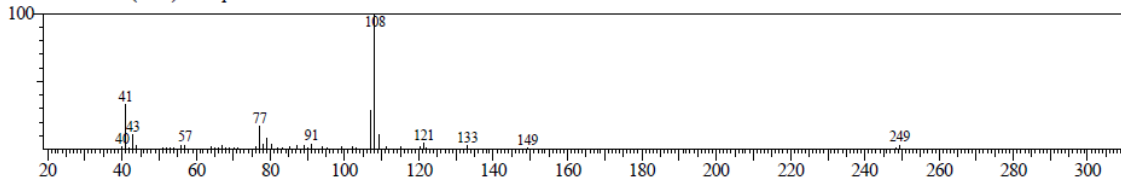


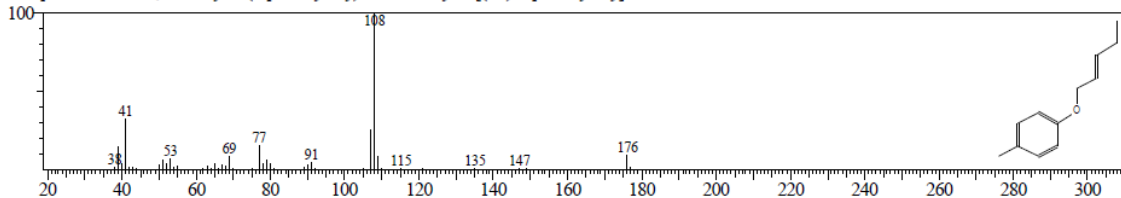
Fig. 4: Line 3 Mass Spectra of Cashew Nut Shell Liquid

<< Target >>

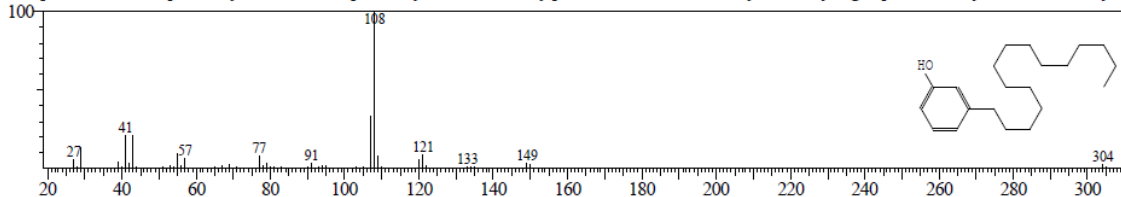
Line# 4 R.Time:20.133(Scan#:2057) MassPeaks:61
RawMode:Single 20.133(2057) BasePeak:108.15(47078)
BG Mode:20.158(2060) Group 1 - Event 1



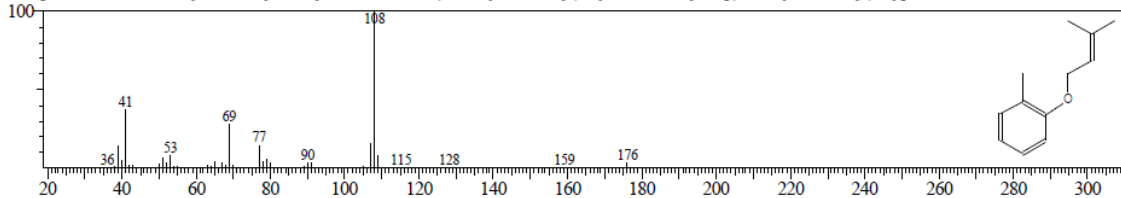
Hit# 1 Entry:27887 Library:NIST05.LIB
SE84 Formula:C12H16O CAS:156089-29-1 MolWeight:176 RetIndex:1388
CompName:Benzene, 1-methyl-4-(2-pentenyl-oxy)- \$\$ 1-Methyl-4-[(2E)-2-pentenyl-oxy]benzene # \$\$



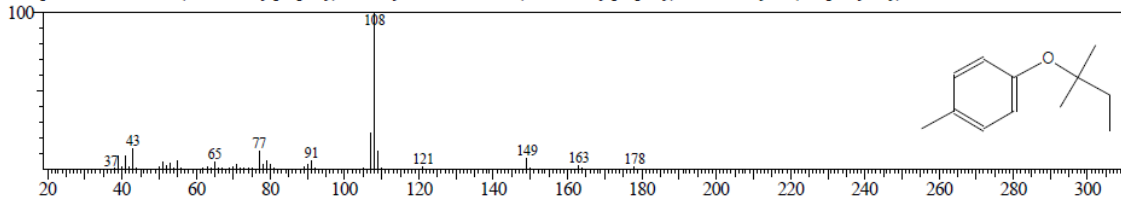
Hit# 2 Entry:23941 Library:NIST05s.LIB
SE84 Formula:C21H36O CAS:501-24-6 MolWeight:304 RetIndex:2406
CompName:Phenol, 3-pentadecyl- \$\$ Phenol, m-pentadecyl- \$\$ m-Pentadecylphenol \$\$ Anacardol, tetrahydro- \$\$ Cyclogallipharol \$\$ Hydrocardanol \$\$ Hydr



Hit# 3 Entry:27886 Library:NIST05.LIB
SE83 Formula:C12H16O CAS:23446-47-1 MolWeight:176 RetIndex:1365
CompName:Ether, 3-methyl-2-butenyl o-tolyl \$\$ Toluene, 2-(3-methyl-2-butenyl)oxy- \$\$ 1-Methyl-2-[(3-methyl-2-butenyl)oxy]benzene # \$\$



Hit# 4 Entry:28960 Library:NIST05.LIB
SE83 Formula:C12H18O CAS:85709-98-4 MolWeight:178 RetIndex:1296
CompName:Benzene, 1-(1,1-dimethylpropoxy)-4-methyl- \$\$ Toluene, 4-(1,1-dimethylpropoxy)- \$\$ 1-Methyl-4-(tert-pentyl-oxy)benzene # \$\$



Hit# 5 Entry:54070 Library:NIST05.LIB
SE81 Formula:C12H14O4 CAS:0-00-0 MolWeight:222 RetIndex:1639
CompName:Oxalic acid, 2-methylphenyl propyl ester

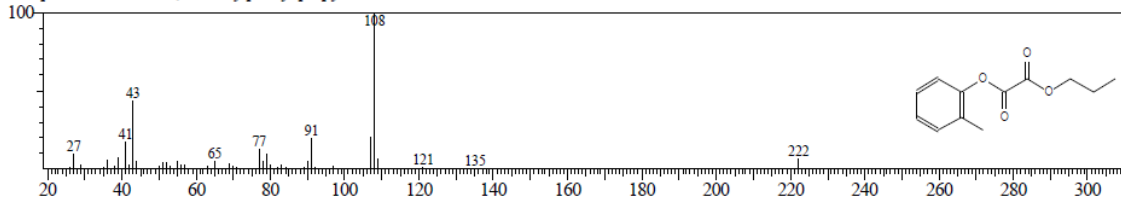


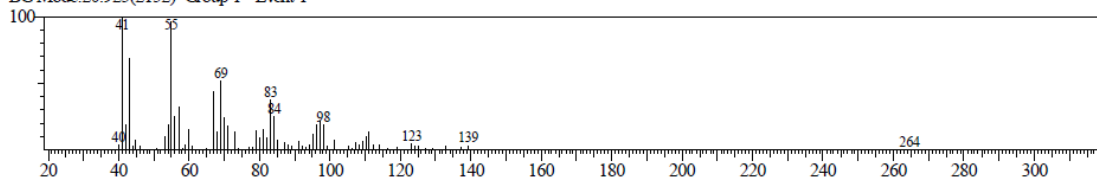
Fig. 5: Line 3 Mass Spectra of Cashew Nut Shell Liquid

<< Target >>

Line# 5 R Time: 20.992 (Scan# 2160) MassPeaks: 77

RawMode: Single 20.992 (2160) BasePeak: 41.00 (32744)

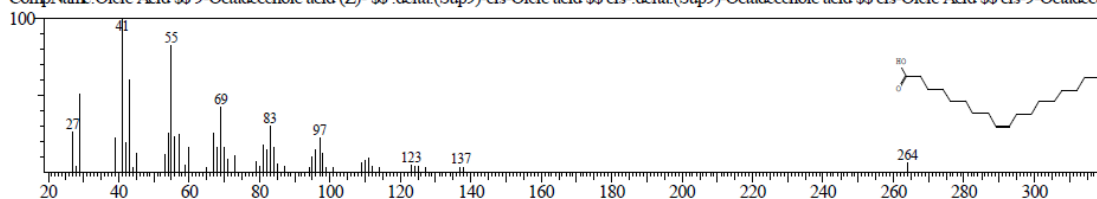
BG Mode: 20.925 (2152) Group 1 - Event 1



Hit# 1 Entry: 22869 Library: NIST05s.LIB

SI: 91 Formula: C18H34O2 CAS: 112-80-1 MolWeight: 282 RetIndex: 2175

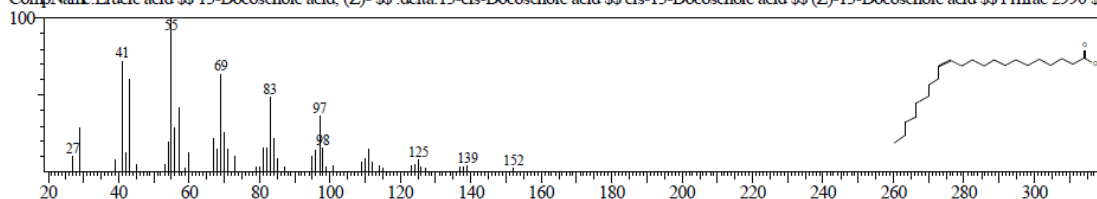
CompName: Oleic Acid \$ 9-Octadecenoic acid (Z)- \$ \$.delta.(Sup9)-cis-Oleic acid \$ \$ cis-.delta.(Sup9)-Octadecenoic acid \$ \$ cis-Oleic Acid \$ \$ cis-9-Octadec



Hit# 2 Entry: 121691 Library: NIST05.LIB

SI: 89 Formula: C22H42O2 CAS: 112-86-7 MolWeight: 338 RetIndex: 2572

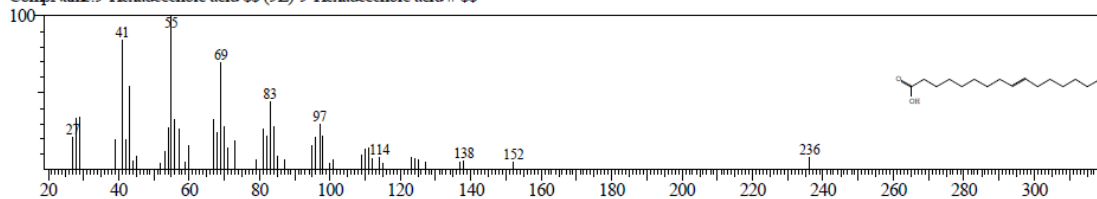
CompName: Erucic acid \$ 13-Docosenoic acid, (Z)- \$ \$.delta.13-cis-Docosenoic acid \$ \$ cis-13-Docosenoic acid \$ \$ (Z)-13-Docosenoic acid \$ \$ Prifrac 2990 \$ \$



Hit# 3 Entry: 73685 Library: NIST05.LIB

SI: 88 Formula: C16H30O2 CAS: 2091-29-4 MolWeight: 254 RetIndex: 1976

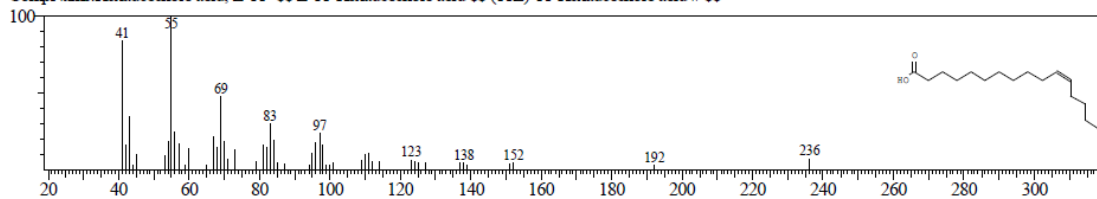
CompName: 9-Hexadecenoic acid \$ (9E)-9-Hexadecenoic acid # \$ \$



Hit# 4 Entry: 21184 Library: NIST05s.LIB

SI: 88 Formula: C16H30O2 CAS: 2416-20-8 MolWeight: 254 RetIndex: 1976

CompName: Hexadecenoic acid, Z-11- \$ \$ Z-11-Hexadecenoic acid \$ \$ (11Z)-11-Hexadecenoic acid # \$ \$



Hit# 5 Entry: 73687 Library: NIST05.LIB

SI: 88 Formula: C16H30O2 CAS: 2416-20-8 MolWeight: 254 RetIndex: 1976

CompName: Hexadecenoic acid, Z-11- \$ \$ Z-11-Hexadecenoic acid \$ \$ (11Z)-11-Hexadecenoic acid # \$ \$

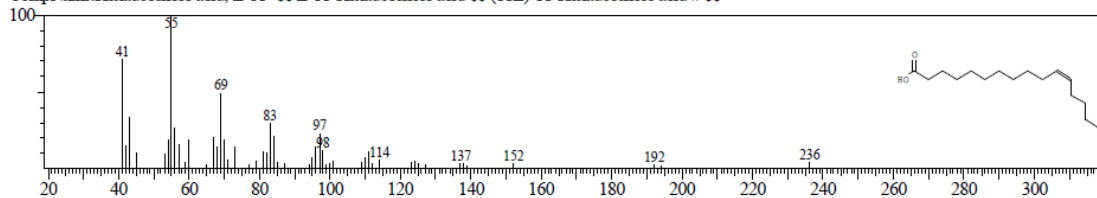
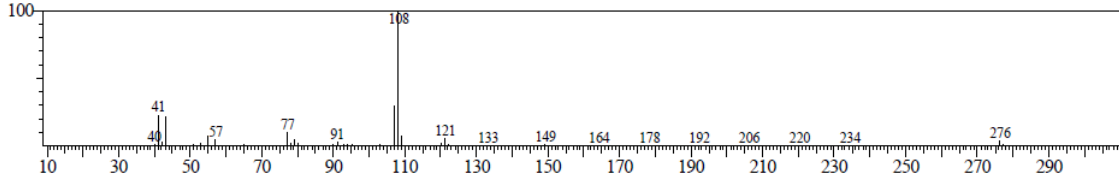


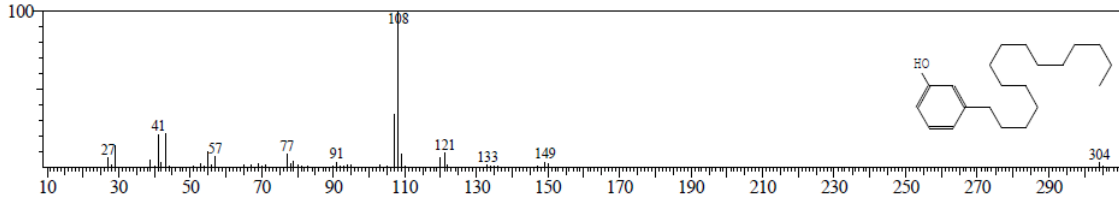
Fig. 6: Line 5 Mass Spectra of Cashew Nut Shell Liquid

<< Target >>

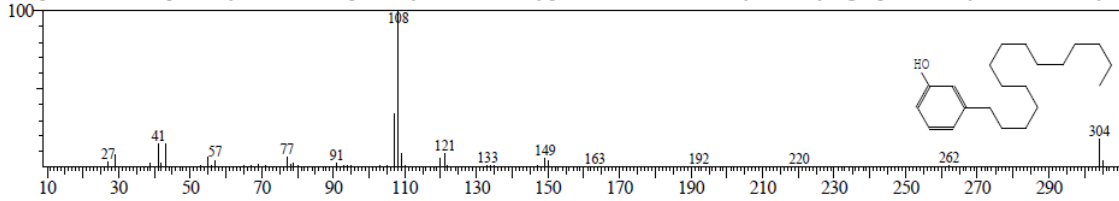
Line#:6 R.Time:22.742(Scan#:2370) MassPeaks:79
RawMode:Single 22.742(2370) BasePeak:108.15(1873970)
BGMode:22.633(2357) Group 1 - Event 1



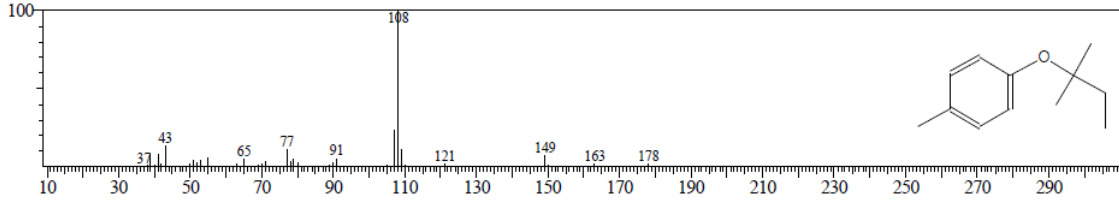
Hit#:1 Entry:23941 Library:NIST05s.LIB
SI:93 Formula:C21H36O CAS:501-24-6 MolWeight:304 RetIndex:2406
CompName:Phenol, 3-pentadecyl- \$\$ Phenol, m-pentadecyl- \$\$ m-Pentadecylphenol \$\$ Anacardol, tetrahydro- \$\$ Cyclogallipharol \$\$ Hydrocardanol \$\$ Hydr



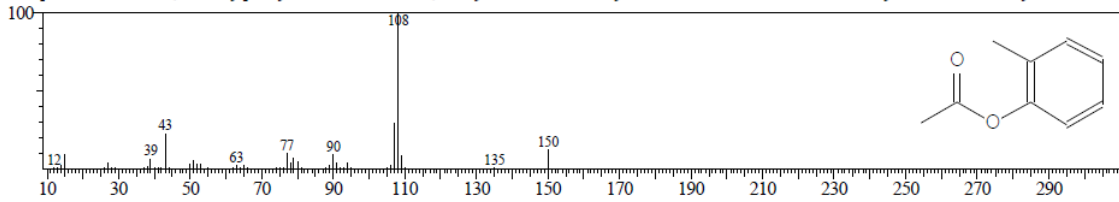
Hit#:2 Entry:23942 Library:NIST05s.LIB
SI:88 Formula:C21H36O CAS:501-24-6 MolWeight:304 RetIndex:2406
CompName:Phenol, 3-pentadecyl- \$\$ Phenol, m-pentadecyl- \$\$ m-Pentadecylphenol \$\$ Anacardol, tetrahydro- \$\$ Cyclogallipharol \$\$ Hydrocardanol \$\$ Hydr



Hit#:3 Entry:28960 Library:NIST05.LIB
SI:87 Formula:C12H18O CAS:85709-98-4 MolWeight:178 RetIndex:1296
CompName:Benzene, 1-(1,1-dimethylpropoxy)-4-methyl- \$\$ Toluene, 4-(1,1-dimethylpropoxy)- \$\$ 1-Methyl-4-(tert-pentyloxy)benzene # \$\$



Hit#:4 Entry:14756 Library:NIST05.LIB
SI:87 Formula:C9H10O2 CAS:533-18-6 MolWeight:150 RetIndex:1174
CompName:Acetic acid, 2-methylphenyl ester \$\$ Acetic acid, o-tolyl ester \$\$ o-Acetoxytoluene \$\$ o-Cresol acetate \$\$ o-Cresyl acetate \$\$ o-Cresylic acetate \$\$



Hit#:5 Entry:23943 Library:NIST05s.LIB
SI:86 Formula:C21H36O CAS:501-24-6 MolWeight:304 RetIndex:2406
CompName:Phenol, 3-pentadecyl- \$\$ Phenol, m-pentadecyl- \$\$ m-Pentadecylphenol \$\$ Anacardol, tetrahydro- \$\$ Cyclogallipharol \$\$ Hydrocardanol \$\$ Hydr

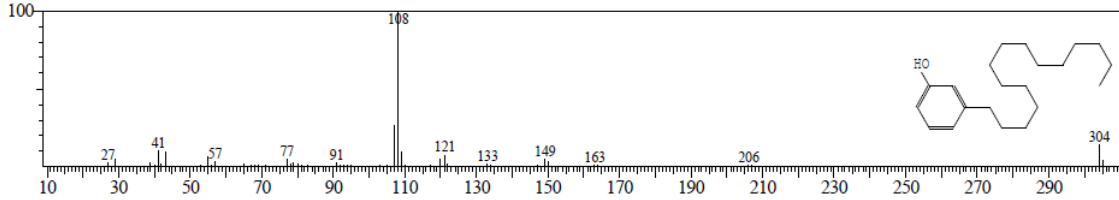
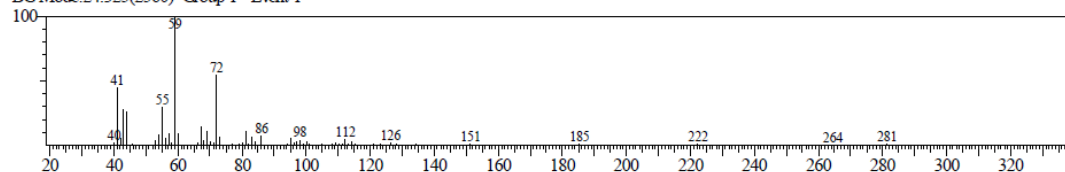


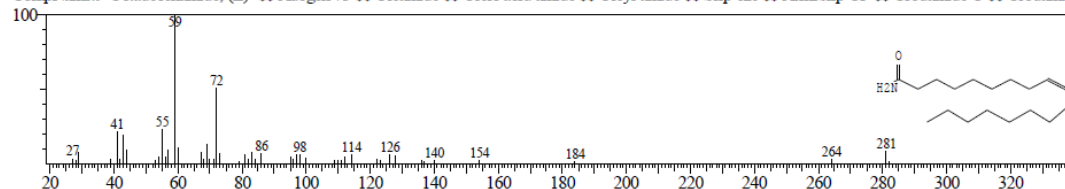
Fig. 7: Line 6 Mass Spectra of Cashew Nut Shell Liquid

<< Target >>

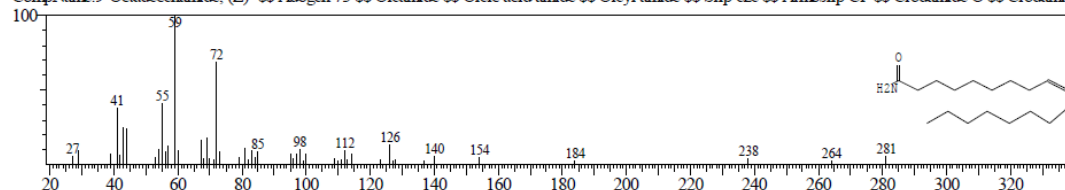
Line#:7 R.Time:24.233(Scan#:2549) MassPeaks:80
RawMode:Single 24.233(2549) BasePeak:59.00(128201)
BG Mode:24.325(2560) Group 1 - Event 1



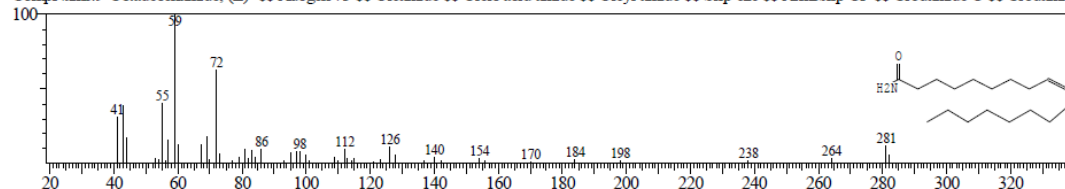
Hit#:1 Entry:89876 Library:NIST05s.LIB
SE89 Formula:C18H35NO CAS:301-02-0 MolWeight:281 RetIndex:2228
CompName:9-Octadecenamide, (Z)- \$\$ Adogen 73 \$\$ Oleamide \$\$ Oleic acid amide \$\$ Oleyl amide \$\$ Slip-eze \$\$ Amoslip CP \$\$ Crodamide O \$\$ Crodamide



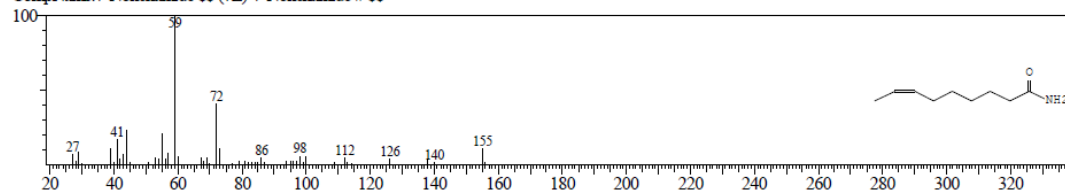
Hit#:2 Entry:22808 Library:NIST05s.LIB
SE88 Formula:C18H35NO CAS:301-02-0 MolWeight:281 RetIndex:2228
CompName:9-Octadecenamide, (Z)- \$\$ Adogen 73 \$\$ Oleamide \$\$ Oleic acid amide \$\$ Oleyl amide \$\$ Slip-eze \$\$ Amoslip CP \$\$ Crodamide O \$\$ Crodamide



Hit#:3 Entry:22807 Library:NIST05s.LIB
SE86 Formula:C18H35NO CAS:301-02-0 MolWeight:281 RetIndex:2228
CompName:9-Octadecenamide, (Z)- \$\$ Adogen 73 \$\$ Oleamide \$\$ Oleic acid amide \$\$ Oleyl amide \$\$ Slip-eze \$\$ Amoslip CP \$\$ Crodamide O \$\$ Crodamide



Hit#:4 Entry:17375 Library:NIST05s.LIB
SE85 Formula:C9H17NO CAS:90949-53-4 MolWeight:155 RetIndex:1333
CompName:7-Nonenamide \$\$ (7Z)-7-Nonenamide # \$\$



Hit#:5 Entry:25161 Library:NIST05s.LIB
SE85 Formula:C22H43NO CAS:112-84-5 MolWeight:337 RetIndex:2625
CompName:13-Docosenamide, (Z)- \$\$ Erucylamide \$\$ Erucyl amide \$\$ (Z)-13-Docosenamide \$\$ 13-Docosenamide \$\$ Amid E \$\$ cis-13-Docosenamide \$\$ cis

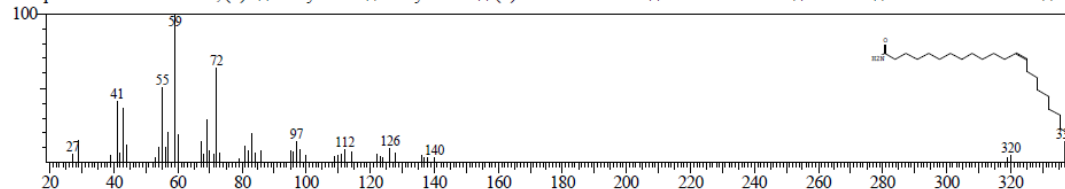
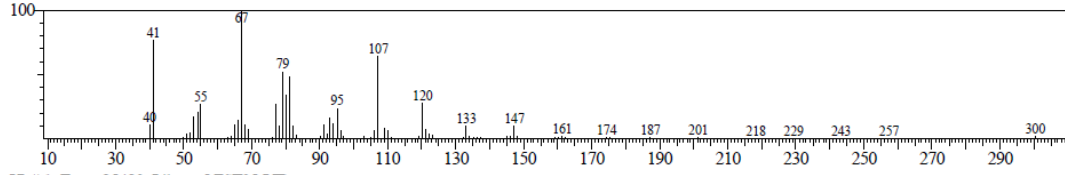


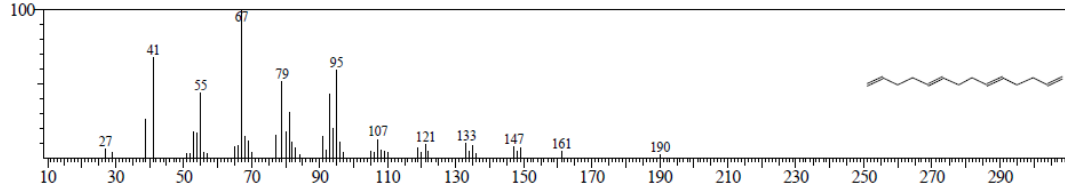
Fig. 8: Line 7 Mass Spectra of Cashew Nut Shell Liquid

<< Target >>

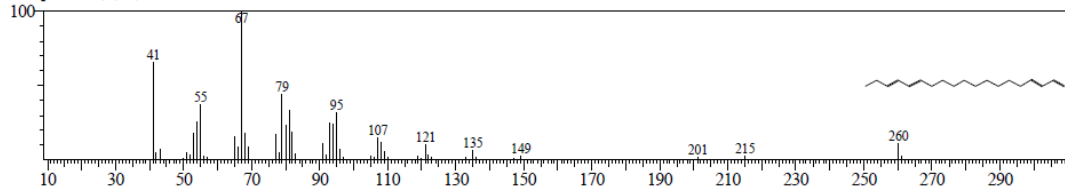
Line# 8 R Time: 25.225 (Scan#: 2668) MassPeaks: 110
Raw Mode: Single 25.225 (2668) Base Peak: 67.00 (680638)
BG Mode: 25.267 (2673) Group 1 - Event 1



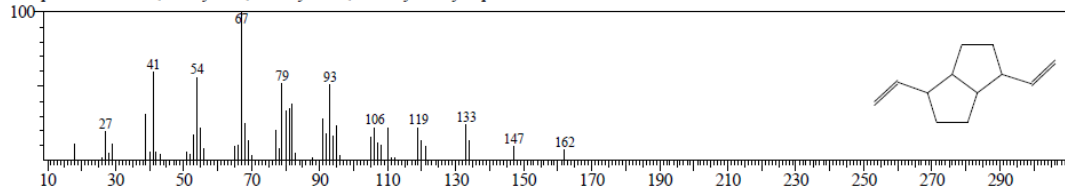
Hit# 1 Entry: 35480 Library: NIST05.LIB
SE: 85 Formula: C₁₄H₂₂ CAS: 51487-38-8 MolWeight: 190 RetIndex: 1409
CompName: 1,5,9,13-Tetradecatetraene (5E,9E)-1,5,9,13-Tetradecatetraene # \$\$



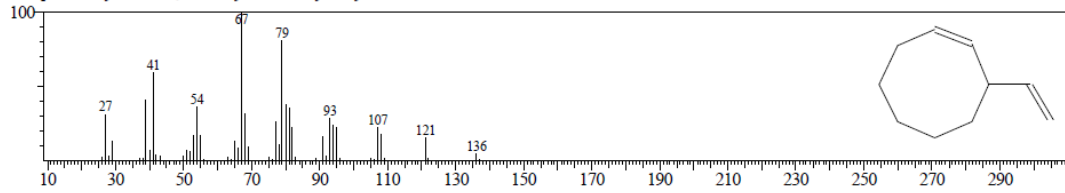
Hit# 2 Entry: 77364 Library: NIST05.LIB
SE: 85 Formula: C₁₉H₃₂ CAS: 0-00-0 MolWeight: 260 RetIndex: 1924
CompName: 1,3,14,16-Nonadecatetraene



Hit# 3 Entry: 20583 Library: NIST05.LIB
SE: 83 Formula: C₁₂H₁₈ CAS: 17572-84-8 MolWeight: 162 RetIndex: 1163
CompName: Pentalene, octahydro-1,4-divinyl- (S)-1,4-Divinyloctahydopentalene # \$\$



Hit# 4 Entry: 9515 Library: NIST05.LIB
SE: 83 Formula: C₁₀H₁₆ CAS: 2213-60-7 MolWeight: 136 RetIndex: 1092
CompName: Cyclooctene, 3-ethenyl- (S)-3-Vinyl-1-cyclooctene # \$\$



Hit# 5 Entry: 9509 Library: NIST05.LIB
SE: 82 Formula: C₁₀H₁₆ CAS: 1124-45-4 MolWeight: 136 RetIndex: 1092
CompName: Cyclooctene, 4-ethenyl- (S)-4-Vinyl-1-cyclooctene # \$\$

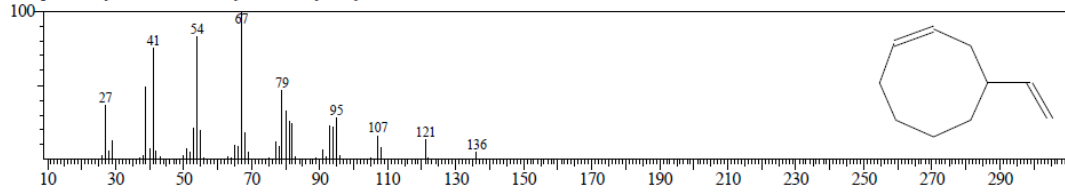
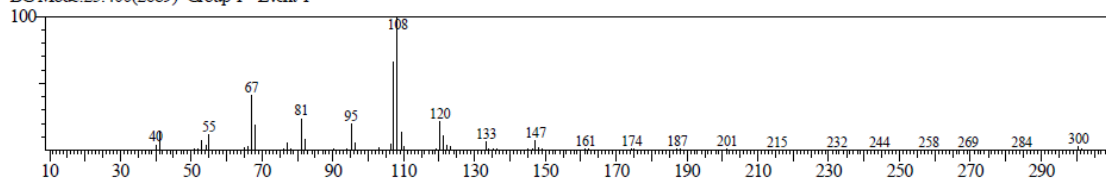


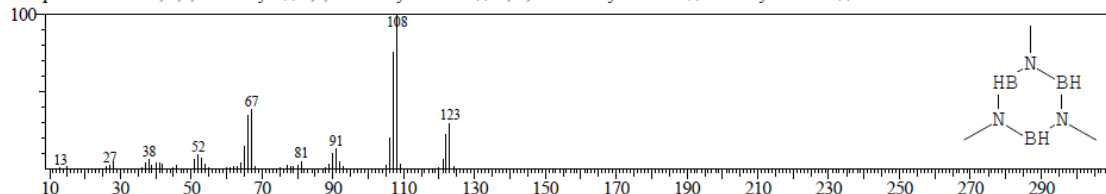
Fig. 9: Line 8 Mass Spectra of Cashew Nut Shell Liquid

<< Target >>

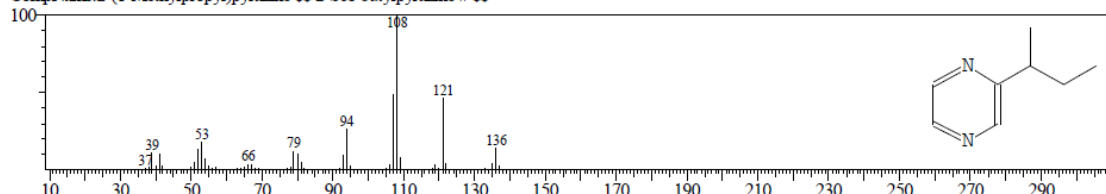
Line#:9 R.Time:25.300(Scan#:2677) MassPeaks:125
RawMode:Single 25.300(2677) BasePeak:108.15(402917)
BG Mode:25.400(2689) Group 1 - Event 1



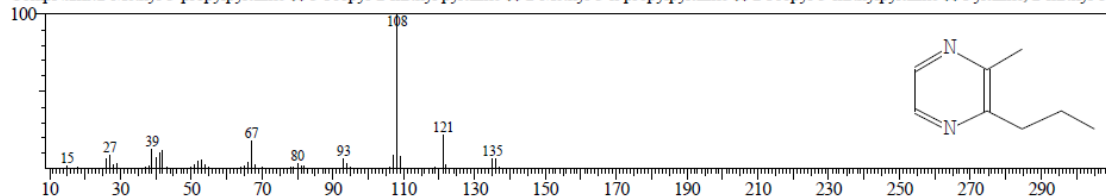
Hit#:1 Entry:5577 Library:NIST05.LIB
SE:73 Formula:C3H12B3N3 CAS:1004-35-9 MolWeight:123 RetIndex:0
CompName: Borazine, 1,3,5-trimethyl- \$\$ 1,3,5-Trimethylborazine \$\$ N,N',N''-Trimethylborazine \$\$ Trimethylborazine \$\$



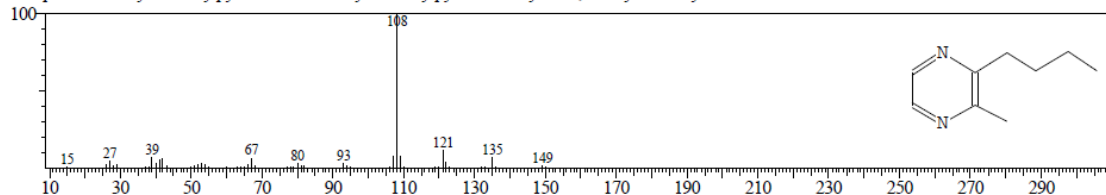
Hit#:2 Entry:9359 Library:NIST05.LIB
SE:73 Formula:C8H12N2 CAS:29460-93-3 MolWeight:136 RetIndex:1015
CompName: 2-(1-Methylpropyl)pyrazine \$\$ 2-Sec-butylpyrazine # \$\$



Hit#:3 Entry:9360 Library:NIST05.LIB
SE:73 Formula:C8H12N2 CAS:15986-80-8 MolWeight:136 RetIndex:1093
CompName: 2-Methyl-3-propylpyrazine \$\$ 3-Propyl-2-methyl pyrazine \$\$ 2-Methyl-3-n-propylpyrazine \$\$ 2-Propyl-3-methylpyrazine \$\$ Pyrazine, 2-methyl-3-



Hit#:4 Entry:8452 Library:NIST05s.LIB
SE:73 Formula:C9H14N2 CAS:15987-00-5 MolWeight:150 RetIndex:1193
CompName: 2-Butyl-3-methylpyrazine \$\$ 2-n-Butyl-3-methylpyrazine \$\$ Pyrazine, 2-butyl-3-methyl- \$\$



Hit#:5 Entry:21454 Library:NIST05.LIB
SE:72 Formula:C10H16N2 CAS:91010-41-2 MolWeight:164 RetIndex:1228
CompName: 2-Isoamyl-6-methylpyrazine \$\$ 2-Isoamyl-6-methylpyrazine \$\$ 2-Isopentyl-6-methylpyrazine # \$\$

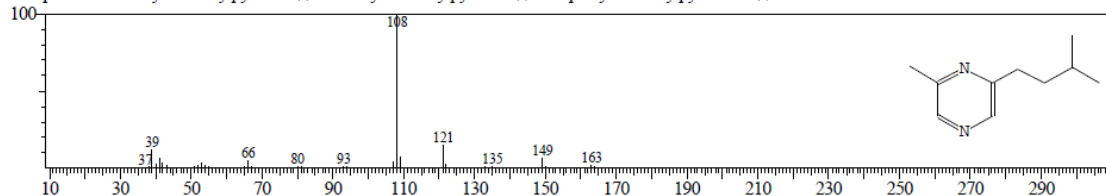
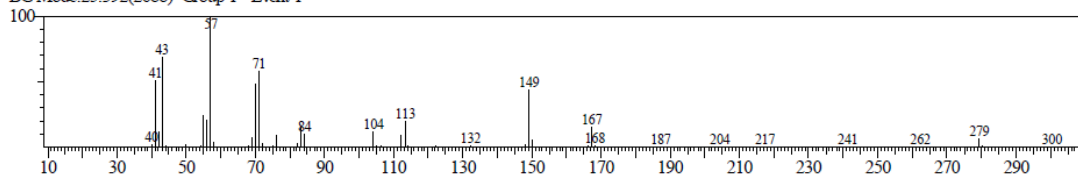


Fig. 10: Line 9 Mass Spectra of Cashew Nut Shell Liquid

<< Target >>

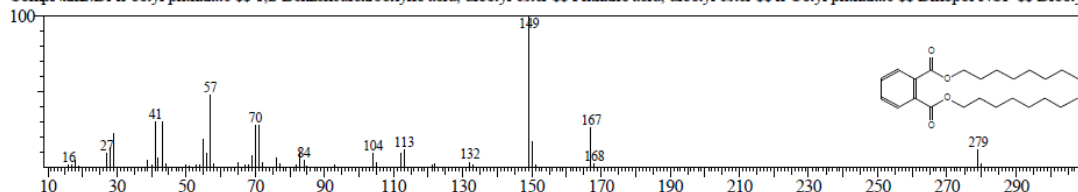
Line#:10 R.Time:25.367(Scan#:2685) MassPeaks:82
RawMode:Single 25.367(2685) BasePeak:57.05(371920)
BG Mode:25.392(2688) Group 1 - Event 1



Hit#1 Entry:26375 Library:NIST05s.LIB

SE:83 Formula:C₂₄H₃₈O₄ CAS:117-84-0 MolWeight:390 RetIndex:2832

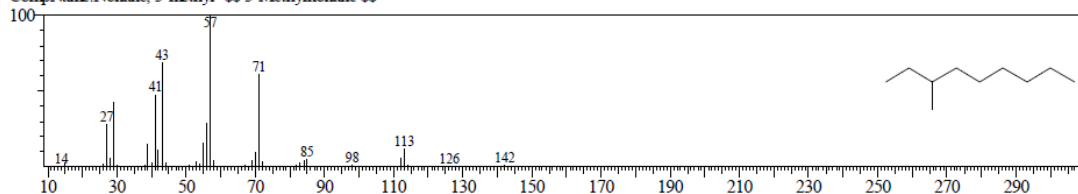
CompName:Di-n-octyl phthalate \$\$ 1,2-Benzenedicarboxylic acid, dioctyl ester \$\$ Phthalic acid, dioctyl ester \$\$ n-Octyl phthalate \$\$ Dinopol NOP \$\$ Dioctyl



Hit#2 Entry:7283 Library:NIST05s.LIB

SE:82 Formula:C₁₀H₂₂ CAS:5911-04-6 MolWeight:142 RetIndex:951

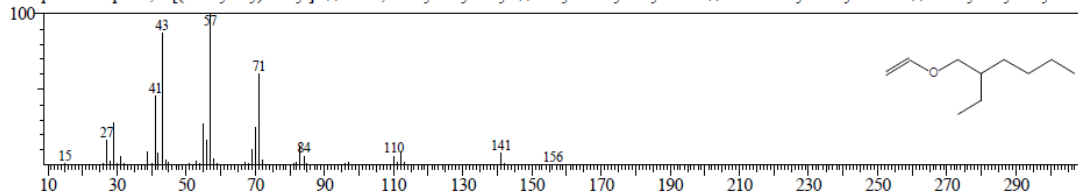
CompName:Nonane, 3-methyl- \$\$ 3-Methylnonane \$\$



Hit#3 Entry:17985 Library:NIST05.LIB

SE:82 Formula:C₁₀H₂₀O CAS:103-44-6 MolWeight:156 RetIndex:1017

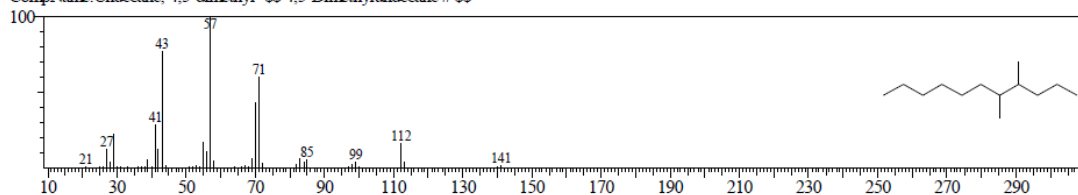
CompName:Heptane, 3-[(ethenoxy)methyl]- \$\$ Ether, 2-ethylhexyl vinyl \$\$ Vinyl 2-ethylhexyl ether \$\$ 1-Ethenoxy-2-ethylhexane \$\$ 2-Ethylhexyl vinyl ether



Hit#4 Entry:32379 Library:NIST05.LIB

SE:82 Formula:C₁₃H₂₈ CAS:17312-79-7 MolWeight:184 RetIndex:1185

CompName:Undecane, 4,5-dimethyl- \$\$ 4,5-Dimethylundecane # \$\$



Hit#5 Entry:23873 Library:NIST05.LIB

SE:82 Formula:C₁₂H₂₄ CAS:50871-03-9 MolWeight:168 RetIndex:1076

CompName:1-Decene, 3,4-dimethyl- \$\$ 3,4-Dimethyl-1-decene \$\$

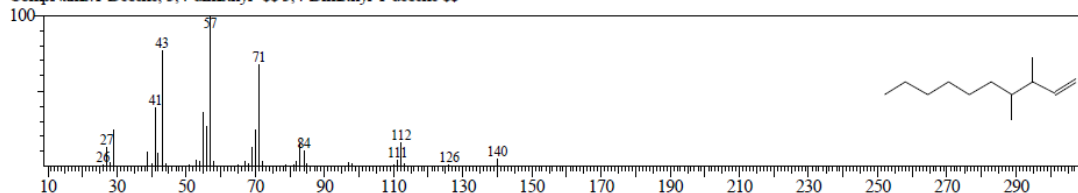
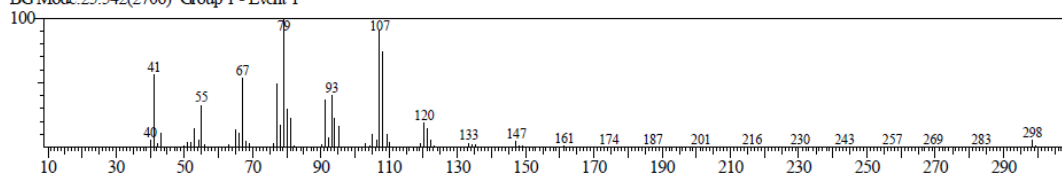


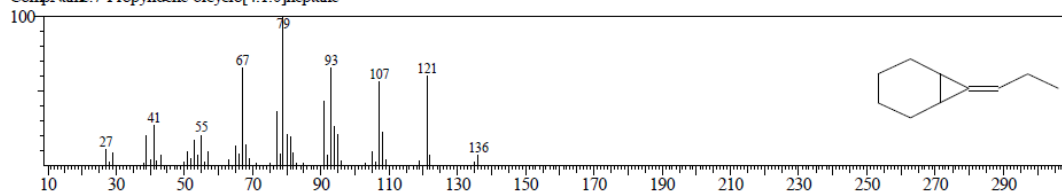
Fig. 11: Line 10 Mass Spectra of Cashew Nut Shell Liquid

<< Target >>

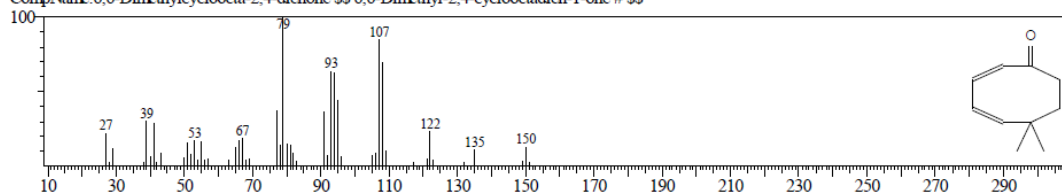
Line#:11 R_Time:25.458(Scan#:2696) MassPeaks:112
RawMode:Single 25.458(2696) BasePeak:79.10(237725)
BG Mode:25.542(2706) Group 1 - Event 1



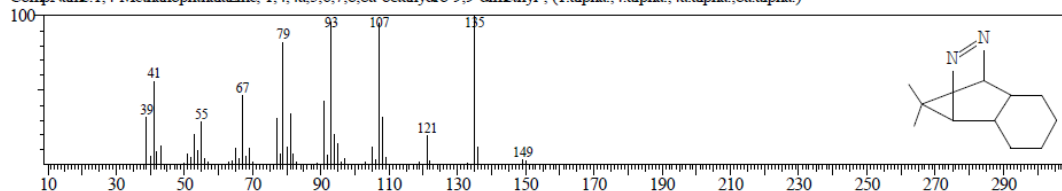
Hit#:1 Entry:9548 Library:NIST05.LIB
SE:86 Formula:C10H16 CAS:82253-09-6 MolWeight:136 RetIndex:1025
CompName:7-Propylidene-bicyclo[4.1.0]heptane



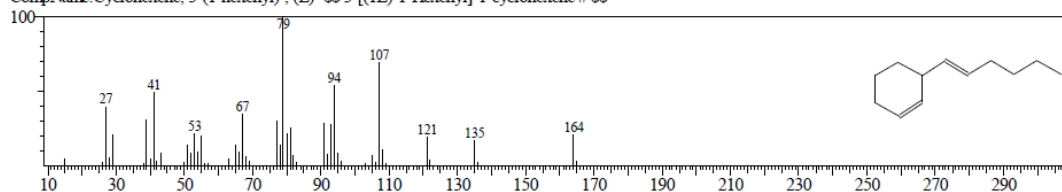
Hit#:2 Entry:14872 Library:NIST05.LIB
SE:86 Formula:C10H14O CAS:91531-51-0 MolWeight:150 RetIndex:1230
CompName:6,6-Dimethylcycloocta-2,4-dienone \$S\$ 6,6-Dimethyl-2,4-cyclooctadien-1-one # \$S\$



Hit#:3 Entry:28893 Library:NIST05.LIB
SE:85 Formula:C11H18N2 CAS:109746-13-6 MolWeight:178 RetIndex:0
CompName:1,4-Methanophthalazine, 1,4,4a,5,6,7,8,8a-octahydro-9,9-dimethyl-, (1.alpha.,4.alpha.,4a.alpha.,8a.alpha.)-



Hit#:4 Entry:21624 Library:NIST05.LIB
SE:85 Formula:C12H20 CAS:55976-11-9 MolWeight:164 RetIndex:1268
CompName:Cyclohexene, 3-(1-hexenyl)-, (E)- \$S\$ 3-[(1E)-1-Hexenyl]-1-cyclohexene # \$S\$



Hit#:5 Entry:43339 Library:NIST05.LIB
SE:85 Formula:C13H20N2 CAS:0-00-0 MolWeight:204 RetIndex:0
CompName:1,4-Methanocycloocta[d]pyridazine, 1,4,4a,5,6,9,10,10a-octahydro-11,11-dimethyl-, (1.alpha.,4.alpha.,4a.alpha.,10a.alpha.)-

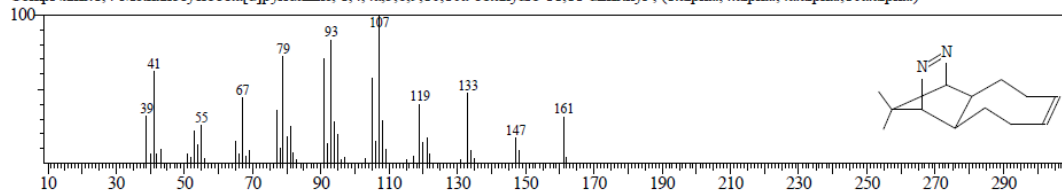
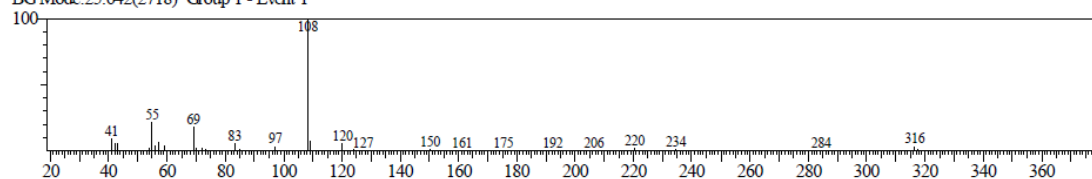


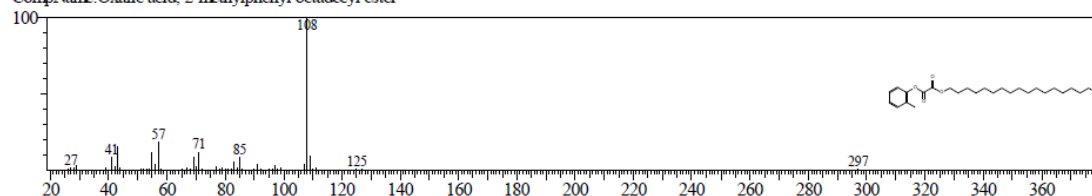
Fig. 12: Line 11 Mass Spectra of Cashew Nut Shell Liquid

<< Target >>

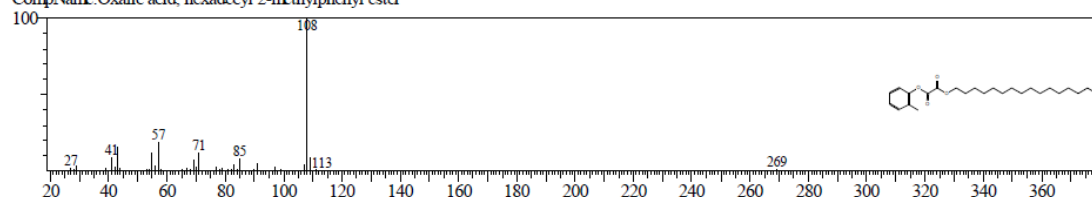
Line#:12 R Time:25.742(Scan#:2730) MassPeaks:59
RawMode:Single 25.742(2730) BasePeak:108.15(227271)
BG Mode:25.642(2718) Group 1 - Event 1



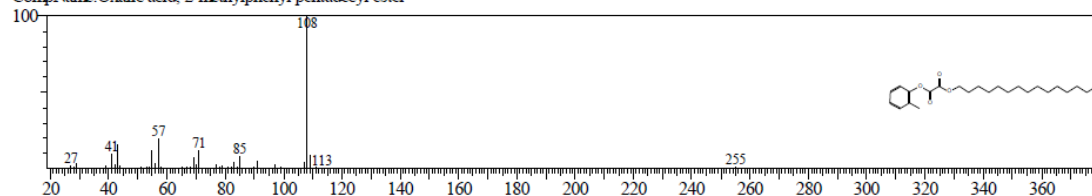
Hit#:1 Entry:150670 Library:NIST05.LIB
SE:80 Formula:C27H44O4 CAS:0-00-0 MolWeight:432 RetIndex:3130
CompName:Oxalic acid, 2-methylphenyl octadecyl ester



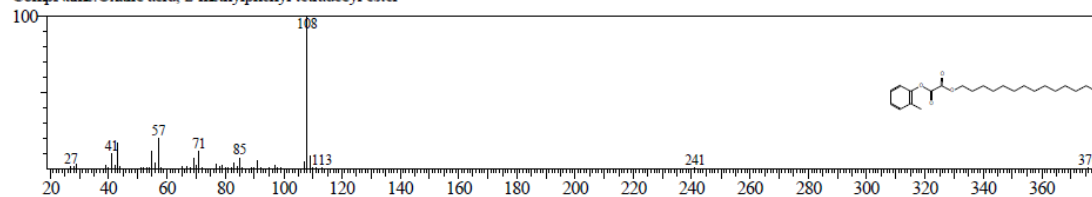
Hit#:2 Entry:145746 Library:NIST05.LIB
SE:80 Formula:C25H40O4 CAS:0-00-0 MolWeight:404 RetIndex:2931
CompName:Oxalic acid, hexadecyl 2-methylphenyl ester



Hit#:3 Entry:142143 Library:NIST05.LIB
SE:80 Formula:C24H38O4 CAS:0-00-0 MolWeight:390 RetIndex:2832
CompName:Oxalic acid, 2-methylphenyl pentadecyl ester



Hit#:4 Entry:137781 Library:NIST05.LIB
SE:79 Formula:C23H36O4 CAS:0-00-0 MolWeight:376 RetIndex:2732
CompName:Oxalic acid, 2-methylphenyl tetradecyl ester



Hit#:5 Entry:132298 Library:NIST05.LIB
SE:79 Formula:C22H34O4 CAS:0-00-0 MolWeight:362 RetIndex:2633
CompName:Oxalic acid, 2-methylphenyl tridecyl ester

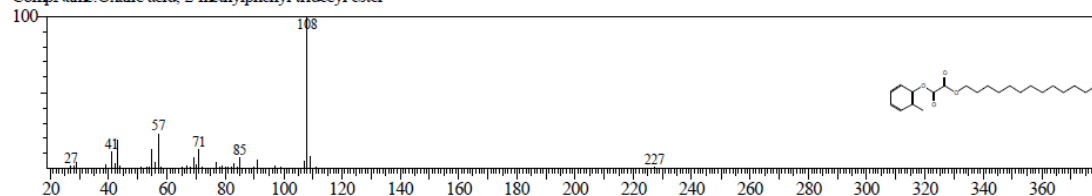
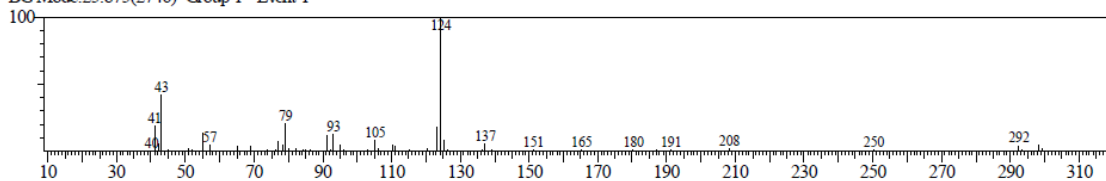


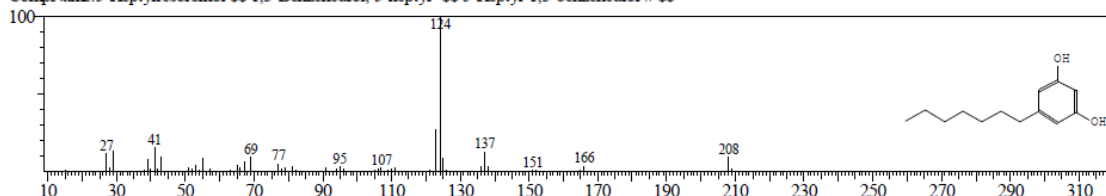
Fig. 13: Line 12 Mass Spectra of Cashew Nut Shell Liquid

<< Target >>

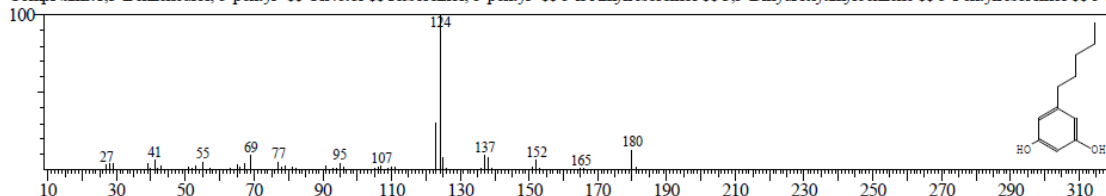
Line#:13 R.Time:25.983(Scan#:2759) MassPeaks:82
RawMode:Single 25.983(2759) BasePeak:124.15(95149)
BG Mode:25.875(2746) Group 1 - Event 1



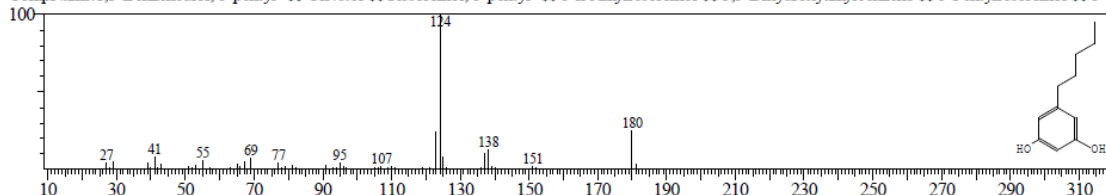
Hit#1 Entry:45946 Library:NIST05.LIB
SE:77 Formula:C13H20O2 CAS:500-67-4 MolWeight:208 RetIndex:1831
CompName:5-Heptylresorcinol \$\$ 1,3-Benzenediol, 5-heptyl- \$\$ 5-Heptyl-1,3-benzenediol # \$\$



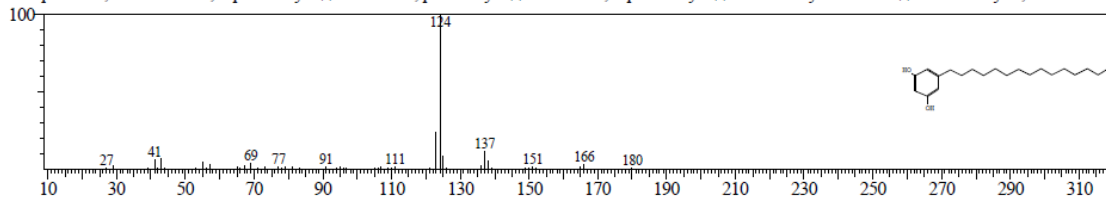
Hit#2 Entry:29977 Library:NIST05.LIB
SE:76 Formula:C11H16O2 CAS:500-66-3 MolWeight:180 RetIndex:1632
CompName:1,3-Benzenediol, 5-pentyl- \$\$ Olivetol \$\$ Resorcinol, 5-pentyl- \$\$ 5-n-Anylresorcinol \$\$ 3,5-Dihydroxyanylbeneze \$\$ 5-Pentylresorcinol \$\$ 5-n



Hit#3 Entry:13451 Library:NIST05s.LIB
SE:75 Formula:C11H16O2 CAS:500-66-3 MolWeight:180 RetIndex:1632
CompName:1,3-Benzenediol, 5-pentyl- \$\$ Olivetol \$\$ Resorcinol, 5-pentyl- \$\$ 5-n-Anylresorcinol \$\$ 3,5-Dihydroxyanylbeneze \$\$ 5-Pentylresorcinol \$\$ 5-n



Hit#4 Entry:112487 Library:NIST05.LIB
SE:74 Formula:C21H36O2 CAS:3158-56-3 MolWeight:320 RetIndex:2626
CompName:1,3-Benzenediol, 5-pentadecyl- \$\$ Resorcinol, pentadecyl- \$\$ Resorcinol, 5-pentadecyl- \$\$ 5-Pentadecylresorcinol \$\$ 5-Pentadecyl-1,3-benzenedic



Hit#5 Entry:18594 Library:NIST05s.LIB
SE:74 Formula:C13H18O3 CAS:7070-24-8 MolWeight:222 RetIndex:1751
CompName:2-Cyclohexen-1-one, 4-hydroxy-3,5,5-trimethyl-4-[(1E)-3-oxo-1-butenyl]- \$\$ 4-Hydroxy-3,5,5-trimethyl-4-[(1E)-3-oxo-1-butenyl]-2-cyclohexen-1-one #

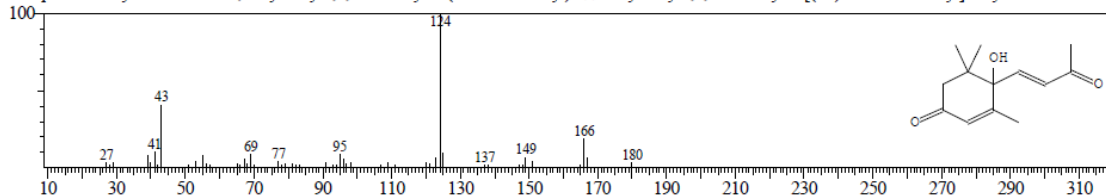
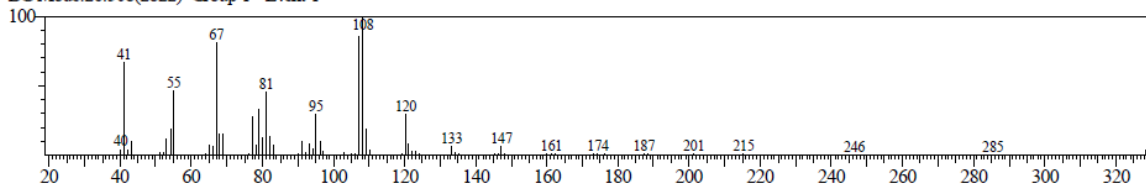


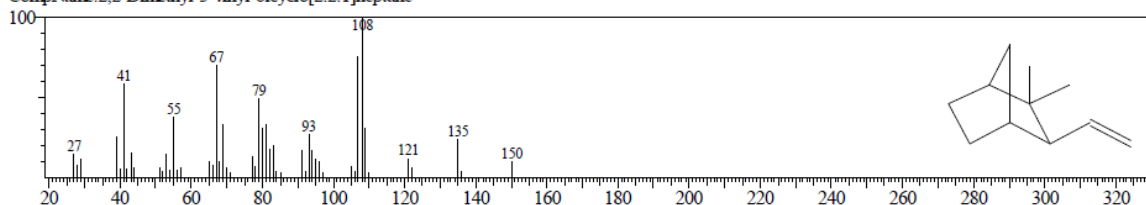
Fig. 14: Line 13 Mass Spectra of Cashew Nut Shell Liquid

<< Target >>

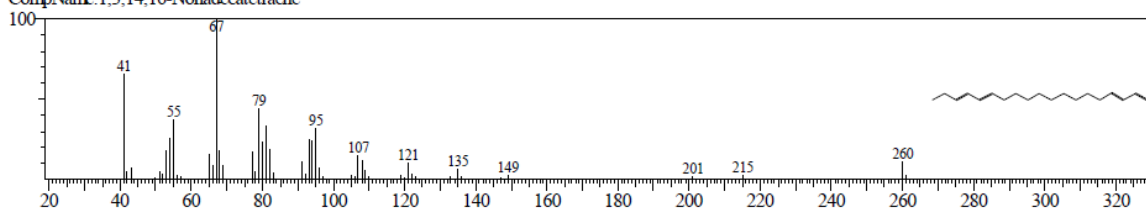
Line#:14 R.Time:26.558(Scan#:2828) MassPeaks:101
RawMode:Single 26.558(2828) BasePeak:108.15(215464)
BG Mode:26.508(2822) Group 1 - Event 1



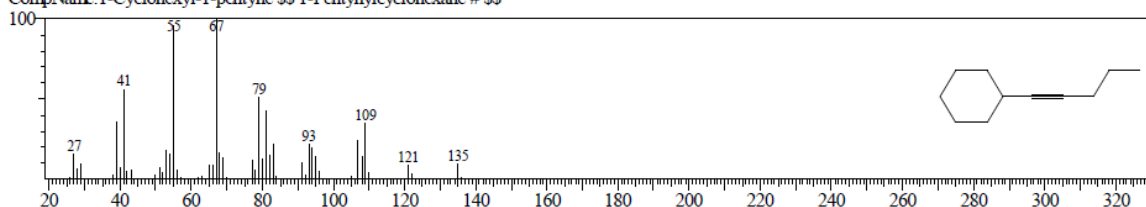
Hit#:1 Entry:15051 Library:NIST05.LIB
SE84 Formula:C11H18 CAS:115948-98-6 MolWeight:150 RetIndex:1027
CompName:2,2-Dimethyl-3-vinyl-bicyclo[2.2.1]heptane



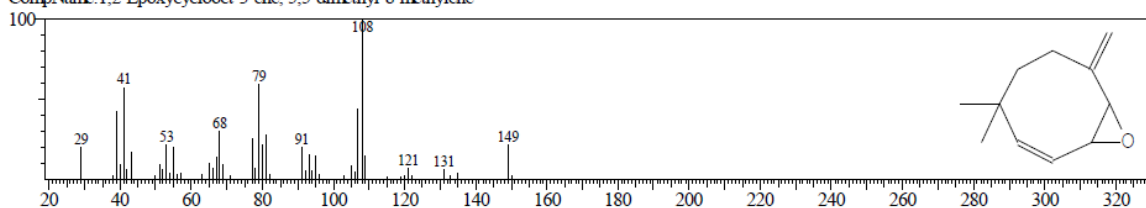
Hit#:2 Entry:77364 Library:NIST05.LIB
SE83 Formula:C19H32 CAS:0-00-0 MolWeight:260 RetIndex:1924
CompName:1,3,14,16-Nonadecatetraene



Hit#:3 Entry:15006 Library:NIST05.LIB
SE81 Formula:C11H18 CAS:67886-53-7 MolWeight:150 RetIndex:1196
CompName:1-Cyclohexyl-1-pentyne \$\$ 1-Pentynylcyclohexane # \$\$



Hit#:4 Entry:21534 Library:NIST05.LIB
SE81 Formula:C11H16O CAS:0-00-0 MolWeight:164 RetIndex:1154
CompName:1,2-Epoxycyclooct-3-ene, 5,5-dimethyl-8-methylene-



Hit#:5 Entry:35480 Library:NIST05.LIB
SE81 Formula:C14H22 CAS:51487-38-8 MolWeight:190 RetIndex:1409
CompName:1,5,9,13-Tetradecatetraene \$\$ (5E,9E)-1,5,9,13-Tetradecatetraene # \$\$

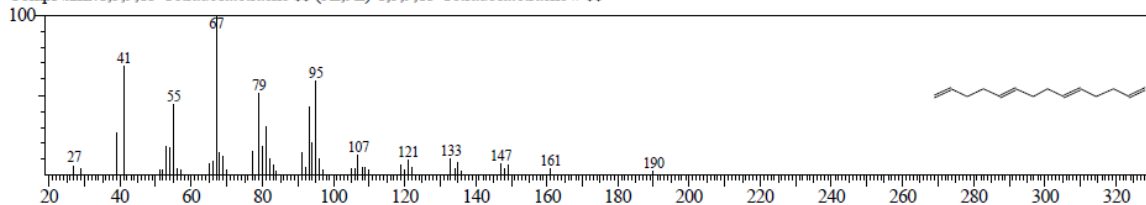
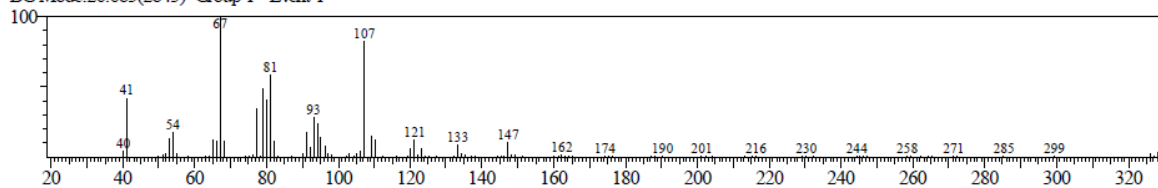


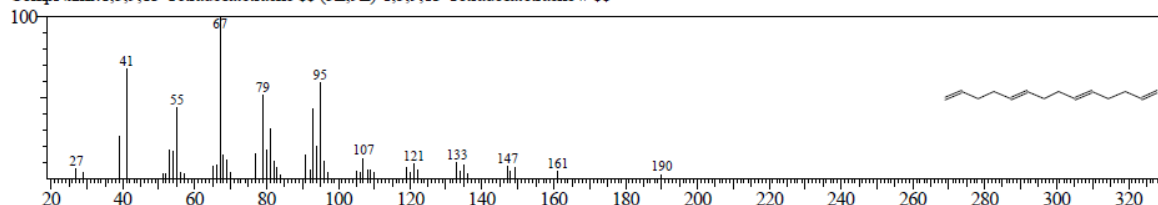
Fig. 15: Line 14 Mass Spectra of Cashew Nut Shell Liquid

<< Target >>

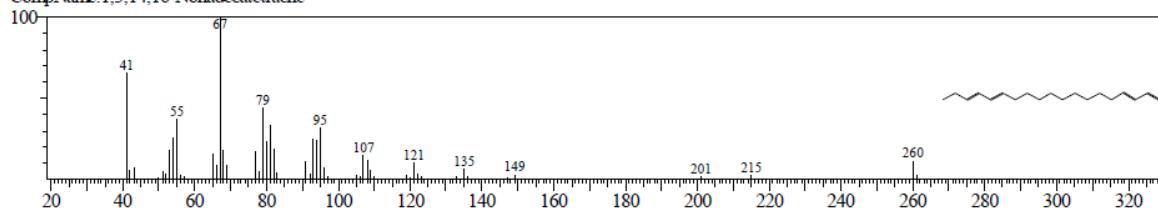
Line# 15 R Time: 26.783 (Scan#: 2855) MassPeaks: 126
RawMode: Single 26.783 (2855) BasePeak: 67.05 (201959)
BG Mode: 26.683 (2843) Group 1 - Event 1



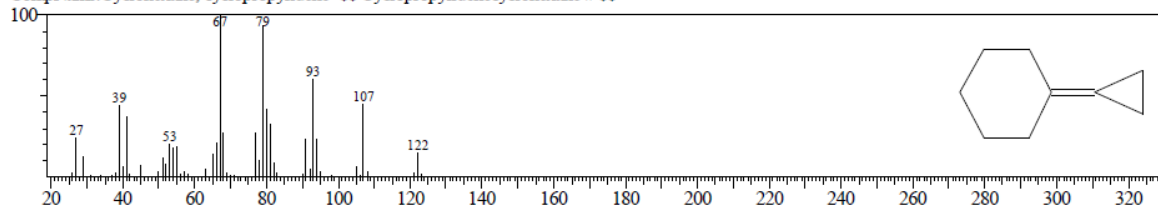
Hit# 1 Entry: 35480 Library: NIST05.LIB
SE: 82 Formula: C14H22 CAS: 51487-38-8 MolWeight: 190 RetIndex: 1409
CompName: 1,5,9,13-Tetradecatetraene (5E,9E)-1,5,9,13-Tetradecatetraene #



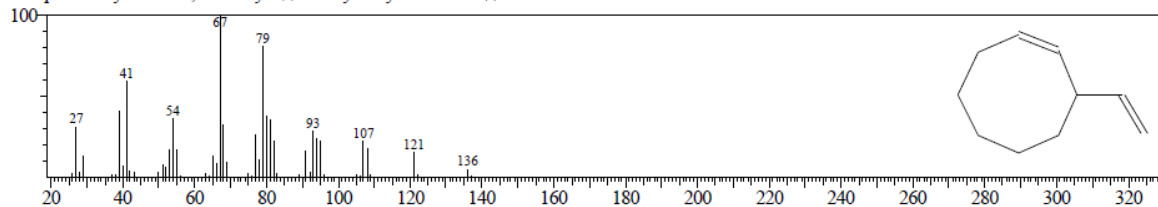
Hit# 2 Entry: 77364 Library: NIST05.LIB
SE: 81 Formula: C19H32 CAS: 0-00-0 MolWeight: 260 RetIndex: 1924
CompName: 1,3,14,16-Nonadecatetraene



Hit# 3 Entry: 5523 Library: NIST05.LIB
SE: 81 Formula: C9H14 CAS: 14114-06-8 MolWeight: 122 RetIndex: 1020
CompName: Cyclohexane, cyclopropylidene- Cyclopropylidencyclohexane #



Hit# 4 Entry: 9515 Library: NIST05.LIB
SE: 81 Formula: C10H16 CAS: 2213-60-7 MolWeight: 136 RetIndex: 1092
CompName: Cyclooctene, 3-ethenyl- 3-Vinyl-1-cyclooctene #



Hit# 5 Entry: 5533 Library: NIST05.LIB
SE: 81 Formula: C9H14 CAS: 0-00-0 MolWeight: 122 RetIndex: 928
CompName: 7-Methylenebicyclo[4.2.0]octane

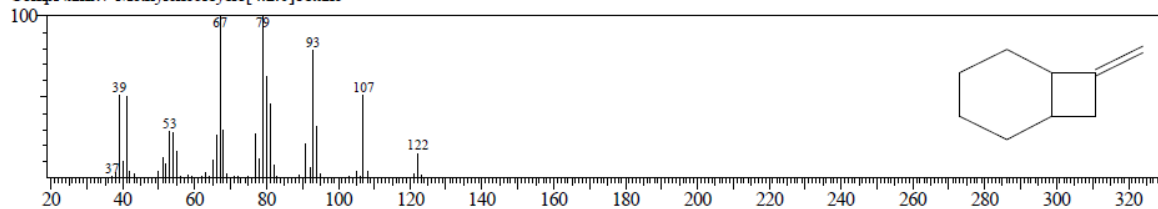


Fig. 16: Line 15 Mass Spectra of Cashew Nut Shell Liquid

CONCLUSION

The results of this study indicate that CNSL could be used as a defoamer for the prevention of foam during production and

application of paint systems as its properties are in consonance with conventional defoamers like polydimethylsiloxane and Linseed oil used in paint formulations.

REFERENCES

1. PMA. (2010). Paints Manufacturers Association of Nigeria Annual Report. A publication of the Paints Manufacturers Association of Nigeria, P. O. Box 67, Ikeja, Lagos, Nigeria.
2. Rodrigues F. H., Francisco C. F., José R. R., Nágila M. P., and Feitosa P. A. (2011). Comparison between Physico-Chemical Properties of the Technical Cashew Nut Shell Liquid (CNSL) and those Natural Extracted from Solvent and Pressing. *Polímeros*, 21 (2):156-160.
3. Akinhami R. F., Atasie V. N. and Akintokun P. O. (2008). Chemical Composition and Physicochemical Properties of Cashew nut (*Anacardium occidentale*) Oil and Cashew nut Shell Liquid. *Journal of Agricultural, Food, and Environmental Sciences*, 2(1): 1 – 10.
4. Adeigbe O. O., Olasupo F. O., Adewale B D and Muyiwa A. A. (2015). A review on cashew research and production in Nigeria in the last four decades. *Academic Journals*, 10(5):196-209
5. Patel, R N., Bandyopadhyay S and Ganesh A (2006). Extraction of cashew (*Anacardium occidentale*) nut shell liquid using supercritical carbon dioxide. *Bioresour. Technology*, 97, 847-862
6. Edoga M O, Fadipe L, Edoga R N (2006). Extraction of Polyphenols from Cashew Nut Shell. *Leonardo Electronic Journal of Practices and Technologies*, 9 (2):107-112
7. Gandhi T, Patel M, Dholakiya B K (2012). Studies on effect of various solvents on extraction of cashew nut shell liquid (CNSL) and isolation of major phenolic constituents from extracted CNSL *J. Nat. Prod. Plant Resour.*, 2 (1):135-142
8. Arayaprane W and Rempel G L. (2007). Effects of cashew nut shell liquid as a plasticizer on cure characteristics, processability, and mechanical properties of 50: 50 NR/EPDM blends: A comparison with paraffin oil. Wanvimon Arayaprane Garry L. Rempel (2007). *Applied Polymer Science*, 106, (4): 2696-2702
9. Sudjaroen Y, Thongkao K, Suwannahong K (2018). Antioxidant, Antibacterial, and Cytotoxicity Activities of Cashew (*Anacardium occidentale*) Nut Shell Waste. *International Journal of Green Pharmacy*, 12 (1) S229-S234
10. Bhunia H. P., Jana, R. N., Basak, A. and Lenka S. (1998). Synthesis of polyurethane from cashew nut shell liquid (CNSL), a renewable resource. *Journal of Polymer Science*, 36(3):391 – 400
11. Marcos A. G. B, Robert R, James I. R. (2017). A preliminary evaluation of bio-based epoxy resin hardeners for maritime application. *Procedia Engineering* 200:186–192

12. Viswalingam K. and Solomon F.E (2013). A Process for Selective Extraction of Cardanol from Cashew Nut Shell Liquid (CNSL) and its Useful applications. *International Journal of Scientific & Engineering Research*, 4(3):1-4
13. Denkov, N. D. (2014). Mechanism of Foam Destruction by oil-based Antifoams. *angmuir*, 20(22): 9463-9505.
14. Asogwa E. U., Mokwunye I. U., Yahaya L. E., and Ajao A. A. (2007). Evaluation of Cashew Nut Shell Liquid (CNSL) as a potential Natural Insecticide against Termite (soldiers and workers castes). *Research Journal of Applied Sciences*, 2(9):939-942
15. Idah P. A, Simeon M. I. and Mohammed M. A. (2014). Extraction and Characterization of Cashew Nut (*Anacardium Occidentale*) Oil and Cashew Shell Liquid Oil. *Academic Research International*, 5(3): 50-54.
16. Deuel H. J. (1951). The lipids: their Chemistry and Biochemistry (Vol 1) New York Inter Science Publishers 53-57.
17. Akintayo E. T., Adebayo E. A., and Arogundade L. A. (2002). Chemical composition, physicochemical and functional
18. Srinivasan A., Czaplá B., Mayo J., and Narayanaswamy A. (2016). Infrared dielectric function of polydimethylsiloxane and selective emission behaviour. *Applied Physics Letters*. 109 (6): 1-7
19. Popa V. M., Gruia A., Raba D., Dumbrava D., Moldovan C., Bordean D. and Mateescu C. (2012). Fatty acids composition and oil characteristics of linseed (*Linum Usitatissimum* L.) from Romania. *Journal of Agroali*
20. Couturier M. (2014). Coating compositions, method of preparation thereof and uses thereof. Available online at: <https://patents.google.com/patent/WO2016090468A1/en>. Accessed: 12/07/2018
21. Owen M. J. (2001). Encyclopedia of Materials: Science and Technology, 2nd Edition, 2480-2482
22. Rajesh K. V., Sumathi C. S., Balasubramanian V., and Ramesh N. (2009). Elementary chemical Profiling and antifungal properties of cashew (*Anacardium occidentale* L.) nuts. *Botany Research International* 2: 253-257.

JOMAR 11(2) 2017, 61 - 72
ISSN: 1597-3204

..

SUITABILITY OF CELLULOSE EXTRACTED FROM NIGERIAN CORN COB WASTES AS INDUSTRIAL EXCIPIENT.

IBE K.A.

Department Of Chemistry, Federal University Of Petroleum Resources, Effurun,
P.M.B. 1221 Effurun, Delta State, Nigeria.
E- mail: ibe.kenneth@fupre.edu.ng. Tel: +2348056401350

ABSTRACT

Industrial excipients like cellulose made from hard woods are very expensive and huge amount of money is spent in their importation. The need to derive them from cheaper and readily available sources such as agricultural wastes has become necessary. Corn cob wastes accumulated in Isele Uku, Aniocha Local Government Area of Delta State, Nigeria were collected, cut into pieces, washed and sun dried before sieving. The cellulose was extracted by hydrolysis and bleaching. The extracted cellulose was characterized together with a commercially available British Drug House(BDH) cellulose against some standard excipient parameters such as p^H , true density, tap density, bulk density, Hausner's ratio, carr's index, powder porosity, moisture content and moisture absorption capacity. The values of some of the parameters(True density,1.61; bulk density, 0.33;Hausner's ratio, 1.27; Carr's index, 21.4) compared relatively well with the commercially available British Drug House (BDH) product. Therefore, cellulose from waste corn cobs has a great potential for use as an industrial excipient.

Keywords: Cellulose, Corn Cob, Industrial Excipient and Hausner's Ratio

INTRODUCTION

Corn is the fourth most important food in the world today [1]. It is used for a variety of foods and related products ranging from industrially produced cereals to locally made delicacies. It can also be consumed directly as food, either boiled or roasted. In Nigeria, corn cobs are a major by-product of local

farming activities. Nigeria is the 10th world largest producer of maize and the largest producer in Africa [2]. The estimated corn production in 2010 was put at about 8,800,000 metric tons with growth rate of 1.68 %, in 2012 [3]. Currently Nigeria produces over 10,000,000 metric tons of maize per annum [2].

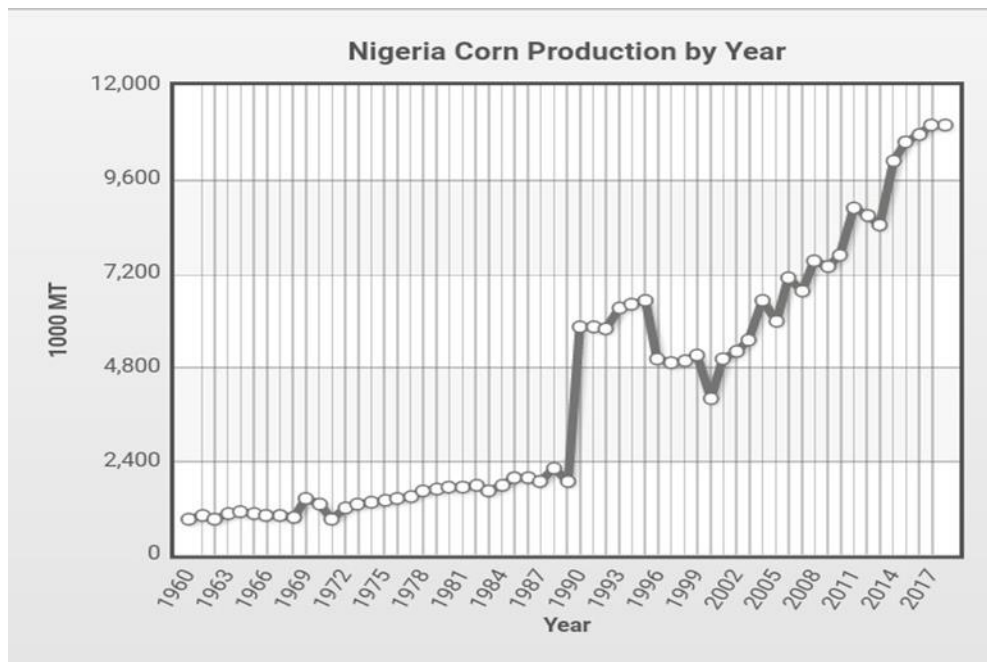


Fig.1: Nigeria Yearly Corn Production [2]

Corn cobs are important by-products of agricultural activities. Each year, farming and other agricultural related activities generate millions of tons of this agricultural residue in Nigeria, and this represents an abundant cheap and readily available source of lignocellulosic biomass [4]. In Egypt, they represent about 15 % of the total corn production of the sweet corn industry [5]

Lignocellulosic biomass is the most abundant renewable biomass with a worldwide production of 1×10^{10} million tons annually [6]. It provides an intriguing almost inexhaustible and sustainable natural polymer that has been used in the form of fiber or its derivatives for thousands of years, for a wide range of materials and product applications [6]. Its major constituents include; cellulose,

hemicellulose and lignin, however the qualities of these major constituents depend on the type of material [7].

Cellulose is a poly-diverse organic polymer of high molecular weight with the formula $(C_6H_{10}O_5)_n$. It consists of a linear chain of several d-glucose units linked by β -(1, 4) glucosidic bonds [8]. It is a major structural component of the primary cell wall of green plants. It exists as a tasteless and odorless white powder which is insoluble in water and most organic solvents.

Cellulose has a very wide range of industrial applications, for instance, in medicine; microcrystalline cellulose and powdered cellulose are used as inactive fillers in drug tablets and other soluble derivatives. In the energy sector, it is used in the synthesis of biofuels. It is also used in science

laboratories as the stationary phase for thin layer chromatography [8].

Cellulose is used in the production of water soluble adhesives and binders such as methyl cellulose and carboxymethyl cellulose. It is also the main ingredient of textiles made from cotton, linen and other plant materials.

Several methods covered by patents have been put forth for the production of cellulose powder. However, commercially available cellulose is produced from hard wood and purified cotton which are highly expensive. Therefore, in this work, the abundant and locally available corn cob wastes in Delta State, Nigeria were harnessed for the extraction of their

cellulose content and characterization for suitability as industrial excipient.

MATERIALS AND METHODS

Description of the Study Area

Corn cobs were obtained from the farmlands in Issele- Uku in Aniocha North Local Government Area of Delta State. Issele-Uku, is in Aniocha-North Local Government Area of Delta state. The town lies approximately six degrees north of the equator, with coordinates; 6°19’11.98 "North and 6°28’36.65 "East. The town has a tropical climate with an average annual temperature of 25.6 °C. The annual rainfall in the town is up to 1807 mm with September having the highest amount of rainfall (324 mm) and December having the least (11 mm) [9][10]

Table I: Monthly average weather conditions in Issele-Uku

Month	Avg. Temperature (°C)	Avg. Temperature (°F)	Precipitation/Rainfall (mm)
January	25.7(0.12)	78.3 (0.12)	15
February	26.7 (0.09)	80.1 (0.09)	32
March	27.4 (0.1)	81.3 (0.1)	95
April	27.2 (0.32)	81.0 (0.32)	141
May	26.1 (0.26)	79.0 (0.26)	213
June	25.1 (0.16)	77.2 (0.16)	246
July	24.1 (0.09)	75.4 (0.09)	256
August	23.9 (0.11)	75.0 (0.11)	195
September	24.4 (0.25)	75.9 (0.25)	324
October	24.8 (0.18)	76.6 (0.18)	231
November	26 (0.1)	78.8 (0.1)	48
December	25.7 (0.15)	78.3 (0.15)	11

*standard deviations are in parenthesis

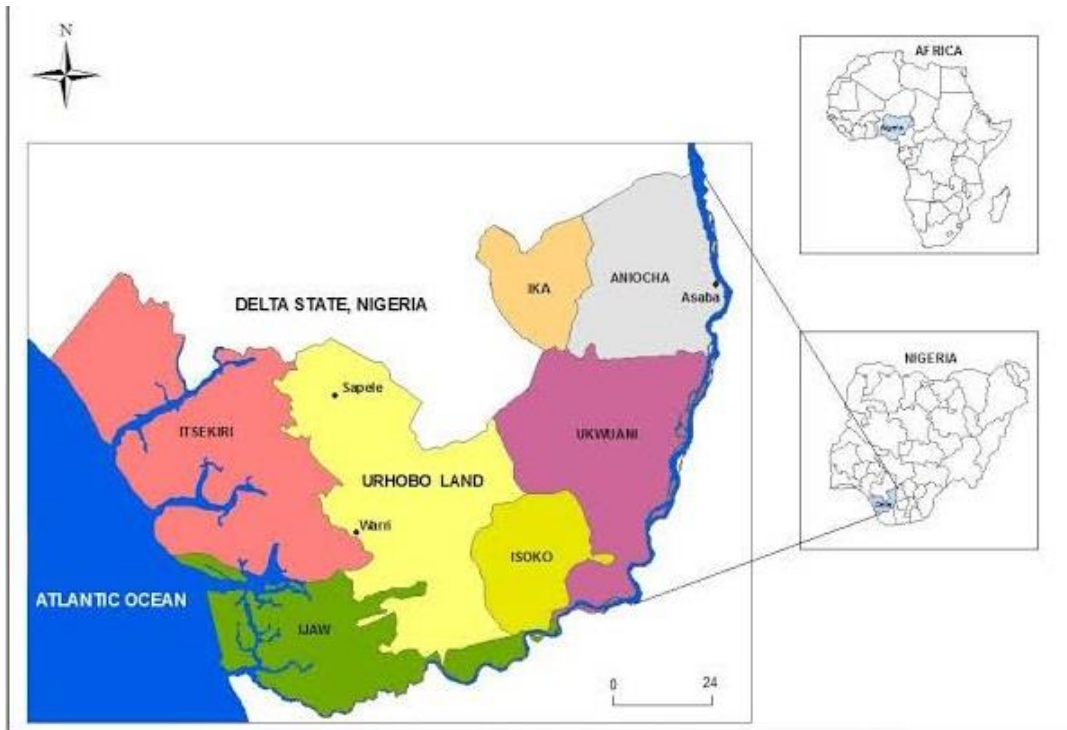


Fig 2: Map of Nigeria showing the Delta state region

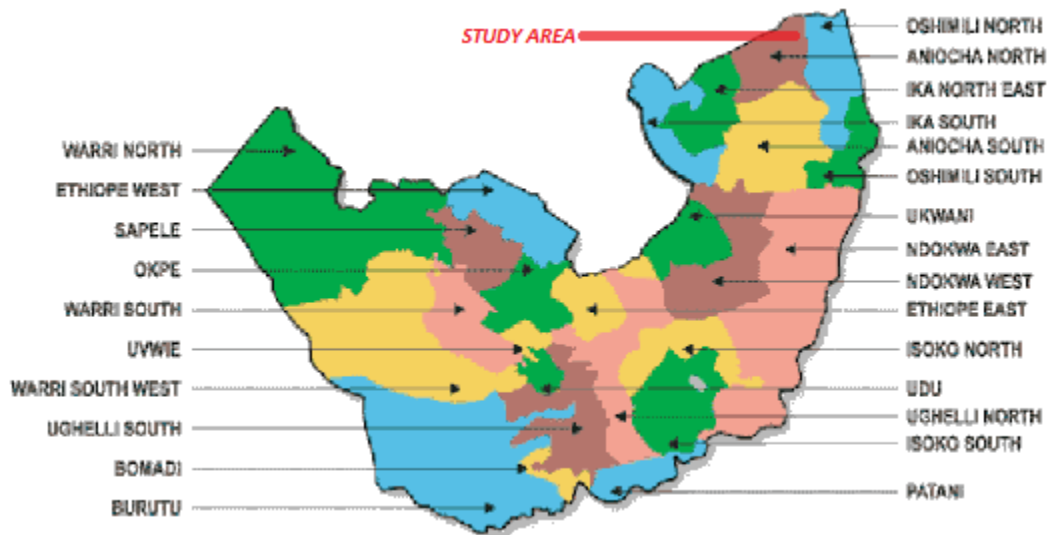


Fig 3: Map of Delta state showing LGA of study area (Aniocha North)

Sample Preparation

The corn cobs were cut into smaller pieces, washed and sun-dried for 48 hours to reduce their moisture content. They were then crushed into powder using a local grinding mill and sieved using an 850 micron sieve. All

the chemicals used in this study were of analytical grade, and are products of BDH

Treatment and Hydrolysis

50 g of the sieved corn cobs was weighed into a beaker and 750 ml of 4 % sodium hydroxide was poured into a beaker in order

..

to obtain a material to liquid ratio of 1:15 [11]. The mixture was then heated at 75 °C for 2 hours to dissolve lignin and other impurities present in the corn powder. It was then washed thoroughly with distilled water and filtered.

750 ml of 40 % sulfuric acid was then added to the washed powder and the mixture was heated at a temperature of 55 °C for about 90 min to obtain microcrystalline cellulose [12], after which the reaction was quenched by pouring the contents of the beaker into an excess of water and then allowed to settle for about 1h, followed by thorough washing with distilled water.



Plate 1a: Extracted cellulose before bleaching

Characterization

The extracted cellulose was put in a beaker and labelled as sample A and BDH cellulose obtained from a chemical shop was labelled as sample B. They were both compared based on the parameters determined as stated by the following.

- **pH:** 2 g of sample A was shaken with 100 ml of distilled water in a beaker for 5 min and the pH of the

The washed powder was further treated with 750 ml of 17.5 % sodium hydroxide to neutralize any residual acid in it. Extraction was completed by treatment with a 500 ml solution of 2 % sodium hydroxide and 2 % sodium sulfite in the ratio 1:1 v/v at 50 °C for 1 h [12]. The sodium sulphite serves as a de-sulphurizing agent as well as a mini-bleaching agent

Bleaching

500 ml of 3.5 % sodium hypochlorite was added to the extracted cellulose in a beaker and the mixture was heated for 90 min at 40 °C [12]. The cellulose was then washed with distilled water, filtered and sundried.



Plate 1b: Extracted cellulose after bleaching
supernatant liquid was determined using a pH meter(Kent meter model 7020). The process was then repeated for sample B.

- **True Density:** A clean, dry 50 ml specific gravity bottle was filled with xylene and its weight was measured and recorded. Some of the xylene was then poured out and 0.5 g of sample A was poured inside, the

bottle was then wiped dry of any excess

fluid and its weight was measured and recorded. The true density of the sample was then calculated using the formula below;

$$D_{true} = \frac{w}{\{(a+w)-b\}} \times SG$$

Where; **w** is the weight of powder, **SG** is specific gravity of solvent, **a** is weight of bottle + solvent and **b** is weight of bottle + solvent + powder [13]. The procedure was repeated for sample B.

- **Bulk Density and Tap Density:** 25 g of sample A was weighed into a 100 ml measuring cylinder and the bulk volume was recorded as (V_0). The cylinder was then tapped against the surface of a table until a constant volume was reached (i.e no further settling of the sample was observed), the volume was then recorded as (V_1). The bulk density (D_{bulk}) and tap density (D_{tap}) were then calculated using the equations below and recorded.

$$D_{bulk} = \frac{W}{V_0}$$

$$D_{tap} = \frac{W}{V_1}$$

Where; **W** is the weight of the powder

- **Hausner's Ratio:** The Hausner ratio [14] for the two samples was calculated using the equation below;

$$Hausner\ ratio = \frac{D_{tap}}{D_{bulk}}$$

- **Carr's Index:** The Carr index [15] for the two samples was calculated using the equation below;

$$Carr's\ index = \frac{D_{tap}-D_{bulk}}{D_{bulk}} \times 100$$

- **Powder Porosity:** The powder porosity (P) of the two samples was evaluated using their respective true and tapped densities by means of the equation below;

$$P = 1 - \frac{D_{tap}}{D_{true}}$$

- **Moisture Content:** 5 g of sample A was weighed into a crucible dried in an oven (Genlab laboratory oven model MINO/040) at 110 °C until a constant weight was reached, and the percentage loss in weight was calculated as the moisture content.

$$\%Moisture\ content = \frac{weight\ of\ sample\ after\ drying}{weight\ of\ sample\ before\ drying} \times 100$$

- **Moisture Absorption Capacity:** 2 g of sample A and sample B were

separately weighed; they were then evenly distributed over the surface of a 70 mm Petri dish separately. The samples were then placed in a desiccator containing distilled water (RH = 100 %) at room temperature

for 72 h. The weight gained by the samples was recorded at intervals of 12 hours. The moisture absorption capacity was calculated from the weight difference.

RESULTS AND DISCUSSIONS

Table II below shows the results of the physiochemical evaluation of the extracted cellulose samples

Table II: Physiochemical evaluation of the extracted cellulose samples

Property	Sample A	Sample B
True density (g/cm ³)	1.61	1.55
Bulk density (g/cm ³)	0.33	0.35
Tap density (g/cm ³)	0.42	0.43
pH	7.9	7.03
Hausner's ratio	1.27	1.23
Carr's index	21.4	18.6
Moisture content (%)	6.10	5.40
Powder porosity	0.74	0.72

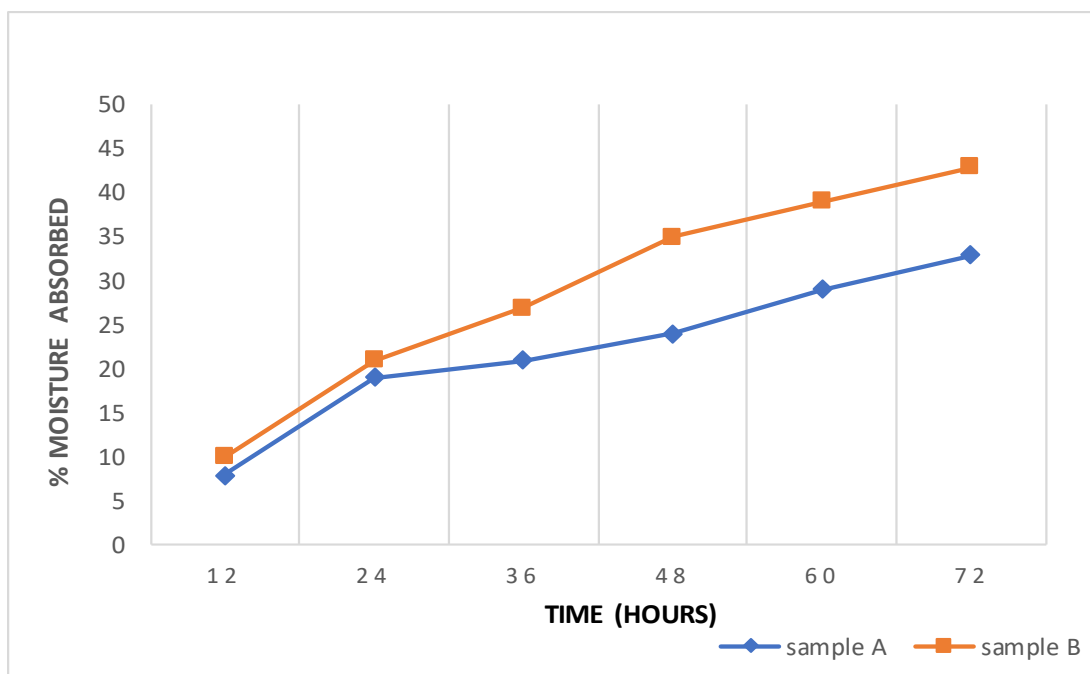


Fig 4: Graph of absorbed moisture with time

pH

From table 2, the results show that both samples A and B have the p^H of 7.9 and 7.03 respectively. The pH of the extracted cellulose is slightly above the required standard of 5.0 – 7.5 for microcrystalline cellulose [16]. However, the value can be adjusted during the extraction process by further washing with a carefully selected weak acid.

True density

The true density of the cellulose powder is an indication of how well the powder can be compressed and it varies directly with the compressibility of the powder i.e. the higher the true density, the higher the compressibility. Both samples would have good compressibility property as they are

both higher than the standard of 1.5 g/cm^3 for microcrystalline cellulose (MCC) [16].

However, the extracted cellulose, having a slightly higher true density, may have better compressibility property than the commercial brand.

Bulk density

The bulkiness or bulk density is a measure of the ability of the cellulose powder to flow during use. Powder flow is a key requirement for pharmaceutical, food and cosmetics manufacturing processes. For example, tablets are often manufactured on a rotary multi-station tablet press by filling the tablet die with powders or granules based on volume. Thus, the flow of powder from the hopper into the dies often determines weight, hardness, and content uniformity of tablets. Understanding of

..

powder flow is also crucial during mixing, packaging, and transportation. And thus, it becomes essential to measure the flow properties of these materials prior to the finishing line. The higher the bulk density, the better the potential of the material to flow [16].

Both microcrystalline cellulose (MCC) samples have almost the same bulk densities, signifying that they could both have good flow potential.

Tap density

Tap density is a measure of how well a powder can be packed in a confined space on repeated tapping. The higher the tap density, the higher the ability of the powder to rearrange under compression [16]. The tap densities of both samples are close. However, the commercial brand of MCC may have better potential of being packed in a tight space than the extracted MCC since it has a slightly higher tap density of 0.43g/cm^3 .

Hausner's ratio

Hausner's ratio is an estimate of the degree of cohesion between particles. It varies inversely with particle flow. A lower Hausner's ratio of materials indicates better flow properties than higher ones. A value of 1.20 or lower indicates that the powder will have good flow properties whereas a value of 1.50 and above indicates poor flow properties [17]. Results on table 1 show that

both cellulose samples have good flow properties.

Carr's index

Carr's index gives an idea of how well a powder can be compressed. It also varies inversely with particle flow. A Carr's index of less than 10 indicates excellent flow properties, values within the range of 12-16 indicate good flow properties; values within the range of 18 -21 indicate fair flow properties while the values within the range of 23-28 indicate poor flow properties [18]. Both cellulose samples fell in the same range of Carr's index classified as fair flow properties.

Powder porosity

Powder porosity indicates the overall flowability and compressibility of the powder. It is an estimate of the voids between the particles as well as the pores [12]. It is also directly related to the particle size i.e. the higher the particle size, the higher the powder porosity. From the results, the commercial microcrystalline cellulose has a higher porosity value than the extracted cellulose and hence has a better compression and flow potential.

Moisture content

The standard range of moisture content for cellulose is between 5 % – 7 % [16], and it varies inversely with particle flow [19]. Both MCC samples fell within the standard range, however, the commercial MCC brand would

..

have a better flow property than the extracted MCC even though both microcrystalline cellulose samples seem to possess fairly the same properties based on the parameters measured. The commercial cellulose brand may have slightly better potential in terms of compressibility and flowability than the extracted cellulose, and this is confirmed by the powder porosity which is an indication of the overall flowability and compressibility of the powder. It is an estimate of the voids between the particles as well as the pores within the particles [12], and it is also directly related to the particle size i.e. the higher the particle size, the higher the powder porosity. From the results, the commercial microcrystalline cellulose has a higher porosity value than the extracted cellulose and hence has a better compression and flow potential.

Moisture sorption capacity (MSC)

Moisture sorption capacity is a measure of the moisture sensitivity of the material. It reflects the relative physical stability of products made from the material when

stored under humid conditions [13]. As shown in fig. 4, both cellulose samples are sensitive to atmospheric moisture although the extracted cellulose seemed more sensitive and hence, less stable under humid conditions.

CONCLUSION

Cellulose extracted from waste corn cob obtained from Issele-Uku, Delta State, Nigeria has a great potential as an excipient. It compared fairly well with the commercial cellulose (BDH brand). However, with slight modification in the chemical extraction procedure, some of the characterization parameters will be improved on thereby enhancing its suitability as an industrial excipient.

ACKNOWLEDGEMENT

I appreciate the efforts of my research assistants who laboured tirelessly to gather the corn cob wastes. I thank the technologists of the Department of Chemistry, Federal University of Petroleum Resources, Effurun who assisted me in the laboratory work.

REFERENCES

1. Abubakar, U.S., Yusuf, K.M., Safiyanu, I., Abdullahi, S., Saidu, S.R., Abdu, G.T. and Indee, A.M. (2016). Proximate and mineral composition of corn cob, banana and plantain peels. *Int. J. of Food Sci. and Nut.* 1(6): 25-27
2. Food and Agricultural Organisation (FAO) (2017). Food and Agricultural Organization Statistics Database online.
3. United States Department of Agriculture (USDA) (2012). Nigeria Yearly Corn Production online.
4. Ruan, R., Lun, Y., Zhang J., Addis, P. and Chen, P. (1996). Structure-function relationships of highly refined cellulose made from agricultural fibrous residues. *Appl. Eng. Agric.*12: 465–468
5. Ashour, A., Amer M., Marzouk A., Shimizu K., Kondo R., and El-Sharkawy, S. (2013); Corncobs as a Potential Source of Functional Chemicals. *Molecules*.18: 13823-13830.
6. Boerjan, W., Ralph, J. and Baucher, M. (2003) "Lignin biosynthesis". *Annu. Rev. Plant Biol.* 54 (1): 519–549.
7. He, J., Cui, S., Wang, S.Y. (2008). Preparation and crystalline analysis of high-grade bamboo dissolving pulp for cellulose acetate. *J. of Applied Polymer Science.* 107: 1029 – 1038.
8. Tosh, B. (2014): Synthesis and sustainable applications of cellulose esters and ethers: A Review. *Int. J. of Energy, Sustainability and Environ. Eng.* 1 (2): 56-78
9. Climate Data (2018). [http://www.accuweather.com/en/ng/Issele Uku](http://www.accuweather.com/en/ng/Issele-Uku)
10. Chi-chung, C. and McCarl, B.A. (2004). Yield variability as influenced by climate; a statistical investigation. *J. of Climate change.* 66: 239-261.
11. Singh, S., Cheng, G., Sathitsuksanoh, N., Wu, D., Varanasi, P., George A., Balan, V., Gao, X., Kumar, R., Dale, B.E., Wyman, C.E. and Simmons, B.A. (2015). Comparison of different biomass pretreatment techniques and their impact on chemistry and structure. *Front Energy Res Bioenergy Biofuels.* 2:1–12.
12. Azubuike, C.P. and Okhamafe, A.O. (2012). Physicochemical, spectroscopic and thermal properties of microcrystalline cellulose derived from corn cobs; *Int. J. of Recycling of Organic Waste in Agric.*1: 9
13. Ohwoavworhwa, F.O. and Adedokun, T.A., (2005). Phosphoric acid mediated depolymerization and decrystallization of α -Cellulose obtained from corn cob: preparation

- of low crystallinity cellulose and some physicochemical properties. Trop. J. of Pharm. Res. 4 (2): 509-516
14. Badiei, M., Asim, N., Jahim, J.M., Sopian, K. (2014). Comparison of chemical pretreatment methods for cellulosic biomass. Procedia Soc. Behavioural Sci. 9: 170–174.
 15. Bowker, M.I. and Stahl, P.H.,. "Preparation of Water-Soluble Compounds through Salt Formation." In Camille Georges Wermuth, ed. The Practice of Medical Chemistry, Macmillan Press, London (2008), pp.747–766.
 16. British Pharmacopoeia (2004). The Stationery Office. The Department of Health, London, p. 405–407
 17. Hausner, H.H.(1967). Friction conditions in a mass of metal powder. Int. J. Powder Metall., 3: 7 - 13
 18. Carr R.L. Jr (1965). Evaluating flow properties of solids, Chem. Eng. 72: 163–168
 19. Peck, G.E., Baley, G.J., Mcurdy, V.E., Banker, G.S.(1989).Tablet formulation and design. In: Lieberman H.A., Lechman L., Schwarz J.B (eds) Pharmaceutical dosage forms. pp.75 – 130. Marcel Dekker, New York.